



Università
Ca' Foscari
Venezia

-
Ca' Foscari
Dorsoduro 3246
30123 Venezia

Master's Degree in
Conservation Science and Technology for
Cultural Heritage

Final Thesis

The wall painting in Santa Maria Assunta Basilica
crypt: new insight on non-invasive and micro
invasive analytical techniques for the analyses of
traditional pigments.

Supervisor

Prof. Elisabetta Zendri
Prof. Diego Calaon

Assistant supervisor

Dr. Delia Paola Lucero Gómez

Graduand

Carmen Esther Piña Torres
Matriculation number 880290

Academic Year

2020 / 2021

ACKNOWLEDGEMENTS

I would like to express my sincere gratitude to all without whom I would not have been able to complete this research. My supervisors, Prof. Elisabetta Zendri and Prof. Diego Calaon for their invaluable guidance, encouragement and support.

Special thanks to Dr. Paola Lucero for her support and patience.

I would like to thank the support of the ministry of Education, Youth and Sports of the Czech Republic, the ERDF/ESF project OA ITI – ARTECA: “Advanced physical-chemical methods of research and protection of cultural and artistic heritage” (CZ.02.1.01/0.0/0.0/17_048/000) that allowed me to obtain Py-GCMS results.

I would like to acknowledge Dr. Francesca Izzo who was so generous to also help the research in regards of the Py-GCMS results.

Finally, thanks to my family, those who left us during these hard times but were always there with their support and love. Thanks to my mother and father for their love, support, and belief in me, to my brother who believes in what I do more than nobody else and Scatty who never ceases to amaze me. Thanks to my friends Marian and Laura for their support and the good laughs, and to Fernando, you were more of a company that you could ever know.

1 CONTENT

2	Aim	3
3	Introduction	4
3.1	Santa Maria Assunta Church	4
3.2	Mural location and its conservation state	8
3.3	Pigments and techniques	11
3.4	Analytical techniques	15
3.4.1	Hyper Spectral imaging	15
3.4.2	Fiber Optic Reflectance Spectroscopy (FORS).....	16
3.4.3	Fourier Transform Infrared spectroscopy	16
3.4.4	Raman spectroscopy	17
3.4.5	Pyrolysis coupled to Gas chromatography and Mass spectrometry (Py-GCMS). 19	
4	Experimental	20
4.1	Archaeological cataloguing	20
4.2	Hyperspectral imaging	24
4.3	Fiber Optic Reflectance Spectra (FORS)	24
4.4	Raman spectroscopy	25
4.5	Fourier Transform Infrared (FT-IR).....	26
4.6	Pyrolysis coupled to Gas Chromatography and Mass Spectroscopy (Py-GCMS)	26
5	Results	27
5.1	Hyperspectral imaging	27
5.2	Fiber Optic Reflectance Spectra (FORS)	31
5.3	Raman spectroscopy	34
5.4	Fourier Transform Infrared FT-IR	41
5.5	Pyrolysis coupled to Gas chromatography and Mass spectrometry (Py-GCMS).	45
6	Discussion.....	47
6.1	Hyper spectral imaging.....	47
6.2	FORS	47
6.3	Raman spectroscopy	51
6.4	Fourier Transform Infrared (FT-IR).....	55
6.5	Pyrolysis coupled to Gas chromatography and Mass spectrometry (Py-GCMS).	57
7	Conclusions	60
8	Bibliography	61
9	Annex 1.....	67

Within the archaeological works in the summer of 2020, a series of wall paintings were uncovered in the Santa Maria Assunta Basilica in Torcello, including the crypt, where a blue backgrounded mural with multi-coloured figures on the apse and removed from the wall fragments that remained behind the altar were exposed. The preserved decoration shows 3 overlaid painting layers.

The present work directed to carry out the characterization of the composing materials of the plaster fragments that belong to the wall painting uncovered during the archaeological works made in 2020 at the Santa Maria Assunta Basilica in Torcello, Venezia. Said characterization entailed the classification and posterior analysis of the recovered fragments, by using non-invasive techniques that enabled the pigment characterization and micro destructive ones that enabled the identification of the use of binders used to paint and consequently the painting techniques.

A systematic cataloguing of the recovered fragments along with the use of non-invasive analytical techniques, hyperspectral imaging, Fiber Optic Reflectance Spectroscopy (FORS), Raman spectroscopy and Fourier Transform Infrared (FTIR) spectroscopy and Pyrolysis coupled to gas chromatography coupled to mass spectrometry (PyGCMS) enabled the characterization of the materials used for the creation of the painting layers.

The cataloguing included the cleaning, photography, labelling, measuring of the surface and of the thickness of the plaster or plasters and colour identification and classification accordingly for more than 3000 recovered fragments.

The hyperspectral imaging enabled the analysis of a higher number of fragments with minimum handling, and to reduce sampling as much as possible. The recording of the reflectance spectra by using FORS allowed the identification of certain pigments. Raman spectroscopy, Fourier Transform Infrared (FTIR) spectroscopy, as well as Pyrolysis Gas chromatography coupled to mass spectrometry techniques were used to identify the binders. All the information recovered from the techniques helped to identify the palette conformed mainly by earth pigments, its mineral composition, and the identification of the painting technique.

3.1 SANTA MARIA ASSUNTA CHURCH

Torcello it is not Venice, and will never be, Torcello did not evolve into Venice, and if anything, it evolved into a medieval Burano, it is a place that finally underwent venetian dominance but always maintained its identity, always recounted different to Venice. Configuring itself as a periphery of the Roman city, Altino, that later would be more important.

It is been know that the islands of the Torcello estuary have been populated long before the Vth century,^{1,2} though the population was scarce. The main activities were agriculture, fishing, or trade with the mainland.¹

Altino, was a Roman Adriatic city of the lagoon type, connected to the ocean by canals and the river delta, giving it a logistic importance.³ One of the richest cities in the venetian gulf during roman times,²it is been theorized that the suffered invasions and looting from the Huns that forced the inhabitants to retreat to the internal islands and over the shores of the lagoon, including Torcello, the nearest island to the mainland.¹ Moreover, its location offered security and it lent itself very well to the Christian refugees.²

After the war, some of the new inhabitants remained in the island, increasing its population and thus its economy, the same as the surrounding islands, Burano, Murano, Mazzorbo, Costanziaca, Amoriano and Ammiano. ¹ Taking the names of every door of their mother city, Altino. Even been known as the Altino estuary.²

Though the archaeological investigations have revealed that in reality, the barbaric invasions had a marginal roll. The excavations in the lagoon and the city show evidence of a gradual path joined to port and commercial activities instead of abrupt passages. A slow passage that began in the Roman era linked to the port system of Altino that gradually became less adapted to the commercial flux and whose activities were taken over by Torcello, Cittanova and Rialto.^{3,4}

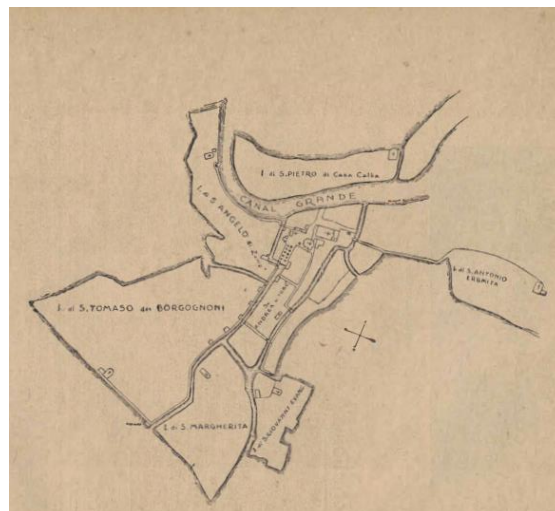


Figure 1 Archipelago in which the Torcello island was located

Giving the new circumstances of the islands, the Patriarch of Grado, Niceta summoned in the year 460, all the bishops, clergy, and senior citizens from the islands to deliberate, giving place to a *Primo Tribuno*, obliged to have residency in Grado and three dependents *Tribuni Maggiori*, one for Rivoalto, one for Candeara and one for Dorsea, residents in Rialto, Eraclea and Torcello respectively. All responsible for the justice impartation of their places of residence.

The sole fact of designating Torcello a tribunal residence over the other islands was a way to acknowledge its importance and higher population.

Later in time, other 10 other *Tribuni inferiori* were designated subordinated to the already existing ones, 5 of them to Torcello.

Subsequently, after the death of Ariovaldo, king of the Longobards. Rotari took the throne in the year 638 and established that in his domains, all the cities must have a catholic and Arian bishop, thus stablishing a bishopric in Torcello, and Paolo was designated.¹

After its designation, the island that until then was *Donio*, *Dorcea* or *Dorceo*, took the name *Nuova Altino*, though the new name was not maintained and, in most chronicles, was referred as an Altino door, *Torricella*.^{1,2}

Not long after of the death of the bishop Paolo, that the new bishop Mauro or Maurizio pledged to the Patriarch the movement of the bishop cathedral from Altino to Nuova Altino or Torcello. The cathedral construction was dedicated to *Nostra Donna*, and relics such as the body of S. Eliodoro Altinate were brought to the church. That would be maintained until the XI century, after which the name *Episcopus Torcellanus*.^{1,2}

After a period, full of disagreements over the tribune government, the need for more government unity arose, and in the 696 for the first time, in the countryside of Eraclea a general assembly took place in which Grado's supremacy was taken off and Eraclea was made the capital of the Venetian duchy. Finally, a *Duca* (subsequently *Doge*) of Venice was appointed with the consensus of the population, nobles, clergy, and bishops as Paolo Lucio Anafesto. Although the tribunal authority did not disappear with the election of the first dodge, their decisions remained contingent to the doge authority. Over the X century they would be known as *Gastaldi Ducali* and on the XII century as *Podestà*. In 810, the government headquarters were moved from Malamoco to Rialto and took the name *Dogado*.

During the reign of king Pepin, over 50 noble families moved to Torcello after the destruction of Eraclea. Other than the nobility, the commerce and navigation contributed to Torcello's prosperity. In fact, it occupied a numerous fleet.

The prosperous and flourishing Torcello was composed of various islets. Divided by a *Canale grande*, similar to the one of Venice, and was intersected by minor canals, their banks were populated by houses and palaces, most of them in stone, and among these the *ponte dei pugni*, a bridge now a days known as the devil's bridge that served for boxing exercise. The churches; *S. Andrea*, *S. Tomasso dei Borgognoni*, *S. Giovanni Evangelista* and *S. Antonio Eremita*.

In the second half of the XII century, Torcello belonged to the *Dogado*, that was divided in *Podesterie* that were named *Reggimenti*. It was extended above good stretch of the lagoon and the mainland. Evidence that even if Venezia was dominating, Torcello always remained a different city. That was governed by their own magistrates of a major and minor council.¹

The downfall of the city was marked by the deterioration of the water quality flowing in the canals, in 1360 the plague struck the city, and even if works were attempted to improve the quality of the water, the efforts were void. In 1509 the island became marsh and unhealthy, the exodus began, and the inhabitants had to emigrate, starting with the most prominent families, and many others followed. In 1615 the island was declared uninhabitable, in 1625 the population still exceeded the 1200 inhabitants, and in 1754 in was reported to be more or less deserted, and the only inhabitants were some religious, nuns and gardeners.^{1,2}

In 1810 the bishopric was totally suppressed and in 1814 was incorporated to the one of Venice.
1,2

All of the most important, rich, sacred, and beautiful goods were moved from Torcello to Venice and handed to the Venetian nobility.

The cathedral consecrated to *Nostra Donna* is probably the most antique of Europe, the construction dating from the first half of the VII century.¹ It has an Italo byzantine style,⁵ in 697 was a reconstruction under the episcopate of Adeodato or Diodato, other reconstructions were ordered in 864^{1,5} and 1008,¹ that involved the magnification of its dimensions, adding two chapels at the sides and magnification of the minor naves.⁵

Nowadays the cathedral that can be seen dates from the 1008 construction.² Though in 1418 the temple needed great repairs and in 1693 other were needed on the roof. In 1816, 1827 and 1853, the weights of the roof were reattached, and restoration on the baptistery, the rectory, the bell tower, and the mosaic.

The temple of Roman style was built to the style of ancient and oblong basilicas, the main door has very ornate jambs on the outside that may belong to the very first construction of the church. The interior is severe without gold frills. Two orders of nine Cipollino marble stone Corinthian columns support three naves.

The length is of 40 meters and the width of 22 meters, and the double in height of the side walls that forms the main nave.

At first, the temple had only one altar, but then two chapels were added, after another one next to the sanctuary was added and finally other four in stone in front of S. Teonisto, S. Liberale, other dedicated to SS. Innocenti and to Maria del Rosario. Urns that contained the corpses of saints Martiri Tabra e Tabrata.

At the end of the middle nave the ancient sanctuary is visible, closed from a balustrade of fine Greek marble with decorated parapets. A lintel surmounted, in ancient times, by statuettes.

In front of the threshold of the *Porta Santa* was the tomb of the bishop Paolo, with an inscription and a figure of the late prelate.

In the centre is the *altar maggiore* from the XVII century, over it an urn with the corpse of the late bishop S. Eliodoro.

After the basilica of San Marco had its *Pala d'oro* in place, Torcello inheritor of the magnificent Altino, got its own *Pala d'oro* in the X century.

Behind the altar, the ancient presbytery was visible, the only with six steps in Italy, has the form of a semicircle.

The presbytery's basin is all decorated with a mosaic of the XII century, depicting the 12 apostles with their respective acronyms and letters expressing their names. The Virgin Mary with Jesus in her arms, and over the cathedral the image of S. Eliodoro dressed in pontifical robes.¹

Under the chorus, the crypt, also known as the *Confessione sotterranea*, where the relics were guarded, and both the lateral chapels had entries and to the major nave. The steps are made from Greek marble¹, in fan shape, it is also furnished with an altar made of three marble slabs. Pilasters were found in archaeological works and identified to be originally topped by colonettes.⁶

After the construction of the new altars around the church the relics were moved to avoid the damage from the marine water that flooded the crypt with the high tides, due to the natural lowering of the building.^{1,2}

The crypt has a ring structure that enabled the processional circulation from north to south and vice versa across the lateral apses. It has been proposed that the wall masonry belongs to the bishop Orseolo phase (1800 reconstruction) due to its connection to the apse system, even if previous studies have distinguished and differentiated the dating of the wall structures due to the revival of the fresco decoration of the apse preceding that mosaic for which various chronological colocations are proposed, another theory arose dating it to the IX century.⁷ Though a doubt persists, why an structure like that would be made in the XI century. Maybe the bishop tried to make a political statement, distancing his patriarchy from the one of Aquileia, underlying the antiquity of the Torcello construction, re building the oriental motifs.⁸

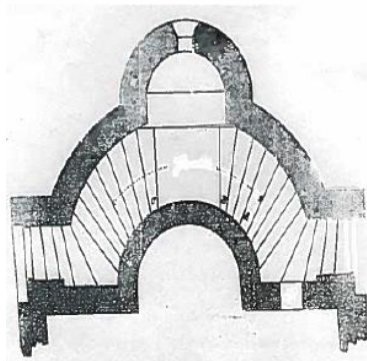


Figure 2 Crypt⁷

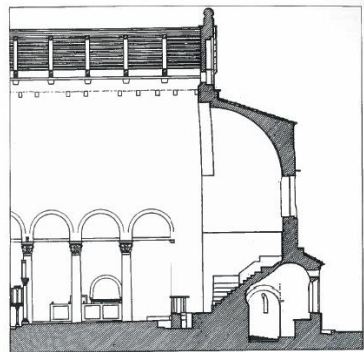


Figure 3 East end and cross section of the presbytery and the crypt⁷

Finally, a mosaic occupies the internal façade of the major nave, it is made up of several allegories to give a complete representation of the *Giudizio finale*, details on the angels and saints, and the cross with two crosspieces show that the Greek way was not abandoned altogether.

In front of the major door of the cathedral, the *Battistero* it is found in the atrium in front of the Basilica.¹



Figure 4 Antique presbytery of the cathedral

3.2 MURAL LOCATION AND ITS CONSERVATION STATE

Archaeological excavations made on Torcello island between February and November 2020, were centred on the Santa Maria Assunta Basilica and its masonry. Within the described works, the crypt of the church was excavated in the period between June 30th and August 6th, 2020.

The works included the consolidation of the masonry with an archaeological assistance that consisted in a survey campaign of the walls where necessary, as well as photographic and photogrammetric survey of the wall, and a surveillance work that encompassed a collaboration with restorers, mosaic professionals, archaeometers and diagnostic experts, operators, and architects.

Overall, 4 areas of the Basilica have been stratigraphically excavated:

1. Area 1100: Extrados of the vault above the mosaic decoration.
2. Area 1200: Confined space placed between the current southern perimeter, the southern minor apse, and the southern internal wall of the diaconicon chapel.
3. Area 1500: Room inside the altar of diaconicon, located in the center of the southern minor apse.
4. Area 1800: Internal compartment of the altar of the annular crypt created by the rectilinear masonry closing the central apse.

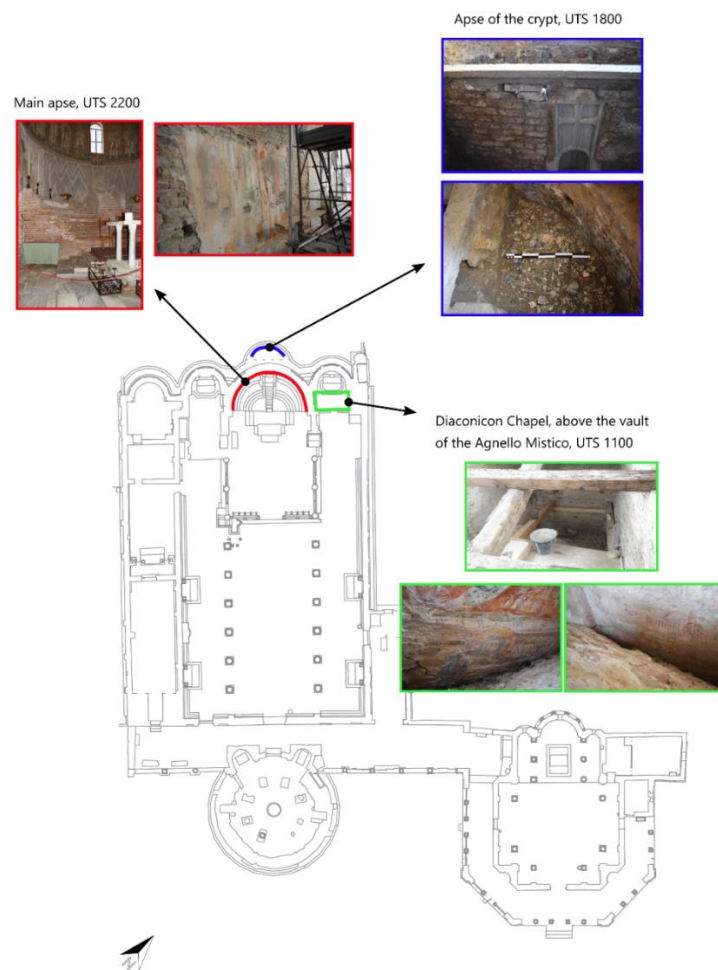


Figure 5 General plan and location of the recovered fragments, Santa Maria Assunta Basilica, Torcello.

In this case, the area of interest is the Area 1800. An inspection due to consolidation needs was made in the annular crypt, a description of the masonry was made but, the intervention was concentrated in the space between the closing walls of the altar set against the sides of the eastern perimeter of the crypt in a space of just over 2 m². The deposits were sieved, in particular US 1814 and 1816, and the evidence was traced to two macro periods, that cover a time span of more than a millennium.



Figure 6 Altar without excavating intervention

The first period (XVII-XX centuries) includes the stratigraphic units relating to the current configuration of the altar of the annular crypt whose construction probably dates back to the XVII century, when the liturgical furnishings of the basilica were modified. The most recent phase (Period I, phase 1) describes the last modifications of the canteen, referable to the massive restoration interventions of the first half of the 20th century, probably made for removal of an offering box attached to the altar.



Figure 7 Stone elements distributed in the inside

The second period (IX-XVII) encompasses the activities related to the original layout of the altar of the annular crypt that affect it in the late medieval and modern age. The works revealed a portion of marble floor slabs and enabled to fully appreciate the morphology of the altar, epigraph, probably from the imperial age, decorated with crosses at the moment of its reuse in the basilica. Currently only the front face is visible since the two sides are hidden by the seventeenth-century wall, while also presenting the raised cross decoration. This detail is not secondary, since it allows to imagine the conformation of the early medieval apse net and the subsequent renovations, with the altar in a central position designed to be visible from three sides.



Figure 8 US 1814. In the background the wall painting can already be seen

A series of findings of considerable importance may help to fully enlighten the picture; the altar fillings, concealed three superimposed layers (UJSS 1820, 1821, 1822) of polychrome painted plaster of which it is still possible to understand the motif, a theory of togate figures preserved only in the lower portion of the bodies. Some clothing elements (tunics, stoles, and shoes) can still be distinguished albeit with difficulty given the state of degradation of the painted surfaces.



Figure 9 Painted plaster US 1820-22

The elements attributable to the background vary from one draft to another but can be traced back to backgrounds of colour or extremely colourful geometric patterns.

Given its actual state, it is difficult to establish the chronology of the wall paintings, though can be roughly placed on a stylistic basis between the XI and XII centuries for the oldest draft. The repetition of subjects in the two most recent plaster levels may indicate chronological proximity, probably due to restoration needs.

Furthermore, the absence of the two oldest plaster layers near on the wall below the window has led to the hypothesis that the surface was not actually frescoed in the first phases described. The altar, perhaps, originally supported a rectangular and oblong table with EW orientation, placed on the stone element US 1806 and embedded in the wall, which would have hidden part of the perimeter from view.⁹



Figure 10 Straightening of the painted wall

3.3 PIGMENTS AND TECHNIQUES

The term *fresco* has been used interchangeably referring to with *mural paintings* and *wall paintings*, but the term has a specific technical meaning, it indicates a pigment technique in which pigments are mixed within water as a suspension and applied on a fresh lime based plaster with a fine aggregate of sand or marble dust, all before the plaster has set¹⁰⁻¹²(painted within about 7h from the application¹³). The pigments are bound to the surface of the wall through the carbonation process,¹⁰ in which the pigment particles are fixed with the newly formed calcium carbonate crystals.¹²

Though, the technique enjoyed brief periods of popularity among ancient Romans and Italians,¹⁰ wall painting precedes the birth of *fresco* by about 20,000 years,¹⁴ painters from all periods and across the world would often use organic binders combined with the *fresco* technique.^{10,14}

Moreover, organic materials, such as, gums, proteins, oils, together or in mixture, employed as binding media in a set plaster (*secco*) vary with the painting technique, époque, and the artists' intention. Its identification is crucial for the characterization of the painting technique, dating and attribution,^{13,14}

Medieval wall paintings also include *mezzo fresco*, is a sort of an intermediate technique, in which pigments are dissolved in lime water or milk of lime and applied into a wet plaster.¹⁵

Binding media allow pigment grains to adhere both to the support surface and each other, the choice of binding media depends on various factors including the pigment used, geography and historical period. The most used in archaeological wall paintings are natural based proteinaceous, lipidic or waxy materials. Egg can be used as a whole or separately. Other common materials are animal glues, milk, casein, oils, waxes and vegetable gums.^{14,15}

The supports for the paintings executed exclusively in *secco* required no special type of plaster ground over the surface of the support, whereas those painted in *fresco* needed one or more calcium hydroxide rich painted layers. However is most common, that paintings executed primarily in *fresco*, have final touches made in *secco*.^{12,16}

In the case of the rock paintings of Altamira and Lascaux, the naturally rich in calcium hydroxide pigments were applied pure on the wall and were impregnated by moisture condensation. The early wall paintings were prepared by using simple procedures. As evidenced by studies carried out on ancient murals in different cultures paintings, plant tempera, using binders of a vegetable

nature to “soften” the pigments of mineral nature. In Ancient Egypt dry paintings were made with organic binders, or based on clay obtained from the Nile or the base of mountain reliefs.¹⁴

On the other hand, although Roman murals painting technique are generally accepted to be *frescoes*, however recent studies have detected the presence of organic binders, opening new perspectives on their wall painting techniques. Moreover, this would explain the presence of not alkali-resistant pigments as its use has been reported by Vitruvius, and whose use on fresh line rendering was warned against by Pliny.^{11,14}

The Middle Ages inherited competences in terms of theoretical and technical treatises yet introduced some technical and stylistic innovations. Regarding medieval craftsmanship and arts, the *Compositiones Variæ* consists of a collection of chemical recipes with instructions on how pigments and dyes should be prepared and used,¹⁵ all but 26 recipes of said document are included into the Latin *The Mappæ clavicula* contains recipes, other sources such as the book *De Diversis Atribus*, the first known treatise written by an artist, Theophilus accounts painting techniques, including colour application and specifically the use of organic binders. Another preserved text that refers to wall painting technique from the VIII century, the manuscript of Lucca, depicts the preparation of mineral pigments and organic colorants. Most medieval wall paintings consist of a combination of *fresco*, *secco* and *mezzo fresco*.¹⁴⁻¹⁶

A pigment can be defined as the component of a paint that contributes colour. This is usually a dry, solid material that can retain its colour when ground to a fine powder. To produce a paint, the pigment must be mixed a binder or “medium”. Traditional, non-synthetic pigments are extracted from plants, animals and mineral encountered in the geological environment. Pigments can be synthesised by a range of chemical and physical processes, dated up to the later Pleistocene, when yellow ochre was heated to produce red ochre. The vast majority of inorganic pigments are either naturally occurring minerals or synthetic, chemically and structurally analogous to occurring mineral.¹⁷

Archaeological evidence in Delos, Pompeii and elsewhere suggests that pigments were mixed prior to painting, possibly to allow the painter to have a wide arrange of colours required for painting. Among those discoveries, are the admixture of red and white to form pink, blue and green, and blue and red to form purple, black and white to form optical blue, and black and white to form grey.¹²

Earth pigments are ubiquitous in painting from most archaeological contexts. They can be broadly divided onto iron rich-ochres, wads, umber, green and white earths, coals and other solid hydrocarbons, and vivianite-rich blue earths.¹⁷ The natural inorganic pigments generally appear to have been of local origin with the only exception celadonite, being most probably mined in Cyprus and exported to other sites within the Easter Mediterranean.¹²

Ochres can be defined as earthy, metal oxide or metal hydroxide rich deposits which form in the surface or near surface environment. Natural occurring ones include a mixture of mineral components, such as quartz, carbonates, clays, and/or micas as well as metal sulphides. Generally, the term refers to iron oxide and hydroxide. Red ochres are dominated by hematite and yellow ochres are typically dominated by goethite, though jarosite group mineral-rich yellow ochres are of local importance.¹⁷

Yellow ochres rich in goethite can be heated and are easily converted to red ochre of various shades when exposed to temperatures from 250 to 300 °C. ¹⁷⁻¹⁹ Yellow ochre was one of the

“austere” pigments of Pliny’s palette. Goethite yellow ochres have been found across the Roman Empire in all contexts.^{15,17}

Hematite rich ochres use has been widely reported throughout periods and traditions from across the globe^{17,18} Geological ochres to transform them into ochre pigments is straightforward and involves a *chaîne opératoire* involving removal of larger impurities (including plant roots and other organic contaminants), grinding, sieving and/or levitation before adding to a medium to produce a paint.¹⁷

Green earths or *terre vertes* are grey green to blue green pigments derived primarily from the minerals celadonite and glauconite, differentiable by using Raman spectroscopy. The two minerals have different geological environments, celadonite is produced through the alteration of basaltic rocks, whilst glauconite is derived from marine clays and sandstones. Green earths were and are the most readily available pure green pigments and as such are known globally in painting.^{15,17,19}

White earth pigments include those made from deposits of chalk, kaolinite, diatomite, and gypsum, used as pigments but also as extenders to bulk out pigments and grounds.¹⁷

Calcium carbonate and calcium sulphate whites are universally used both as ground and pigments.

The blue and green mineral pigments are rarer minerals, and some are synthetic analogues of naturally occurring minerals. Considered precious throughout art story. As primary colours they can only be represented by pure, single phases and not mixtures. The copper carbonate hydroxides, malachite and azurite are well-known and relatively common green and blue minerals. In addition to malachite and azurite, several copper salts and related compounds are found within the supergene enrichment products associated with copper mineralisation and with the corrosion of copper and bronze metals. The rock lapis lazuli, which is rich in the dark blue, sulphur-bearing *haüyne* phase lazurite is probably the best known of all mineral pigments.

The extraction of lazurite from lapis lazuli leaving aside other blue minerals such as sodalite as well as carbonates and pyrite is no simple task, and natural sources of ultramarine often contain trace amounts of these minerals as impurities.¹⁷

Egyptian Blue is the most important blue pigment used in North African, European, and Middle Eastern archaeological contexts. It is a calcium copper silicate, analogous to the rare naturally occurring mineral cuprorivaite. Egyptian Blue is easy to synthesise, and the process was described by the Roman author Vitruvius.^{15,17}

Name	Formula
Hematite	Fe ₂ O ₃
Goethite	FeO (OH)
Glauconite	K (Mg, Fe ²⁺) Fe ³⁺ (Si ₄ O ₁₀)(OH) ₂
Celadonite	(K, Na) (Mg, Fe ²⁺ , Fe ³⁺)(Fe ³⁺ , Al)(Si, Al) ₄ O ₁₀ (OH) ₂
Calcite	CaCO ₃
Kaolinite	Al ₂ (Si ₂ O ₅) (OH) ₄
Lazurite	Na ₆ Ca ₂ (Al ₆ Si ₆ O ₂₄) (SO ₄ , S, S ₂ , S ₃ , Cl, OH) ₂
Egyptian Blue	CaCuSi ₄ O ₁₀

Table 1 Mineral pigments and their formulae¹⁷

The range of pigments used for a *fresco* paint, as stated before, was limited to the one that could withstand an alkaline environment, including yellow and red ochres, vine and ivory blacks, green earths and Egyptian blues.¹⁵ Colours generally used in *secco* paintings that do not withstand alkaline environments include few organic pigments and inorganic ones such as, lead and arsenic based pigments as well as ultramarine, prepared from lapis lazuli pigment.¹⁵

It has been highlighted the lack of availability of raw materials in the Middle Ages and difficulty of the purchase for economic reasons, some pigments such as red and blue pigments were imported from Germany (azurite ($2\text{Cu}(\text{CO}_3)_2\text{Cu}(\text{OH})_2$)) or from Afghanistan (lapis lazuli ($\text{Na}_8(\text{Al}_6\text{Si}_6\text{O}_{24})\text{Sn}$)) they were expensive and therefore were reserved for important areas of wall paintings. Indeed, in the iconographic tradition, the use of the blue pigment takes on a symbolic value.²⁰

A wide arrange of techniques has been use to uncover the traditional colours of the medieval period; haematite, goethite, vermilion, red lead, carbon black and calcite.^{15,20,21} Sometimes, analyses have revealed the available budget for the execution of paintings, as the identification of the colour palette and the availability of pigments.^{20,22}

Pigments and binding media are fundamental elements affecting the appearance of the paint layer; its colour depends on the pigment, considering that the binding medium in which the pigment is dispersed is colourless.¹⁴

However, the nature of the binding medium is responsible for the transparency of a pigment owing to its optical properties being determined primarily by its refractive index. When a pigment is mixed with a binding medium, the degree of chemical and physical compatibility of the two phases in the suspension renders each pigment more appropriate in a specific medium. The latter should also have the property of film-forming so that upon drying it can create a stable, coherent film with good adhesive, mechanical and optical properties. Aside from colour, pigments also influence the appearance of a paint layer, since the diffusion or scattering of the light is directly linked to the nature and particle size of the pigment. In general, the finer the pigment particles the greater the diffusion and hence the opacity of the paint layer. In addition, this hiding power of the pigment (or opacity) is influenced by the difference between the refractive index of the pigment and the medium, the tonality of its colour and its concentration in the medium. Based on the hiding power of a paint layer as determined by the properties of the pigment and the binding medium, ancient artists were able to create transparent paint layers and enhance the colour qualities of pigments.¹⁴

The preparatory drawing for painting (between IV and I centuries) followed a standard practice, primarily incised or painted using a dilute colour.¹² In the early Middle Ages, the thickness in preparatory layers was smaller and the plaster was no longer smoothed, after smoothing the surface, lines were imprinted by a snapping cord and drawings were sketched. Compasses were used to trace curved lines.¹⁵

Throughout the Middle Ages, copying existing works was central to artistic production, reflecting the value attributed to tradition within the technical and practical customs of artistic practice. It was carried out using tools intended to facilitate the process, referred as models.¹⁵

3.4 ANALYTICAL TECHNIQUES

Due to the complex nature of Cultural Heritage elements, a single analytical technique is not enough to elucidate the materials present, not only because the environmental impact to the materials, but the chemical reactions that can occur in the boundaries or inner parts of the objects and, a multi analytical approach is critical in such situations.^{20,23}

Among the most adequate techniques to study elements are the ones of portable and non-destructive nature, as they facilitate the study of immobile works preserving the integrity of the artifacts^{20 23}

A short description of the used analytical techniques, non-invasive and micro destructive, is given below.

3.4.1 Hyper Spectral imaging

The large expanse of painted surface that usually characterises a wall painting, and the possibility to scan the whole surface with non-invasive imaging methods and point analysis are highly desirable. These techniques can detect the presence of different types of materials and thus guide sampling, reducing to a minimum and enhancing the effectiveness of the sampling operation itself.¹⁶

Originally developed for remote sensing and aero spatial applications, it has been adapted to the study of cultural heritage.²³⁻²⁶ Imaging hyperspectral methods, allow to map the chemical composition and its spatial distribution with respect to what is visible to the naked eye.¹⁴

The hyper spectral imaging data consists of hundreds of reflectographic images that are acquired in spectrally contiguous narrow bands, covering an extended spectral range, typically from the visible and near infrared regions up to the short wave near infrared (800 to 2500 nm). This data set which is called image-cube includes spectral (indicating the intensity of the reflected radiation at a given wavelength) and spatial information, that locates the pixel of the imaged area on the examined surface. Starting from the image cube, a high-resolution reflectance spectrum can be associated to each pixel of the imaged scene.²⁷ Depending on the spectral resolution, it may be possible to calculate a full spectrum per image pixel from the acquired spectral cube.²⁶ This enables the identification and mapping of the artists materials, including pigments and other pictorial materials. Additionally, a reflectance spectrum is acquired in the visible range that is exploitable for colorimetric analysis. This technique offers the possibility to characterize polychrome surfaces, including pigment identification, hints in the ageing process, to monitor the conservation treatments, and the distribution of materials in the surface.^{26,27}

Hyper spectral imaging systems used in conservation science can vary a lot, but overall, all include: a spectrographic head, an illumination system, and a mechanical structure to mount either the spectrographic head or the artwork. The systems are PC controlled. A spectrographic head includes a spectrograph, an optical module (objective and lens system to project the object image onto the entrance slit plane), and a camera for data acquisition. By varying the technical features, systems can be tailored for different applications.²⁴

One of the most used and effective approach of data processing is the spectral angle mapping (SAM); this method represents the spectra as vectors in the n-dimensional space of wavelengths and clusters them by calculating their angular difference with respect to a set of reference spectra. Basically it compares spectral shapes and it's not affected by spectral intensity scaling, useful for uneven surfaces, and has been successfully applied to map distributions of pigment mixtures not known a priori.²⁴

3.4.2 Fiber Optic Reflectance Spectroscopy (FORS)

Visible reflectance spectroscopy is based on the principle of selective light absorption²⁸, the system acquires a percentage of the reflectance spectra vs. wavelength in a certain range. The electromagnetic radiation in the studied range is projected through optical fibres onto the surface of the object, which responds according to its optical properties. The incident radiation will be transmitted, absorbed, or reflected by the surface of investigation. Reflection can be either diffused or specular. The diffused component is collected by fibre optics and delivered to a spectrum analyser, where is separated into components and analysed to provide the reflected percentage¹⁰

The spectral behaviour of a painted surface to a source emitting the visible wavelength range can give information about its composition.²⁹

The results of this analysis are reflectance spectra in which both reflected and scattered light is recorded; it depends on the refractive index of the pigment and the suspending medium, and on particle size relative to the wavelength of the incident light. Even if in general, the superficial inhomogeneity and compositional complexity of pictorial material can make discrimination difficult, this is a helpful toll for pigments identification.²⁹

A disadvantage is the simultaneous detection of the light reflected and scattered by the sample, and second, the contact between the device and the sample, solved by the use of optical fibres.³⁰

The FORS is also currently applied for the identification of organic binders in particular on wall paintings.^{10,13,14,30}

3.4.3 Fourier Transform Infrared spectroscopy

Infrared spectroscopy has been a primary tool for the identification, monitoring of chemical reactions, determination of chemical changes and degradation, the ascertaining of damage of specific conditions, and evaluation of material stability. In the field of cultural heritage conservation, FTIR has been used as means to characterize constituent materials (organic and inorganic) of paintings, from the support to the outer layers of varnish, determining the components of the paint samples, binders, as well as to examine archaeological objects, to determine corrosion products, and to characterize the effects of storage materials and cleaning products in museum collections³¹⁻³⁶

The FTIR spectroscopy is a simple and fast method to obtain information about the organic components (by identifying the class of materials present) and the inorganic materials, through the interpretation of the characteristic vibrational modes of the functional groups when they interact with MIR light.^{14,37}

Light and matter can interact, the interactions are characterized by the energy of the radiation and its effect on materials. Infrared radiation supplies enough energy to produce translational, rotation, and vibrational motion in molecules. The measurement of the characteristic IR energies that correspond to these transition results in a spectrum, unique for each molecule or material based on its atomic structure. The specific number and position of absorption bands for any molecule are governed by its degrees of freedom, its functional groups, and the IR selection rules.

The absorption bands in a spectrum exhibit three important parameter: frequency, shape, and intensity. Frequencies indicate the presence of certain functional groups in a material. The shapes provide information concerning the group functionality as well as material purity.

Symmetrical in nature, deviations indicate the presence of an overlapping band, or the molecule has been modified, the width can be increased by inter or intra molecular interactions. The intensity provides information on the amount of specific functional groups present.

Additionally, since functional groups (combinations of atoms) produce absorptions at or near the same frequency, regardless of the rest of the molecule, the presence or absence of certain functional groups can be determined by interpretation of the IR spectrum.

An IR spectrum displays detector response as percent transmittance (%T) or absorbance (A) on the y-axis, and IR frequency in terms of wavenumber (cm^{-1}) on the x-axis. The detector response indicates the extent of interaction of the IR electromagnetic radiation with the sample as it is proportional to the resultant intensity of IR radiation that reaches the detector after passing through the sample.

Generally, for IR analysis, a homogeneous sample can be ground or filed to form fine particles, then analysed by either KBr pellet or micro pellet.

Samples from works of art, however, may be complex mixtures of components that are difficult to completely identify by IR spectroscopy alone. However, IR spectral analysis can characterize the material class(es) present within the sample and thus supply a basis for the selection of an additional analysis method for further separation of sample components and their identification.

In paints, pigments are dispersed in an organic binder. This usually does not hinder the determination of the pigment, but it may make it difficult to determine the binder if it is present in low concentrations.³¹

However, IR spectroscopy becomes less useful when investigating objects that vary in shape, size, and fragility, and thus are difficult to sample,³⁶ other problems of different nature can arise, inorganic components such as oxides or sulphides, which are inactive in the mid infrared region.³⁸ Efficacy of the techniques also rely on the availability of spectral reference libraries and reference materials.³⁶ IR spectroscopy is also demanding and time consuming with regard to sample preparation. Samples must be embedded in a suitable substance, typically KBr, that is transparent in the infrared region, microtomed under certain conditions, and only after a delicate sample preparation procedure.³⁹

3.4.4 Raman spectroscopy

Raman spectroscopy is also widely used for the analysis of Cultural Heritage objects.^{32,40} It has been used on inorganic material and organic materials, including pigment/binder mixtures.^{14,19,23,32}

The possibility to study many different kind of materials from crystalline to amorphous, organic and inorganic, even when largely heterogeneous, thanks to its micrometric space resolution, made Raman an unique tool for the study of archaeological materials.¹⁹ Raman spectroscopy can very often help to answer questions that aim to characterize materials, that can spread light on its provenance. Intervention in this field may concern the identification of significant minerals in the pottery or porcelain body, in the glaze or at their interface or in the composition of the glazes, glass or enamels.⁴¹

The inelastic light scattering that results from the interaction of a monochromatic, coherent beam of light produced by a LASER (light amplification by stimulated emission of radiation) with

(liquid, solid or gas) matter is called Raman scattering, from the name of Sir Chandrashekhara Venkata Râman who obtained The Nobel Prize for that in 1930.⁴¹

When a LASER beam is casted upon a sample and interacts with it, originates scattered light that has a different frequency to the one casted upon it, giving birth to Raman scattering, the effect is achieved when a photon is absorbed, excites the molecule and the posterior de-excitation leads to transitions between vibrational levels. The Raman spectra can be predicted from analysis of the functional groups present and the normal bonds. .⁴¹

In the field of Cultural Heritage, Raman mapping can also be made of flat samples, there also mobile setups available since 2000.

A Raman spectrum displays a peak fingerprint symmetric with respect to the elastic scattering (Rayleigh) signal, located at the same wavenumber/energy as the laser. The intensity of the anti-Stokes peaks decreases very rapidly as the distance from the Rayleigh peak increases, because the population of the upper vibrational level decreases to zero. Usually, only Stokes side is considered, and the cm^{-1} scale is measured with respect to the excitation energy.

The disadvantages of the technique involve the physics of the light-matter interaction, as the Raman intensity observed depends on the type of bonds present in the material, whereas it is almost null for ionic bonded compound, in the covalent bonded ones, the intensity increases with higher number of electrons involved in the bond. The spectra depend on the kind of laser used and is limited to modes involving the chromophore, which restricts the databases. Another problem that may arise is fluorescence, a slow phenomenon (10^{-3} s) that appears when transitions between electronic levels lead to its emission, it is strong and broad and can mask the spectrum.⁴¹

There are three types of instruments available: bench top, usually exited with two lasers, sometimes more; the mobile Raman setups, connected by optic fibres to a remote head, and handheld instruments.

The accurate use of portable Raman spectrometers allow the non-destructive approach towards the work of art.²⁰

The choice of portable Raman relies on a compromise between the available features of the instruments, such as tunability of the laser power, speed of analysis, analysed of spot size, spectral range, even the total weight of the setup and ease of positioning, and the needs of the project at hand, for example, organic substances can be now analysed in situ.⁴² But sometimes polymers and organic compounds, especially those processed with solvents or natural organic/inorganic mixtures like ivory, exhibit strong fluorescence: in that case IR laser excitation (785 or 1064 nm) can limit or avoid fluorescence generation and a good Raman spectrum can be recorded.⁴¹ Most portable instruments use the 785 nm line of a laser diode as excitation, which is considered one of the best compromises between efficiency and low fluorescence.¹⁹

One of the most widespread applications concerns pigments of different sorts, ages, dispersion mediums and decorating various materials. Notwithstanding, it must be taken in consideration that databases are often not sufficient for identification, due, to for example, to pigment degradation caused by the uprising of reactions in mixtures or by the high incident laser power and/or energy, though degradation can be simulated to verify spectral changes.⁴¹

The collected spectra can represent a challenge in identification because certain source laser wavelengths may be absorbed by specific pigments, leading to large fluorescence backgrounds

which obscure weak Raman signals. To identify a Raman spectrum a “finger printing approach is often used, its imperious to analyse by the most intense peak to the less intense to confirm identification.²¹

3.4.5 Pyrolysis coupled to Gas chromatography and Mass spectrometry (Py-GCMS).

Py-GCMS is a micro-destructive technique that through the decomposition of a material at high temperature and in the absence of oxygen to break the molecular bonds in a large molecule and to form pyrolysis products. The idea behind this is to reduce the complexity of the original molecule and study some of its features by looking at simpler and smaller pyrolysis products.^{43,44} Rendering the technique ideal for organic material characterised by a macromolecular nature: such as natural polymers (proteins or plant gums) or those that undergo oligomerisation or cross-linking as a reaction to exposure to light and air.⁴⁵

Temperatures used usually range between 400 °C and 800 °C to avoid combustion the entire process occurs in the absence of oxygen,⁴³ this range will fragment macromolecules such as polymers, ranges used between 100 °C and 400 °C correspond more to thermal desorption and allow the detection of low molecular weight components and are normally used in double and multiple shot analysis.⁴⁶⁻⁴⁹

There are two main types of pyrolyzer used in analytical work, filament; equipped with a metal coil at the end of the probe that is introduced into a pyrolysis chamber and electrically heated, furnace or micro-furnace, have a pre-heated pyrolysis chamber, the sample is loaded at the top of the chamber and then dropped inside by a releasing mechanism. The pyrolyzers can be directly coupled with a detector but, gas chromatographic separation is often interposed between the pyrolyzer and the mass spectrometer (Py-GC-MS), where all pyrolysis products are separated in the gas chromatography column and therefore can be identified one by one.^{43,50}

This is the most straightforward configuration for the pyrolysis system. In fact, coupling the diagnostic power of mass spectrometry with the separation capability of the gas chromatographic system enhances the potential of pyrolytic methods. Although the chemical structures of the molecules originally present in the sample are not always straightforwardly related to the final pyrolysis products, pyrolysis is a valid fingerprinting technique.⁴⁵

The main advantage of this technique over other chromatographic techniques is that no sample preparation is required, and the sample can be analysed in solid state, reducing the analysis costs and time.⁴³

The disadvantages relate to the low volatility of pyrolysis products arising from natural and some synthetic macromolecules. In fact, the polar acidic, alcoholic and aminic moieties are not really suitable for gas chromatographic analysis. This can cause that the pyrolysis products may not be completely eluted by the gas chromatographic column, and may be retained in cold areas of the pyrolyzer and the transfer line system.⁴⁵

To overcome the problems related to the formation of polar pyrolysis products, unspecific compounds, and to match the requirement of the pyrolysis products to be sufficiently volatile to undergo gas chromatography, derivatization agents are used directly *in situ* with the solid sample.^{43,45}

The most commonly used agents are tetramethylammonium hydroxide (TMAH), for methylation, and hexamethyl disilazane (HMDS) for silylation. Their function is to substitute

polar OH groups thereby reducing the polarity of the pyrolysis products and enhancing their volatility.^{43-45,51}

Another limitation is that this is not a quantitative technique, while materials can be identified, it is difficult to assess how much is present in each mixture. This is because each material has its own pyrolysis yield, an intrinsic property that is difficult to predict due to the presence of many materials and inorganic compounds, and one material can generate many pyrolysis products, though it can be used in a semi quantitative way.⁴³

In the field of cultural heritage, the technique's main use is the identification of organic materials in composite samples⁴³, for example; paint samples⁵², specially binding media^{44,53} (oils, proteins and gums) and coating materials (resins and waxes), lacquers characterization⁵⁰, modern materials; synthetic formulations⁵⁴, fibers⁵⁵, lignocellulosic materials and degradation material⁵⁶.

4 EXPERIMENTAL

For the experimental analysis, a systematic approach was taken considering the characteristics of each technique and the information that could be obtained of them, starting with the non-destructive techniques and concluding with micro destructive ones.

The first step towards the identification of the pigments and painting techniques was the cataloguing of the fragments and, it encompassed the use of an imaging technique, as is the photography, along with the description of the fragments.

The second step involved a first selection of fragments considering the representative characteristics among the grouped catalogued samples, that was subjected to another imaging technique, hyperspectral imaging. Considering the results obtained and the characteristics of the equipment, another selection of fragments was made to be analysed by other non-destructive technique, FORS, whose results were complementary to the ones obtained from the hyperspectral imaging.

Subsequent analysis were the micro destructive ones (Raman, FTIR and Py-GCMS), as they involved the scraping of the selected fragments, and in the case of FTIR and Py-GCMS a subsequent treatment of the samples.

4.1 ARCHAEOLOGICAL CATALOGUING

3226 fragments recovered from the inside of the altar of the basilica's crypt were cleaned, photographed, measured, and labelled. The complete identification entailed giving each fragment an ID that consisted in stating the archaeological stratigraphic unit (SU) in which the fragments were found along with a number assigned. A significant remark is the fact that some fragments were double, or triple layered, and a consecutive numeration was made for each layer and catalogued as a single fragment while making notes of the particularity of the fragment. A group class was assigned according to their predominant painted colour and noting plaster colour, this was done according to the Munsell colour system and using the Munsell soil colour chart. The obtained catalogue is depicted in Annex 1 and, an example of the photograph made is depicted in Figure 11.



Figure 11 Catalogued fragment, TORSMA 001.

32 groups were obtained from the grouping by colour and are depicted in Table 2.

Group class	Munsell code	Number of fragments	Group class	Munsell code	Number of fragments	Group class	Munsell code	Number of fragments
1/a	5G 2.5/2	149	11/a	2.5YR 4/1	176	21/a	N 7/	73
2/a	5PB 2.5/1	406	12/a	10B 2.5/1	14	22/a	10YR 4/1	2
3/a	N 3/	633	13/a	10B 4/1	311	23/a	10YR 9.5/1	59
4/a	7.5YR 5/6	160	14/a	5GY 3/2	103	24/a	7.5YR 6/4	9
5/a	10YR 6/8	107	15/a	10YR 2/1	14	25/a	10B 6/1	2
6/a	10R 4/6	260	16/a	7.5YR 4/6	21	26/a	5YR 4/2	101
7/a	2.5YR 3/6	132	17/a	10R 3/2	2	27/a	2.5YR 5/8	4
8/a	5G 6/1	135	18/a	5G 8/1	32	28/a	2.5Y 2.5/1	15
9/a	2.5YR 6/4	92	19/a	5G 4/2	8	29/a	10Y 6/2	21
10/a	5R 2.5/1	136	20/a	10YR 7/8	86	30/a	7.5YR 6/6	21
31/a	10GY 3/1	20	32/a	5GY 4/2	17			

Table 2 Group classes, Munsell system colour code and the number of fragments of each class

The archaeological cataloguing in the form of identifying the Munsell colour of the fragments gave origin to 32 groups, as mentioned before. The Munsell code assigned first pointed to a preliminary identification of the minerals present in the pictorial layer.

The Munsell system allowed a direct comparison of the pigment to the soil colour as it can be used as a clue to the mineral content of soil. Relatively large crystals of goethite give the ubiquitous yellow pigment of aerobic soils. Smaller goethite crystals produce shades of brown. Hematite (Greek for blood-like) adds rich red tints. Large hematite crystals give a purplish-red colour to geologic sediments that, in a soil, may be inherited from the geologic parent material.⁵⁷

A correlation between the assigned codes with the Munsell colours⁵⁷ Table 3 and the assigned Munsell to studied pieces was made. The assigned Munsell colour to groups 4 and 20 coincided with the ones reported of goethite. In the case of group 5/a, a goethite identification by colour was possible as the hue of the mineral of size between 1-2 μm , although the value and chroma are different. Group 6/a assigned colour code, was the same of the reported for hematite of grain size around 0.1 μm , in the case of group 7/a, the colour code is shared with ferrihydrite mineral, it is not used as a pigment though. But the fact that it is composed of hydrated iron,

indicates the presence of a pigment rich in iron, same as group 11/a in the case of lepidocrocite. Group 3/a colour code was coincident with iron sulphide.

Mineral	Formula	Size (µm)	Munsell	Colour	Group
goethite	FeOOH	1-2	10YR 8/6	yellow	20/a
goethite	FeOOH	~0.2	7.5YR 5/6	strong brown	4/a
hematite	Fe ₂ O ₃	~0.4	5R 3/6	red	
hematite	Fe ₂ O ₃	~0.1	10R 4/8	red	6/a
lepidocrocite	FeOOH	~0.5	5YR 6/8	reddish-yellow	
lepidocrocite	FeOOH	~0.1	2.5YR 4/6	red	11/a
ferrihydrite	Fe (OH) ₃		2.5YR 3/6	dark red	7/a
glaucosite	K(Si _x Al _{4-x}) (Al, Fe, Mg) O ₁₀ (OH) ₂		5Y 5/1	dark grey	
iron sulphide	FeS		10YR 2/1	black	3/a
pyrite	FeS ₂		10YR 2/1	black (metallic)	
jarosite	K Fe ₃ (OH) ₆ (SO ₄) ₂		5Y 6/4	pale yellow	
todorokite	MnO ₄		10YR 2/1	black	
humus			10YR 2/1	black	
calcite	CaCO ₃		10YR 8/2	white	
dolomite	CaMg (CO ₃) ₂		10YR 8/2	white	
gypsum	CaSO ₄ ·2H ₂ O		10YR 8/3	very pale brown	
quartz	SiO ₂		10YR 6/1	light grey	

Table 3 Reported properties of minerals reported versus the assigned groups

To complete and simplify the analysis, representative fragments of each group class were selected and then a partial regrouping simplifying the colour by hues was made, and group classes were analysed grouped as depicted in Table.

Colour	Group class
Green	1/a, 8/a, 14/a, 18/a, 19/a, 31/a, 32/a
Blue	2/a, 13/a, 25/a
Black	3/a, 28/a
Yellow	4/a, 5/a, 16/a, 20/a, 30/a
Red	6/a, 7/a, 12/a, 27/a
Brown	9/a, 10/a, 11/a, 16/a, 17/a, 21/a, 26/a, 29/a
Grey	15/a, 21/a, 22/a
White	23/a
Skin	24/a

Table 4 Regrouped group classes

To reduce the number of groups and to simplify further analysis, groups of 10 to 15 fragments, were separated from each class group to reduce the number elements to be studied. The

election criteria were the colour saturation of the painted layer and size of the fragment. The fragments ID as well as their characteristics and the analysis made to each one is depicted in Annex 1.

As part of the visual examination, previous to the use of any analytical techniques, an additional step was made considering only the two- and three-layered pieces, and their recorded visual characteristics such as the distinction between layers in the double three-layered ones, and their plaster colour in the double and three layered. This was made as an attempt to locate the groups made in the layers and associate the results obtained to each layer.

A heat map was prepared to locate the proportion of pieces belonging to each group per pictorial layer. The map is presented in Figure 12, and it presents the proportion of pieces used in each group per pictorial layer, this could be an important aid to establish the pigments and if possible, the painting technique used in each layer, along with the colour scheme used.

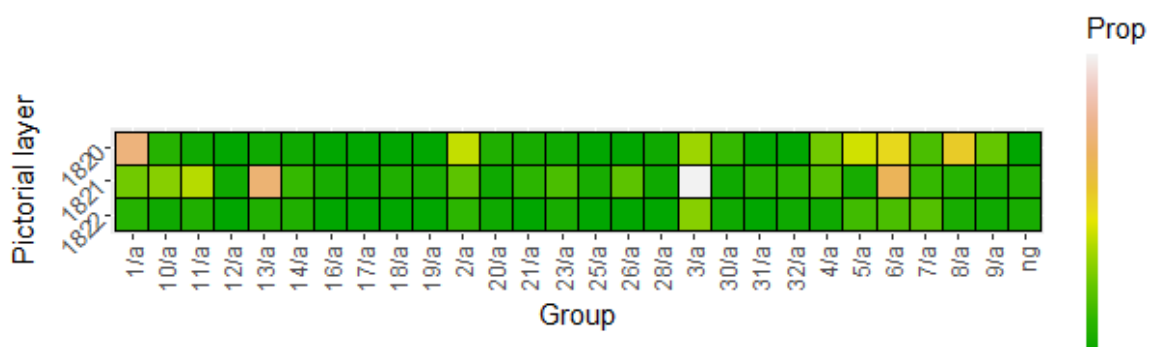


Figure 12 Heat map of groups per pictorial layer

It is evident that there was a change of colour scheme and palette across time, at least in the background colours as there is evidence that the colours that have a bigger proportion by layer is not consistent over time.

While the oldest pictorial layer (1822) does not show a high proportion of any of the colours, the heat map gave information regarding the intervention it might have suffered. Regarding the prevalent colours, group 6/a (red) was preserved and is even more present in the subsequent layer, though its use decreased a little in the most recent one, meaning that the use of hematite increased over time.

Group 5/a (ochre colour) was vastly used in layer 1822, then decreased in 1821 and finally its use increased dramatically in 1820. The pigment that corresponds to this colour is goethite

Group 7/a (red) is a slightly dark shade of red that is rather prevalent in layer 1822, though its use was continued over time, it was never used as a predominant colour in subsequent layers, probably reserving its use mainly to smaller areas.

Group 3/(blue-black) a is an interesting case. In proportion, the colour was used marginally in layer 1822 but in the subsequent layer its use increased dramatically only to diminish again in 1820. An explanation could be the purpose of the colour, a dark colour such as this could be used to outline the figures present in layer 1822, whereas in layer 1821 it could have been used as a background. Signalling a change in colour scheme between the first and the second layer

Group 11/a (dark reddish brown) is primarily present in the middle layer, as this is a dark shade of colour, and considering a very dark background, it may correspond to some piece of clothing that dressed one of the figures, rather than corresponding to the background.

Group 13/a (blue grey) is a group that contains a shade of blue that is only present in large quantities in the middle layer, probably part of the rigged geometric pattern of the background, along with group 6/a (red).

Group 10/a (reddish black) is a group only present in the middle layer, though probably relegated to a place detailing over the background or tunics. Group 26/a (dark reddish grey) appears in similar proportion to colours such as previous one, suggesting a similar treatment.

Finally, the most recent layer exhibits yet again a change in colour scheme where group 1/a (green) and group 8/a (greenish grey) both green shades, they may be used to replace the blue scheme for a green one but preserving the colour accents made with red and yellow tones.

4.2 HYPERSPECTRAL IMAGING

The hyperspectral images of each group were taken using the full hyper spectral camera Specim IQ. In total 344 pieces were analysed, though the pieces were arranged to photograph each group separately.

The camera works within the 400 nm - 1000 nm range (VIS-NIR, sensor 512X512px, 204 spectral bands, with spectral resolution FWHM 3 nm). The images obtained were processed by using Specim IQ Studio computer software.

The Specim IQ camera integrates into a single compact and portable device that houses a hyperspectral sensor, colour camera and data storage. The camera allows the visualization of the scene and adjustment of focus.²⁸

An identification model was built for each group class taking a saturated point in one sample and obtaining a fake colour image that indicates the points in which the reflectance spectrum of the point previously chosen coincides with the image according to the selected similarity threshold, over 0.9893. This operation was repeated on various times with the same photograph selecting different points to ensure that the fragments were correctly assigned to each class group.



Figure 13 Specim IQ arrangement (left) and software (right).

4.3 FIBER OPTIC REFLECTANCE SPECTRA (FORS)

The Fiber-Optic Reflectance Spectra analysis were performed using the ASD FieldSpec 4 Standard-Res Spectroradiometer, with a contact plant probe. The instrument records reflectance wavelength range between 350 nm to 2500 nm and spectral resolution of 3nm at

700nm and 10 nm at 1400/2100 nm. Three detectors, a VNIR (350-1000nm) detector of 512 element NIR-enhanced silicon array, SWIR 1 (1000-1800 nm) detector of Graded Index InGaAs Photodiode, 2 Stage TE Cooled and a SWIR 2 (1800-2500 nm) detector of Graded Index InGaAs Photodiode, 2 Stage TE Cooled. At least three spectra were acquired each time. A total of 89 fragments were analysed, and their characteristics are depicted in Annex 1.

4.4 RAMAN SPECTROSCOPY

The Raman spectrometer used is a Bruker BRAVO handheld Raman spectrometer, equipped with fluorescence mitigation s SSE™ (Sequentially Shifted Excitation) and Duo LASER™ excitation.

14 fragments were analysed by using the portable characteristic of the equipment, and in some cases, the equipment allowed the sampling of various zones of single fragments. 18 fragments were analysed by using the powdered pigment sampled from the pictorial layer of each. The fragments studied are depicted in Table 5.

The sampling was made to overcome the characteristics of the fragments, the use of two or more shades of the colour in the same fragments, as in fragments 1687, 2464 and 2659 and in other cases the deteriorated surfaces that prevented the analysis of the paint due to wide faded surfaces.

Fragment ID	Direct contact	Scrapped sample
TORSMA2020_0665	x	
TORSMA2020_1384		x
TORSMA2020_1423	x	x
TORSMA2020_1500		x
TORSMA2020_1671		x
TORSMA2020_1681	x	
TORSMA2020_1687	x	
2 colours analysed		
TORSMA2020_1808		x
TORSMA2020_1849	x	
TORSMA2020_1866		x
TORSMA2020_2053		x
TORSMA2020_2131	x	x
TORSMA2020_2133		x
TORSMA2020_2232	x	x
TORSMA2020_2317	x	x
2 colours analysed		
TORSMA2020_2464	x	x
2 colours analysed		
TORSMA2020_2516		x
TORSMA2020_2659	x	x
3 colours analysed		
TORSMA2020_2664		x
TORSMA2020_2676	x	x
TORSMA2020_2795		x
TORSMA2020_2796	x	
TORSMA2020_2814	x	
TORSMA2020_2832		x
TORSMA2020_2886	x	

Table 5 Fragments analysed by Raman spectroscopy with the type of analysis made

4.5 FOURIER TRANSFORM INFRARED (FT-IR)

18 fragments were examined by a double beam Thermo Nicolet Nexus 670 FT-IR spectrometer, associated to Omnic E.S.P. 10 software to elaborate IR spectra, recorded within a 4000-400 cm^{-1} range with a resolution of 4cm^{-1} , accumulating 20 scans. The samples were taken mechanically scraping the pictorial layer from the fragments, and then KBR pellets were made for its examination in transmittance. The fragments analysed are depicted in Table 6.

Fragment Id	Group
TORSMA2020_1384	13/a
TORSMA2020_1423	2/a
TORSMA2020_1500	13/a
TORSMA2020_1672	8/a
TORSMA2020_1686	13/a
TORSMA2020_1808	5/a
TORSMA2020_1866	9/a
TORSMA2020_2053	14/a
TORSMA2020_2131	13/a
TORSMA2020_2232	6/a
TORSMA2020_2317	9/a
TORSMA2020_2464	10/a
TORSMA2020_2516	2/a
TORSMA2020_2659	1/a
TORSMA2020_2676	4/a
TORSMA2020_2795	4/a
TORSMA2020_2814	11/a
TORSMA2020_2832	8/a

Table 6 Fragments analysed by IRTF

4.6 PYROLYSIS COUPLED TO GAS CHROMATOGRAPHY AND MASS SPECTROSCOPY (PY-GCMS)

In order to unequivocally determine the presence of organic materials a Py-GCMS chromatographic system was used to analyse the fragments.

The instrumentation consists of a Frontier Pyrolizer EGA/Py-3030D (Frontier Lab) coupled to a gas chromatograph 8890 Agilent Technologies (USA) equipped with an Agilent UA5-30M-0.25F capillary column (stationary phase 5% diphenyl-95%dimethyl-polysiloxane, (30 m x 250 μm x 0.25 μm) and with a deactivated silica pre-column (1.3 m x 100 μm , Agilent Restrictor MSD). The GC was coupled with an Agilent 5977B Mass Spectrometer.

Chromatographic conditions: initial temperature 50 $^{\circ}\text{C}$, 10 min isothermal; 20 $^{\circ}\text{C}/\text{min}$ up to 260 $^{\circ}\text{C}$, 10 min isothermal; 20 $^{\circ}\text{C}/\text{min}$ up to 290 $^{\circ}\text{C}$, 5 min isothermal; 20 $^{\circ}\text{C}/\text{min}$ up to 320 $^{\circ}\text{C}$, 10 min isothermal. Analyses were performed under a helium constant flow (3 mL /min) with a split ratio 1:60.

The mass spectrometer was operated in EI positive mode (70 eV, scanning m/z 50–650)., Ion source 280 $^{\circ}\text{C}$

Analysis on the whole sample were conducted by placing around 1 mg of powder into the metallic cup. Derivatization was performed by adding a solution of HMDS 99% and TMCS 1%. These samples were analysed with the described chromatographic method.

Additionally, extractions were conducted on samples (1-2 mg) were placed into clean vials, 40 μL of a $\text{CH}_3\text{Cl}/\text{CH}_3\text{OH}$ 2:1 v/v solution was added along with 40 μL mL water, the obtained solution was subjected to 20 min of ultrasound bath, after separating the organic phase, a second extraction was made repeating the procedure without the water, the obtained extraction was dried in a N_2 flux, then derivatized with HMDS 99% and TMCS 1% and subjected to the Py-GCMS analysis arrangement described above. These samples were analysed using the same chromatographic method.

The selected samples came from fragments 2832, 1866, 2795, 2464 (light and dark), 2516, 2676, and 2131.

5 RESULTS

5.1 HYPERSPECTRAL IMAGING

Each group was studied by selecting points that could explain as much of the fragments' surface as possible, in some cases 2 points were needed to completely explain the colours, mainly due to surface weathering and in consequence flatter reflectance spectra with little information.

Groups 4/a, 5/a, and 20/a that exhibit different shades of red colour, reflectance spectra (Figure 14) share maxima at 450 nm and 750 nm and, minima at 500 nm additional to an inflection at 548 nm, although the groups differ in their reflectance factors, it is consistent with the different shades of ochre colour.

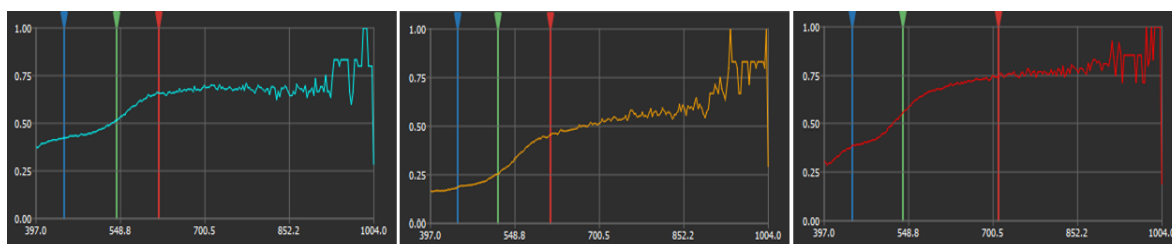


Figure 14 Group 4/a, 5/a, and 20/a respectively.

The orange colour found in group 12/a slightly different spectrum from ochre groups, the minima is found at 480 nm, but the inflection at 548 nm is the same of the ochre groups (Figure 15).

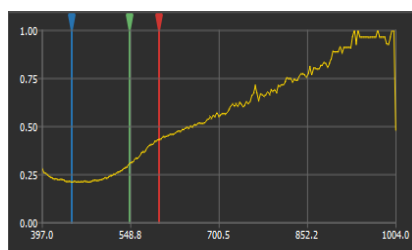


Figure 15 Group 12/a.

Brown hues of more pink tones (9/a,17/a), as well as the skin colour (group 24/a) of white background, share the maxima and minima values with the orange group (Figure 16), although a lower reflectance factor is observed.



Figure 16 Groups 9/a, 17/a, and 24/a

Group 16/a shares a similar spectrum with the previous groups, although a lower reflectance factor is found in comparison with groups with a yellow/ochre tone, but higher than brown and pink tones. Figure 17.

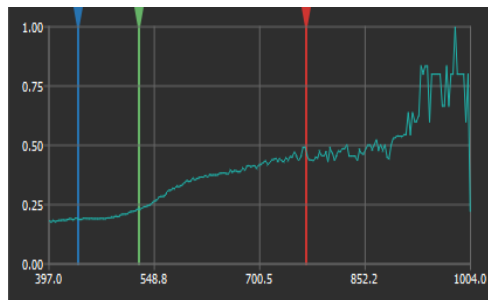


Figure 17 Group 16/a

Red groups, 6/a, 7/a, and 27/a share overall similarities, minima at 450 nm, and 850 nm, an inflection at 580 nm, and maxima at 700 nm (Figure 18). The 7/a, and 27/a groups show similar reflectance factors, consistent with the similar shade of colour of the fragments, as the one of groups 6/a show a lighter tone.

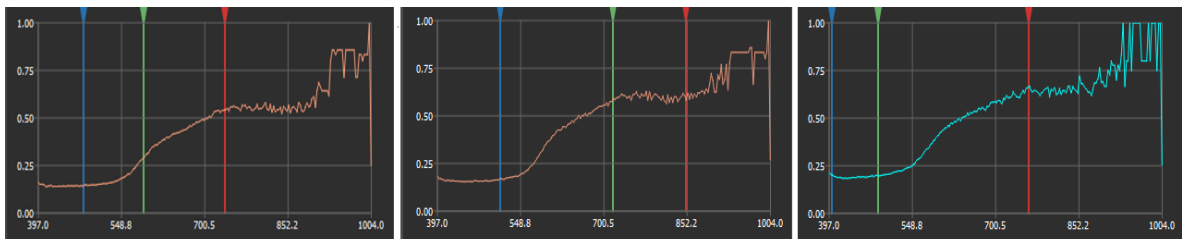


Figure 18 Groups 6/a, 7/a, and 27/a

Some other groups, such as the ones pertaining to darker shades of brown 10/a, 11/a, and 29/a, share almost flat spectra (Figure 19), but perceptible minima at 450 nm, inflections at 550 nm and maxima at 700 nm. The same relevant points are present in group 24/a, particularly in those pieces with green background, the difference is observed in the reflectance factor, as it is significantly higher in those pieces.

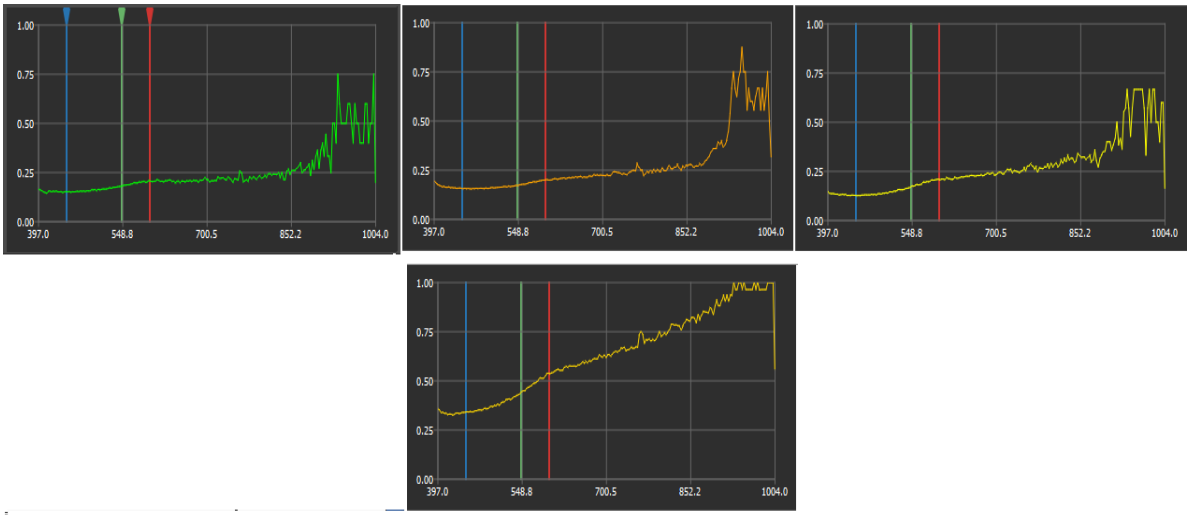


Figure 19 Groups 10/a, 11/a, and 29/a, 24/a below.

Groups 1/a, 8/a, and 19/a, all with some green hue colour, share the same spectra that show a maximum at 550 nm and, even though group 1/a has a darker tone, the reflectance factor is very similar. Figure 20.

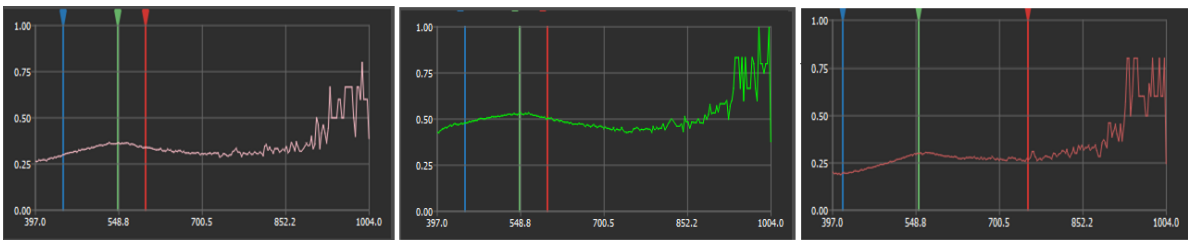


Figure 20 Groups 1/a, 8/a, 19/a

Groups 14/a, and 18/a, also of green hue colours, have reflectance spectra where an inflection at 510 nm and a maximum at 610 nm are visible (Figure 21), although group 18/a spectrum has a higher reflectance factor, both have the same relevant points.

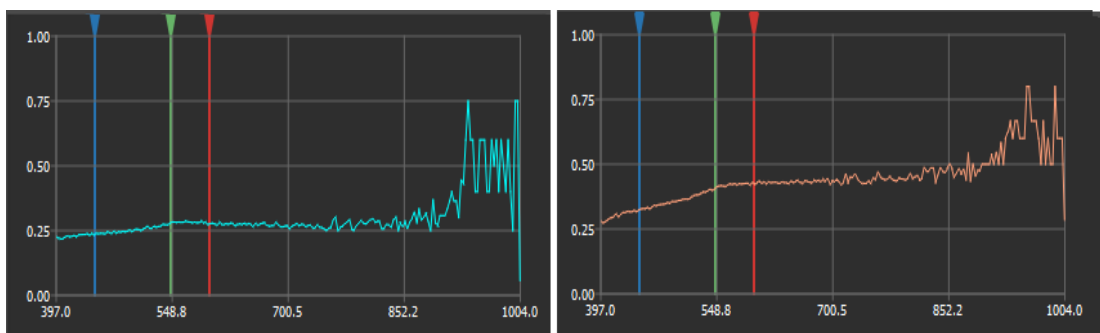


Figure 21 Groups 14/a, and 18/a

Regarding the blue hue colour groups, slightly different spectra were recorded, group 2/a spectrum has maxima at 460 and 770 nm and, minima at 610 nm and 870, these values are shared with the blue accents that appear in group 21/a. The difference relies in a maximum at 397 nm and a minimum at 400 nm found in the first group, that are not present in the accents of the other group (Figure 22).

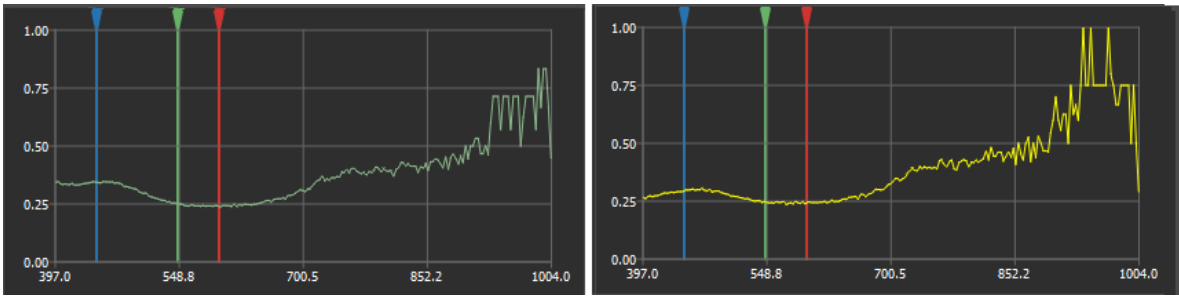


Figure 22 Groups 2/a, and 21/a.

On the other hand, group 13/a pieces, whose grey tone approaches to the light blue tone of the other blue fragments. The reflectance spectrum (Figure 23) is flat with no clear similarities to other blue spectra.



Figure 23 Group 13/a.

The spectra groups exhibited by groups of grey hue (15/a, 21/a, and 22/a) only show a diagonal line with low slope across the complete range (Figure 24).

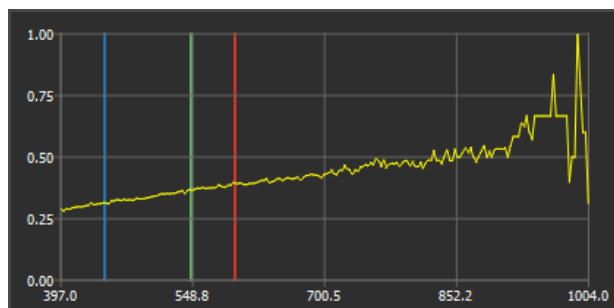


Figure 24 Group 21/a

Group 23/a is composed by pieces mainly white coloured with maxima at 405 nm and, 700 nm and, a minimum at 420 nm (Figure 25).

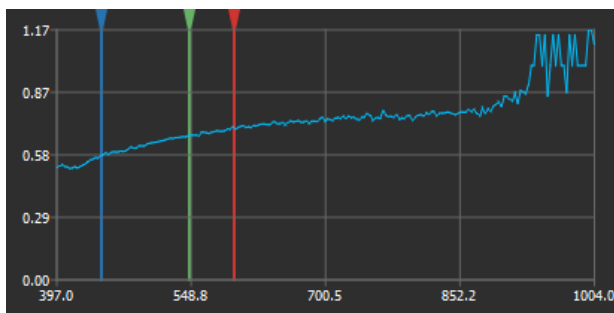


Figure 25 Group 23/a.

5.2 FIBER OPTIC REFLECTANCE SPECTRA (FORS)

To enlarge the information obtained from the reflectance spectra, FORS analysis were performed and larger range of information that could help to not only corroborate the groups made, but also give information about the pigments and binders if used.

According to the preliminary data that the hyperspectral images gave, the data was regrouped, the ochre, yellow, brown, pink, and orange hues fragments were grouped together, all coincide with peaks at 750, 610, 1270, 1670, 2146 and 2375 nm, the inflection around 550 nm served to distinguish two sets of spectra, one set the inflection displaced below that point. There are also some differences in signals at 1419, 2174 and 2208 nm.

The group 4/a fragments showed different spectra than the other groups assigned to this batch, where the characteristic inflection is displaced to 560 nm, and the signal at 592 nm is more evident and well defined, as well as the signals at 1419, 2174 and 2208 nm (Figure 26). This kind of spectra was identified of being hematite.

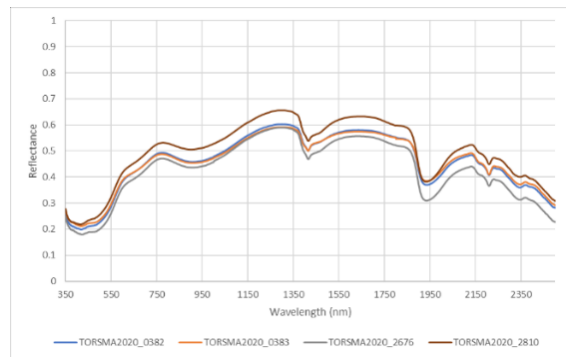


Figure 26 Group 4/a FORS spectra

The rest of the spectra corresponding to groups 5/a, 9/a, 16/a, 20/a, 24/a, 27/a, and 30/a are closer in their reflectance factor, as well as an overall softening of signals, including the inflection at 550 nm, the minimum at 1419 nm and the signal at 2174 nm was reduced to a shoulder (Figure 27). Overall, they show a special resemblance to goethite.

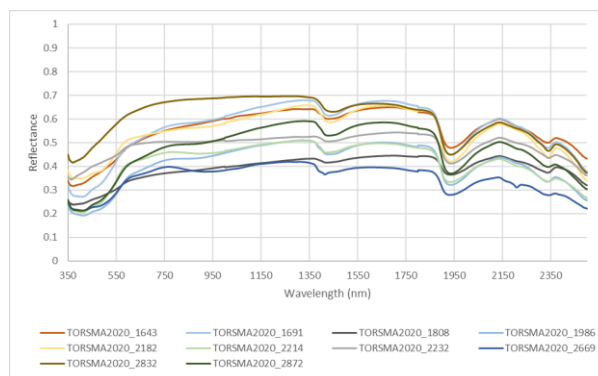


Figure 27 Groups 5/a, 9/a, 16/a, 20/a, 24/a, 27/a, and 30/a FORS spectra

The spectra of the red painted fragments were paired together for their further analysis (Groups 6/a, 7/a, 10/a, 17/a, and 26/a) (Figure 28). The same pattern of distinction was made as with the previous set of groups where a group of spectra show softer features whereas the other shows sharper peaks and a displacement of the first inflection to 592 nm.

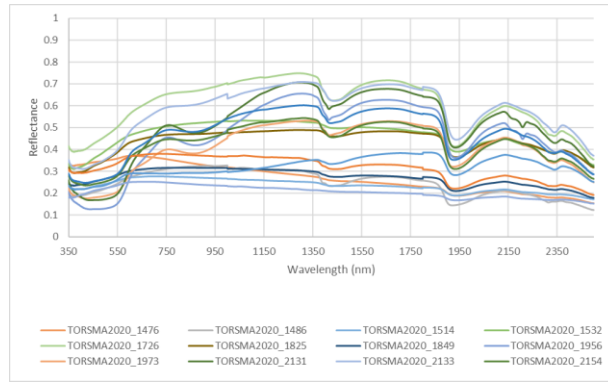


Figure 28 Groups 6/a, 7/a, 10/a, 17/a, and 26/a FORS spectra

The first group, represented with fragments from group 6/a, has minima at 466 nm, 875 nm, 1420 nm, 1468 nm, 1803 nm, 2170 nm, 2210 nm, 2354 nm, and 2406 nm. It is important to notice that the minima, inflections, and overall shape up to the shoulder at 1266 (Figure 29). This spectrum was identified before as hematite as part of ochre groups.

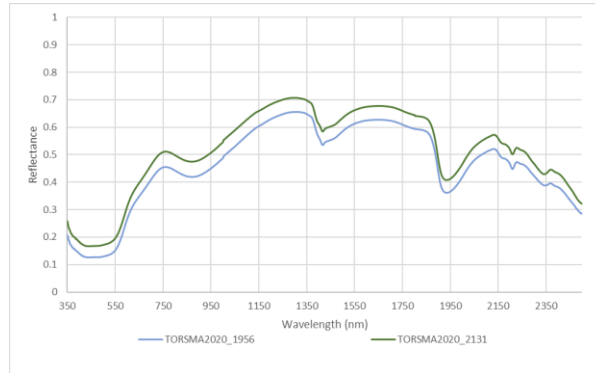


Figure 29 6/a reflectance spectra

And the second, represented with the remaining red hue groups. They show minima at 428 nm, 876 nm, 1446 nm, 1934 nm, 1928 nm, 2312 nm, inflections at 673 nm, shoulders at 1839 nm, and 2226 nm, and maxima at 2138 nm. Like the one of goethite.

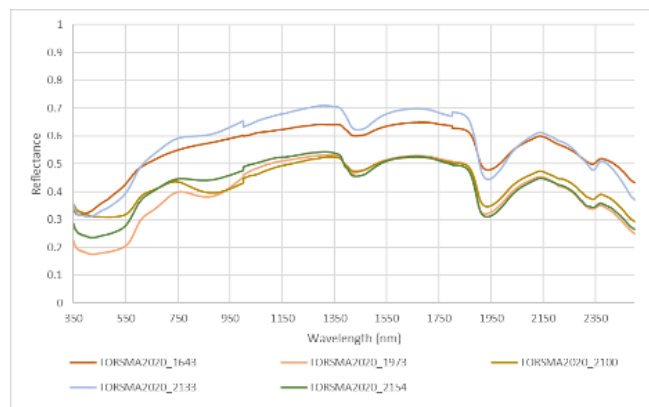


Figure 30 7/a reflectance spectra

The green hue include groups 1/a, 8/a, 14/a, 18/a, 19/a, 31/a, and 32/a. Overall, the most important feature is a maximum at 575 nm especially evident in fragments corresponding to

groups 1/a, 8/a, 14/a, 19/a, 31/a, and 32/a (Figure 31), whereas in groups 14/a, and 18/a (Figure 32), this maximum turns into a shoulder. The rest of the bands are a shoulder at 865 nm, and 1380 nm, and 1681 nm, a peak at 2150 nm, a minimum at 1420 nm, 1919 nm, and 2302 nm, and another maximum at 2381 nm. This kind of spectra was identified as a green earth pigment, particularly glauconite.

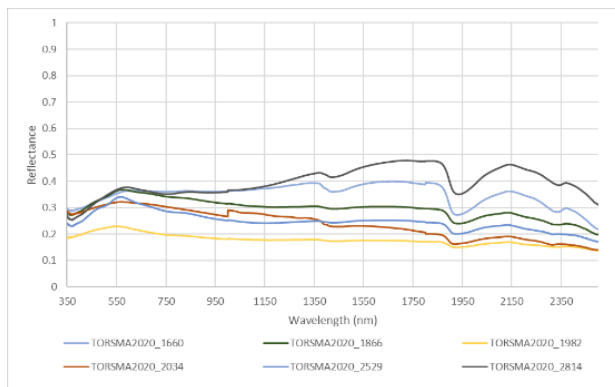


Figure 31 1/a, 8/a, 19/a, 31/a, and 32/a reflectance spectra

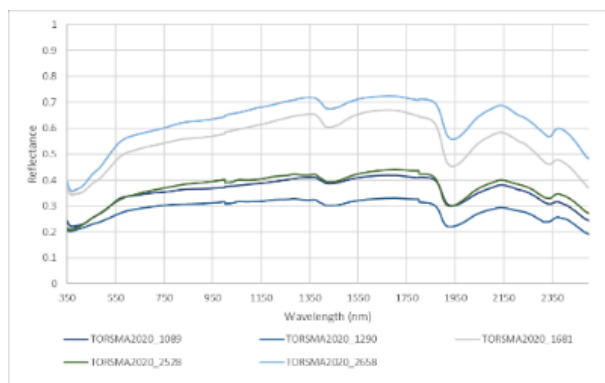


Figure 32 14/a, and 18/a reflectance spectra

The fragments catalogued under blue hue groups are 2/a, and 3/a. The first group, in the lighter tones exhibit spectra with maximum at 490 nm, a minimum at 600 nm and another maximum at 750 nm. The darker shades of blue only shows a maximum at 490 nm. But both sets have signals at 1411, 1904, 1928, 2107, 2150, 2137 nm (Figure 33). These spectra share characteristics with Egyptian blue and lazurite reflectance spectra, further analysis will help to completely characterize the pigment used.

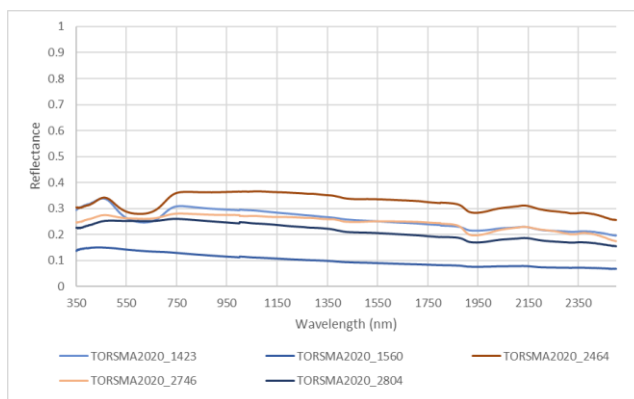


Figure 33 2/a, and 3/a reflectance spectra

The white hue group (23/a). Signals at 382 nm, 1429 nm, 1932 nm, 2204 nm, and 2350 nm (Figure 34).

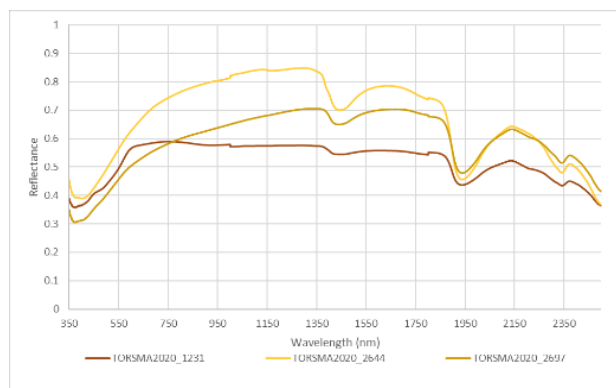


Figure 34 23/a reflectance spectra

There are several signals (1429 nm, 1932 nm, 2204 nm, and 2350 nm) that are present in all samples, indicate the presence calcium carbonate (CaCO_3) most likely used along egg and an oil, as their signals that coincide in (1723 nm, 1760 nm, 1930 nm, 2049 nm, 2132 nm, 2303 nm, and 2350 nm, situation that replicates among every studied group except 4/a, and 6/a.

5.3 RAMAN SPECTROSCOPY

Overall, 25 different fragments were analysed by Raman, and their analysis went as according to the data and preliminary identifications made analysing the reflectance spectra, and their spectra and peaks are depicted in Table 7, as well as the form in which the spectra was obtained. In some cases, more than one colour from the pictorial layer was analysed.

Though the spectra were primarily overshadowed by the presence of calcium carbonate, some signals that belong to the pigments used could be observed.

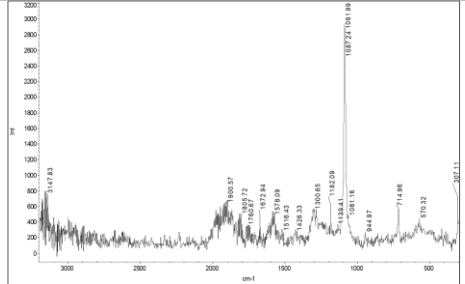
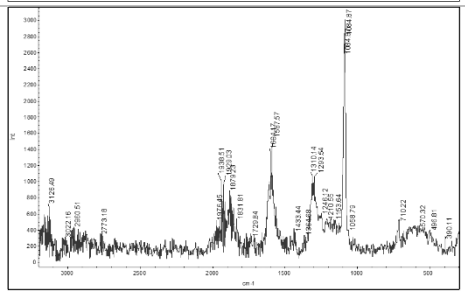
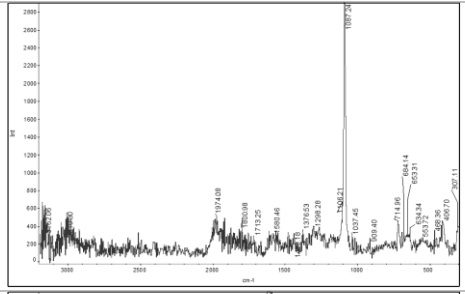
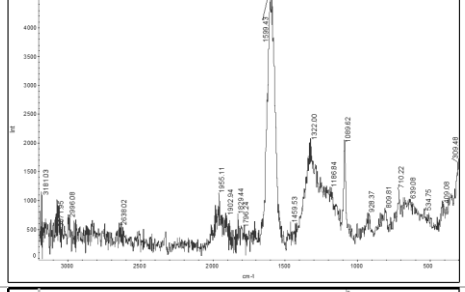
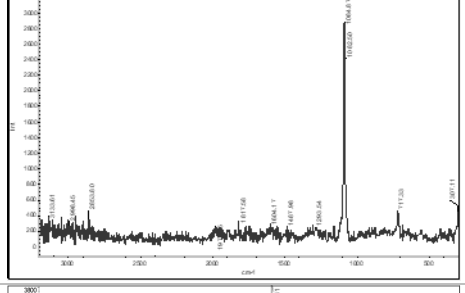
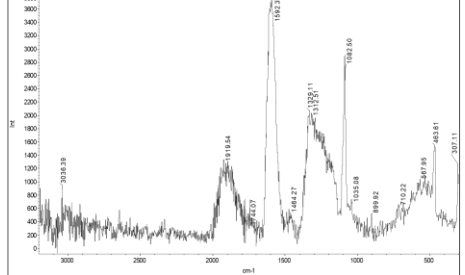
Fragments 2131 and 2676 belonging to groups 6/a, and 4/a respectively were compared together, and the identification of hematite used as pigment could be sustained. On the other side, the presence of goethite was identified used in its mineral form, but also heated to obtain darker shades including orange, pink, red and brown colours. This is the case with fragments 665, 1686, 1808, 2232, 1849, 2133, 2317, 2659, 2795, 2796, and 2886.

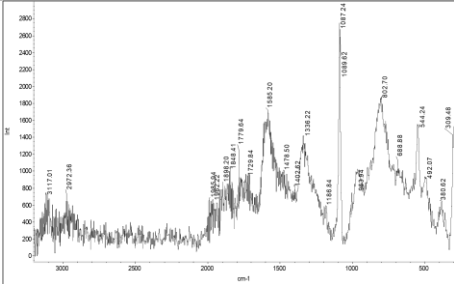
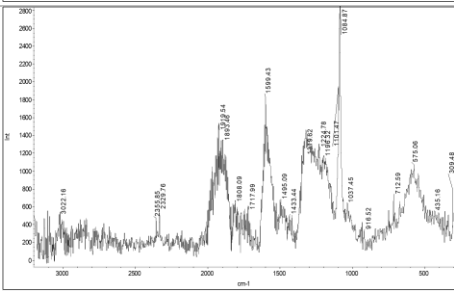
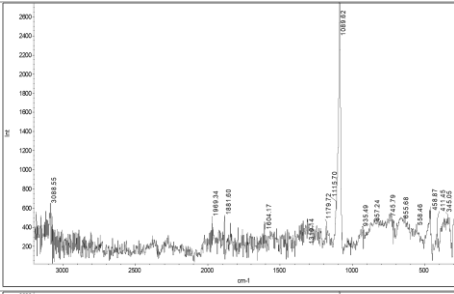
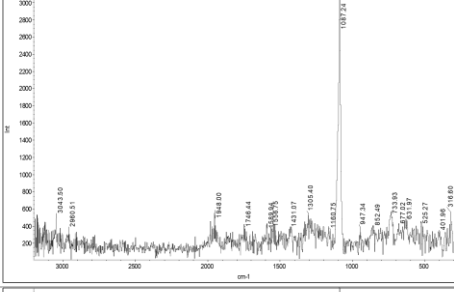
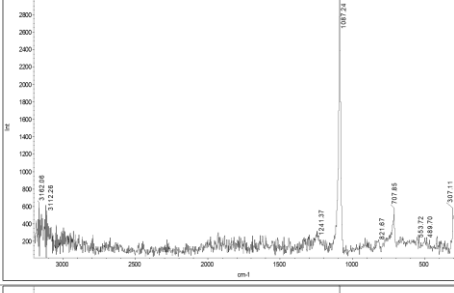
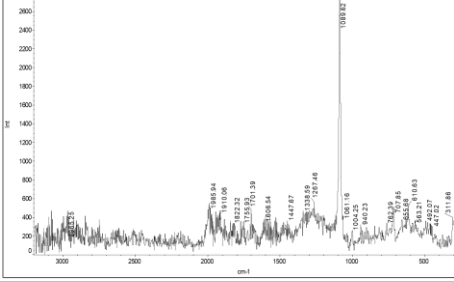
The green earth pigment, glauconite pigment was identified in fragments 1671, 1681, 1866, 2516, and 2814

Finally, the Raman spectra taken from lighter and brighter shades of the blue fragments enabled the recognition of characteristic peaks of lazurite mineral used as a pigment.

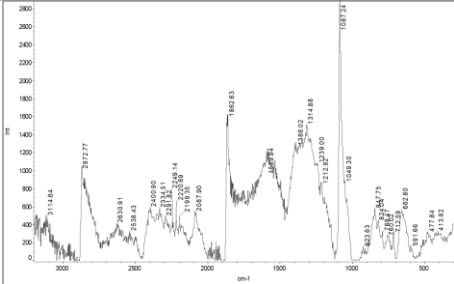
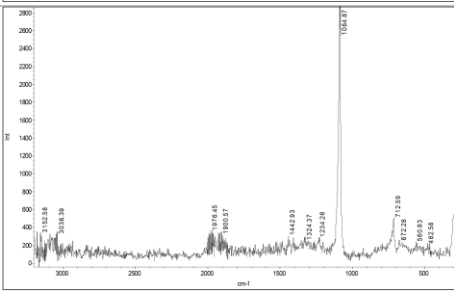
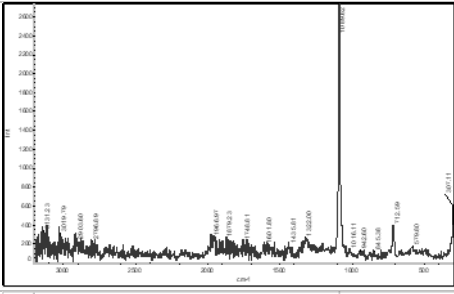
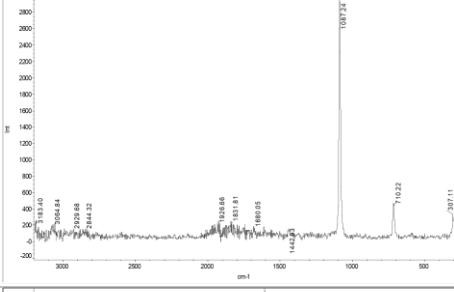
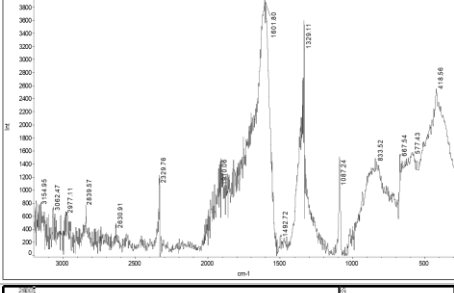
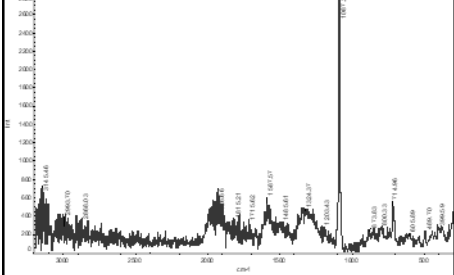
There were also peaks that were identified to be akin to those of proteins present in the eggs and to those that belong to oils such as linseed oil, that is traditionally used in this context, in all fragments but fragments 665, 1849, 2131, 2317, and 2676.

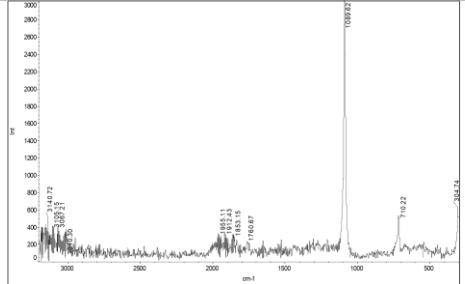
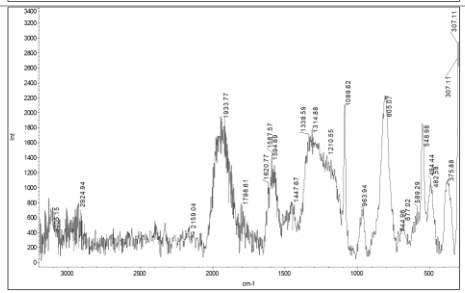
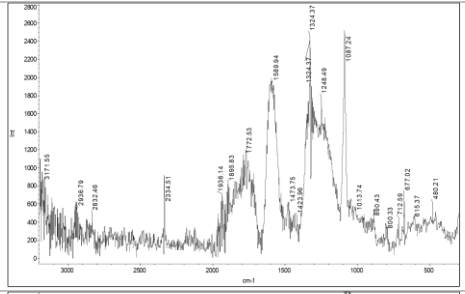
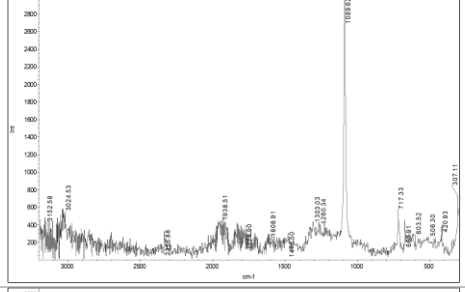
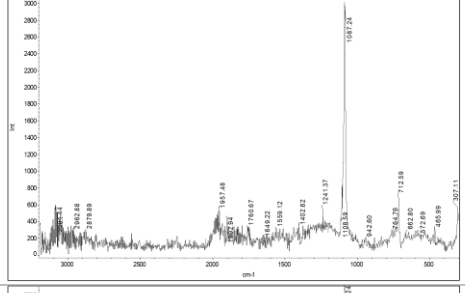
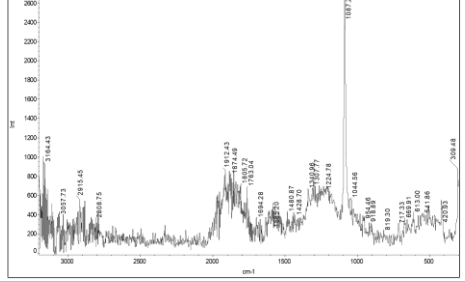
Fragment	Raman count (cm ⁻¹)	Spectrum
1384	307.11, 387.74, 482.58, 551.31, 677.02, 714.96, 800.33, 904.66, 954.46, 973.43, 1084.87, 1300.65, 1454.76, 1587.57, 1597.06, 1611.28, 1706.13, 1748.81, 1817.58, 1917.17, 2083.16, 2109.24, 2329.68, 2929.68, 3178.66	
1423	307.11, 354.54, 382.99, 501.55, 544.24, 710.22, 816.93, 1091.99, 1298.28, 1597.06, 1983.57, 3038.76, 3159.69	
1500	304.74, 530.01, 717.33, 1089.62, 1303.03, 1585.20, 1601.80, 1841.29, 2609.57, 2889.37	
1671	636.71, 719.71, 831.15, 1084.87, 1293.54, 1440.56, 1594.69, 1952.74, 2894.11, 3019.79, 3181.03	
1686	333.20, 511.04, 622.49, 750.53, 928.37, 1087.24, 1295.91, 1566.23, 1734.59, 1924.28, 3041.13, 3145.46	
1804	508.67, 608.26, 712.59, 1087.24, 1928.28, 1599.43, 1606.54, 1964.60, 2884.63, 3157.32	

<p>1866</p>	<p>714.96, 1091.99, 1300.65, 1578.09, 1805.72, 1900.57, 3147.83</p>	
<p>2053</p>	<p>570.32, 710.22, 1084.87, 1293.54, 1310.14, 1433.44, 1587.57, 1879.23, 1929.03, 3126.49</p>	
<p>2131</p>	<p>307.11, 406.70, 486.36, 714.96, 1087.24, 1298.28, 1580.46, 1800.98, 1974.08, 3010.30, 3162.06</p>	
<p>2232</p>	<p>309.48, 409.08, 639.08, 710.22, 809.81, 928.37, 1089.62, 1186.84, 1322.0, 1599.43, 1796.24, 1955.11, 2638.02, 2996.08, 3071.95, 3181.03</p>	
<p>2317</p>	<p>307.11, 717.33, 1084.67, 1239.54, 1487.98, 1604.17, 1817.58, 1976.45, 2853.80, 2998.45, 3133.61</p>	
<p>2464 Dark</p>	<p>307.11, 463.61, 1082.50, 1312.51, 1329.11, 1592.31, 1919.54, 3036.39</p>	

<p>2464 Light</p>	<p>309.48, 380.42, 492.07, 544.24, 802.70, 963.94, 1087.24, 1336.22, 1585.20, 1729.84, 1779.64, 1848.41, 1962.22, 2972.36, 3117.01</p>	
<p>2516</p>	<p>575.06, 1084.87, 1224.78, 1319.62, 1599.43, 1919.54, 2329.76, 2355.85</p>	
<p>2659 Orange</p>	<p>354.05, 458.87, 655.68, 745.79, 1089.62</p>	
<p>2659 Red</p>	<p>733.93, 1087.24, 1305.40, 1556.75, 1948.0</p>	
<p>2659 Yellow</p>	<p>307.11, 707.85, 1087.24, 1241.37, 3112.26, 3162.06</p>	
<p>2676</p>	<p>311.86, 468.36, 714.96, 1087.24, 1305.40, 1433.44, 1582.83, 1924.28, 2934.42, 2988.96, 3176.29</p>	

<p>2795</p>	<p>307.11, 420.93, 503.92, 541.86, 641.46, 719.71, 804.07, 1080.13, 1174.98, 1305.40, 1589.94, 1739.33, 1865.00, 2614.31, 2872.77, 3185.77</p>	
<p>2814</p>	<p>307.11, 579.80, 752.90, 914.15, 1087.24, 1286.43, 1563.86, 1988.31</p>	
<p>2832</p>	<p>337.94, 616.74, 736.30, 928.37, 1089.62, 1293.54, 1876.86, 2913.08, 3140.72</p>	
<p>Direct contact with the fragment</p>		
<p>665</p>	<p>307.11, 712.59, 1084.87, 1891.09, 1945.63, 3105.15</p>	
<p>1423</p>	<p>307.11, 364.02, 546.61, 712.59, 814.55, 973.43, 1089.62, 1208.18, 1329.11, 1502.21, 1594.69, 1701.39, 1881.60, 2334.51, 2882.26, 3074.33</p>	
<p>1681</p>	<p>309.48, 432.79, 556.09, 679.39, 714.96, 1089.62, 1298.28, 1599.43, 1860.26, 1952.74, 2863.29, 2960.51, 3114.64</p>	

<p>1687 Grey</p>	<p>307.11, 420.93, 650.94, 710.22, 812.18, 1087.24, 1314.88, 1594.69, 1763.04, 1857.89, 1948.0, 2329.76, 2875.14, 3133.61</p>	
<p>1687 Yellow</p>	<p>304.74, 669.91, 714.96, 1084.87, 1879.23, 1959.85, 3062.47, 3147.83</p>	
<p>1849</p>	<p>307.11, 712.59, 1089.62, 1322.0, 1435.81, 1601.80, 1748.81, 1879.23, 1966.97, 2796.89, 2903.60, 3019.79, 3131.23</p>	
<p>2131</p>	<p>307.11, 710.22, 1087.24, 1442.93, 1680.05, 1831.81, 1926.66, 2844.32, 2929.68, 3064.84, 3183.40</p>	
<p>2232</p>	<p>418.56, 577.43, 667.54, 833.52, 1087.24, 1329.11, 1601.80, 1910.06, 2329.76, 2630.91, 2839.57, 2977.11, 3062.47, 3154.95</p>	
<p>2317 Brown</p>	<p>399.59, 489.70, 714.96, 800.33, 873.83, 1087.24, 1324.37, 1587.57, 1815.21, 1926.66, 2868.03, 2993.70, 3145.46</p>	

<p>2317 Yellow</p>	<p>304.74, 710.22, 1089.62, 1853.15, 1912.43, 1955.11, 3010.30, 3067.21, 3105.15, 3140.72</p>	
<p>2464 Light blue</p>	<p>307.11, 375.88, 494.44, 548.98, 589.29, 677.02, 805.07, 936.94, 1089.62, 1314.88, 1447.67, 1798.61, 1933.77, 2159.04, 2924.94, 3105.15</p>	
<p>2464 Dark blue</p>	<p>480.21, 677.02, 712.59, 800.33, 890.43, 1087.24, 1248.49, 1324.37, 1589.53, 1772.53, 2334.51, 2832.46, 2936.79, 3171.55</p>	
<p>2659 Orange</p>	<p>307.11, 420.93, 669.91, 717.33, 1089.62, 1260.34, 1478.50, 1608.91, 1774.90, 1938.51, 2336.88, 3024.53, 3152.58</p>	
<p>2659 Yellow</p>	<p>307.11, 572.69, 712.59, 764.76, 1087.24, 1241.37, 1559.12, 1957.48, 2879.89, 2962.88, 3081.44</p>	
<p>2659 Red</p>	<p>309.48, 420.93, 541.86, 1087.24, 1224.76, 1307.77, 1585.20, 1874.49, 1912.43, 2808.75, 2915.45, 3057.73, 3164.43</p>	

2676	309.48, 712.59, 1089.62, 1719.50, 1907.69, 2004.91, 2922.57, 3010.30, 3119.38, 3176.66	
2796	430.42, 515.78, 589.29, 679.39, 710.22, 895.18, 994.77, 1087.24, 1329.11, 1618.40, 1753.56, 1902.94, 1655.11, 2327.39, 2887.0, 3052.98, 3169.17	
2814	309.48, 546.61, 717.33, 1084.87, 1174.98, 1319.62, 1592.31, 1734.59, 1867.38, 1943.25, 2322.65, 3045.87, 3166.80	
2886	575.06, 667.54, 731.56, 1089.62, 1246.12, 1438.18, 1831.81, 1955.11, 3062.47	

Table 7 Raman results for the samples analysed

5.4 FOURIER TRANSFORM INFRARED FT-IR

The Fourier Transform Infrared analysis allowed to distinguish the painting technique as a *secco*, using *tempera grassa* as bands that are present in egg and linseed oil were observed.

The organic binders show bands in the mid infrared spectral range, CH stretching at 2900-2800 cm^{-1} , NH stretching of amide groups at 3300-3280 cm^{-1} , at about 3090 cm^{-1} the first overtone of amide II is located. A band in the range between 1500 and 1800 cm^{-1} corresponds to the carbonyl bond absorption whose position varies due to the type of carbonyl, ester groups in a lipidic medium present it at $\sim 1740 \text{ cm}^{-1}$, in proteinaceous binders it presents at $\sim 1650 \text{ cm}^{-1}$ (amide I) together at $\sim 1550 \text{ cm}^{-1}$ (amide II) and $\sim 1450 \text{ cm}^{-1}$ (amide III) in a stair like form, though lime can distort the bands of organic compounds.¹³

On the other hand, the pigment identification made analysing the results of FORS and Raman techniques the also possible this way. By FTIR means, the inclusion of aluminium a silicon clays on the goethite pigment could be identified, the presence of lazurite, hematite and lazurite was confirmed, the pigment identification is depicted on Table 8.

Identification	Group	Fragment
Hematite	4/a, 6/a	2131, 2676
Goethite	5/a, 7/a, 9/a, 10/a, 11/a	665,1686, 1808, 2232, 1849, 2133, 2317, 2659, 2795, 2796, 2886
Glauconite	1/a, 8/a, 14/a, 19/a	1671, 1681, 1866, 2516, 2814
Egyptian blue/lazurite	2/a, 13/a	1384, 1423, 1672, 2053, 2664, 2464
Calcium Carbonate	24/a	2832

Table 8 Pigment identification

Table 9 depicts the results obtained from the FTIR analysis of every sample taken.

Sample	Wavenumber (cm ⁻¹)	Spectrum
1384 grey	412.32, 448.69, 471.51, 540.4, 712.87, 874.24 , 910.17, 1031.03, 1083.11, 1443.97 , 1542.11, 1559.77, 1580.38, 1616.36, 1797.44, 2515.78, 2872.61, 2971.69, 3452.48, 3616.65, 3694.98	
1423 blue	451.88, 425.94, 713.01, 874.45 , 1011.94, 1085.99, 1143.63, 1430.90 , 1561.63, 1575.74, 1616.45, 1798.14, 2517.53, 2864.37, 2930.66, 3461.72	
1500 grey	408.55, 440.35, 472.06, 539.98, 712.84, 848.36, 872.70 , 913.92, 1005.28, 1025.46, 1077.34, 1441.02 , 1797.50, 2514.75, 2874.65, 2981.80, 3450.76, 3691.55, 3694.74	
1672 Light green	460.53, 526.82, 613.29, 713.14, 874.14 , 1015.99, 1083.11, 1163.81, 1447.86 , 1545.05, 1559.77, 1574.49, 1621.59, 1797.92, 2517.08, 2870.14, 2971.02, 3461.38	

1686 yellow	405.76, 449.0, 472.06, 713.03, 728.41, 774.70, 797.76, 874.09 , 1026.16, 1085.99, 1166.69, 1448.19 , 1797.97, 2518.33, 2875.44, 2982.60, 3428.47, 3685.83	
1808 Pink/ orange	408.65, 417.29, 428.82, 460.53, 712.94, 874.47 , 1005.28, 1028.34, 1083.49, 1166.69, 1443.39 , 1797.51, 2515.16, 2599.20, 2870.14, 2976.78, 3428.93	
1866 green	411.40, 458.14, 713.15, 874.16 , 1016.95, 1456.50 , 1558.69, 1582.23, 1620.49, 1798.18, 2516.30, 2610.63, 2875.60, 2982.65, 3399.51, 3529.50, 3617.33, 3694.31	
2053 grey	459.39, 534.64, 713.19, 874.22 , 1008.99, 1032.84, 1084.42, 1444.29 , 1535.14, 1558.69, 1576.34, 1617.54, 1798.13, 2513.81, 2867.48, 2978.0, 3433.09, 3619.91, 3695.46	
2131 red	469.15, 547.73, 712.23, 797.07, 874.52 , 907.59, 1007.15, 1030.14, 1101.99, 1430.91 , 1791.75, 2510.13, 2611.44, 2863.79, 2981.68, 3443.82, 3615.33, 3689.01	
2232 Pink/ orange	406.56, 458.14, 712.90, 848.26, 873.71 , 1022.82, 1084.42, 1420.32 , 1616.20, 1797.26, 2514.19, 2598.54, 2871.16, 2974.31, 3417.32, 3677.96	

2317 red	401.12, 439.52, 712.80, 874.03 , 1024.33, 1083.05, 1447.69 , 1797.35, 2513.81, 2863.79, 2922.74, 2978.00, 3432.92	
2464 light blue	447.49, 611.94, 659.04, 712.75, 873.75 , 1008.40, 1076.89, 1143.14, 1451.72 , 1618.04, 1794.63, 2512.36, 2340.55, 2869.39, 2920.92, 2983.49, 3433.79	
2464 dark blue	712.75, 873.40 , 1018.08, 1083.71, 1432.34 , 1797.77, 2512.36, 2582.30, 2869.39, 2979.81, 3433.16	
2516 green	458.77, 712.79, 775.46, 801.76, 873.78 , 1016.14, 1417.71 , 1797.0, 2512.36, 2596.39, 2885.71, 2979.81, 3434.79	
2659 ochre	418.05, 454.85, 708.82, 789.80, 873.78 , 1021.68, 1076.89, 1429.86 , 1794.63, 2512.36, 2593.34, 2869.39, 2979.81, 34321.54	
2659 orange	462.15, 712.79, 797.16, 873.86 , 1030.22, 1076.89, 1165.23, 1444.30, 1790.95, 2512.36, 2869.39, 2976.13, 3433.98	

<p>2659 Red</p>	<p>780.82, 873.86, 1030.36, 1080.36, 1447.45, 1794.63, 2512.36, 2865.71, 2979.81, 3093.91, 3277.95, 3434.07</p>	
<p>2676 ochre</p>	<p>471.77, 528.47, 712.50, 797.16, 874.42, 907.11, 1007.83, 1030.76, 1082.54, 1440.93, 1790.95, 2508.68, 2600.70, 2869.39, 2976.13, 3612.89, 3693.87</p>	
<p>2795 grey</p>	<p>467.34, 535.83, 712.50, 874.28, 910.87, 1004.93, 1029.32, 1442.21, 1794.63, 2508.68, 2604.38, 2885.71, 2979.81, 3441.81, 3609.21, 3690.19</p>	
<p>2814 Light green</p>	<p>405.23, 458.62, 712.85, 727.22, 797.16, 873.49, 1023.33, 1089.11, 1169.91, 1410.67, 1797.47, 2516.04, 2869.39, 2976.13, 3020.30, 3428.86</p>	
<p>2832 Skin (white sample)</p>	<p>712.81, 793.48, 873.90, 1027.50, 1083.86, 1410.67, 1797.31, 2512.36, 2589.66, 2869.39, 2979.81, 3421.50</p>	

Table 9 Infrared spectra obtained

5.5 PYROLYSIS COUPLED TO GAS CHROMATOGRAPHY AND MASS SPECTROMETRY (PY-GCMS).

In order to confirm or discard the presence of binders of any kind, Py-GCMS analysis were performed in fragments selected by the results previously obtained on FTIR and Raman analysis Table 10, Taking a sample in which binders were not identified previously (2131), and a set of samples whose characteristics suggested binders.

Fragment ID sampled	Lipidic material	Proteinaceous material
2832	X	X
1866	X	X
2795	X	X
2464 (light and dark)	X	X
2516	X	X
2676	X	X
2131	-	-

Table 10 Samples studied along with the markers found in them

As mentioned before, analyses were performed with direct methylation and also performing a previous acidic extraction, the latter enabled to identify proteic markers, as opposed to the direct to encountering just lipidic markers, the characteristic Py-GCMS chromatograms of the samples containing markers are presented in Figure 35, and their identifications Table 11.

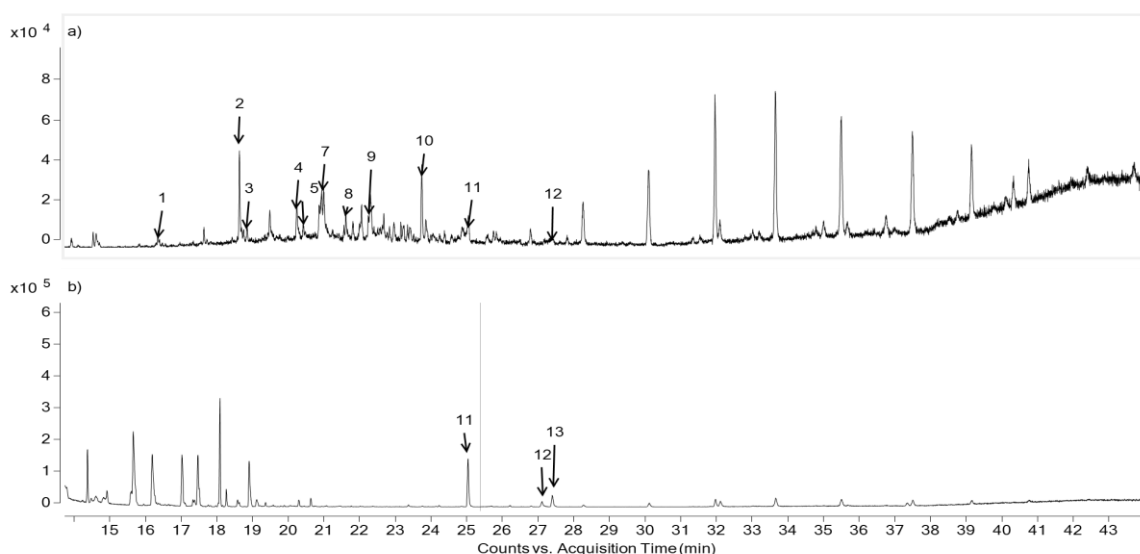


Figure 35 Py-GCMS chromatograms of a) sample extracted, b) sample without both chromatograms correspond to samples taken from fragment 2832.

N° Assigned chromatographic peak	Peak identification	Main ions (m/z)
1	Indole	70, 83,117
2	Cyclo(Pro-Ala)1	70, 83, 97, 111,125,168
3	Cyclo(Pro-Ala)2	70, 83, 97, 111,125,168
4	Cyclo(Pro-Val)1	70, 72,125,154,196
5	Methyl indole	71, 130, 131
6	Octanedioic, -OTMS ester, di-TMS ester	73,203,291,406
7	Cyclo(Pro-Val)2	70,72,125,154,196
8	Cyclo(Pro-Leu)	70, 86, 125, 154
9	Cyclo(Pro-Met)	70,135,154,167,228
10	heptadecanitrile	57,71,83,97,110,124,138,152,166,208,222
11	Palmitic acid TMS ester	73, 117, 129, 313, 328
12	Oleic acid TMS ester	73, 117, 129, 339, 354
13	Stearic acid TMS ester	73, 117, 129, 341, 356

Table 11 Peak identification of the marker found in the studied fragments

6.1 HYPER SPECTRAL IMAGING

The photographs taken from each of the 32 groups contained a reflectance spectrum of each acquired point, in this way by choosing a point in one sample, a false colour heat map was produced over the previous image. Choosing one or two points each time was enough to produce false images that covered the colour in the studied fragments, and little discrepancies were observed among the groups made.

The confirmed groups were rearranged to reduce its number and ease the study of them by reducing the information (Table 12).

Hue group by reflectance	Group class
Green	1/a, 8/a, 14/a, 18/a, 19/a, 31/a, 32/a
Blue	2/a, 13/a, 25/a
Black	3/a, 28/a
Yellow	4/a, 5/a, 16/a, 20/a, 30/a
Brown	9/a, 10/a, 11/a, 16/a, 17/a, 21/a, 26/a, 29/a
Skin	24/a
Red	6/a, 7/a, 12/a, 27/a
Grey	15/a, 21/a, 22/a
White	23/a

Table 12 Rearranged groups

The analysed reflectance spectra led to a wider grouping, yellow ochre pigments could already be identified by the inflection around 550 nm (Figure 14, Figure 15, Figure 16, Figure 17)⁵⁸, the red ochre pigments were identified by the inflection at 580 nm (Figure 18).⁵⁸ The colour of the ochres is related to their granulometry, and although it doesn't impact the reflectance curve trend.⁵⁹

Blue colour groups spectra have relevant points that can lead to identify them as either lazurite or Egyptian blue, as some decisive signals could be overlapped by the noise present on the reflectance spectra.

6.2 FIBER OPTIC REFLECTANCE SPECTRA (FORS)

The first step of the analysis involved the hyperspectral image taking of selected samples and reflectance spectra were obtained, though the usable range between 400 to 700 nm. The recorded range between 700 and 1000 nm exhibited noise that made impossible a complete identification, but it did give reasonable data to ensure that the groups made by colour identification were correct and duplicated groups were merged.

Reflectance information continued to be acquired by FORS means on selected samples, and were compared directly to reference samples taken from U.S. Geological Survey Spectral Library.⁶⁰ The results obtained for yellow, red, orange, pink and brown samples coincide with the flex points of iron-based pigments, goethite and hematite.

The yellow set of reflectance spectra was divided as stated before and group 4/a spectra were compared with the ones of hematite and goethite, and it was identified as hematite as the slope is shifted towards larger wavelengths (580 nm) Figure 36. The same procedure was done with the other groups of the set

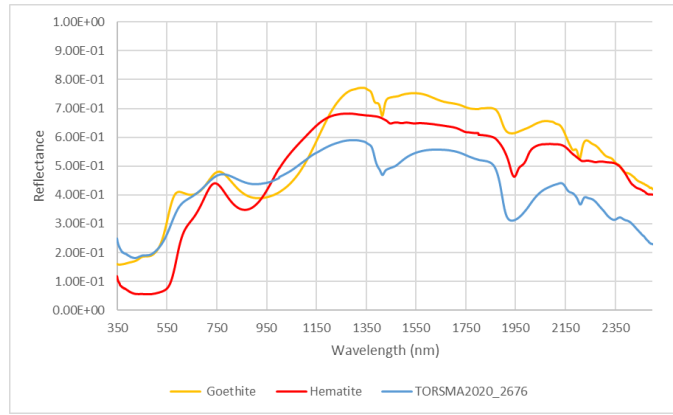


Figure 36 Group 4/a comparison with goethite and hematite

The remaining spectra were also compared and its resemblance to goethite was evident in all cases. Figure 37.

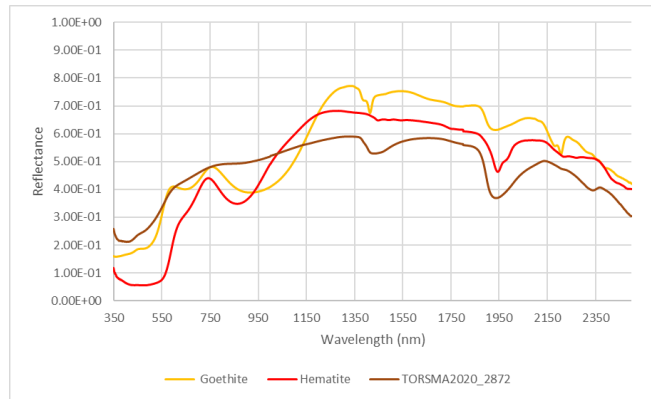


Figure 37 Group 5/a comparison with hematite and goethite

On the other hand, the red set of groups was also treated as the previous set, and group 6/a was confirmed as hematite as the slope at 580 nm is characteristic of this mineral. Figure

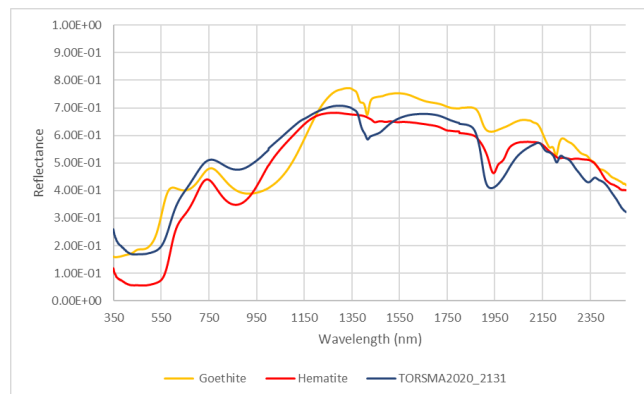


Figure 38 Group 6/a comparison with hematite and goethite

The rest of the groups showed a slightly different spectra, whose slope is shifted towards lower wavelengths (450 nm). Figure 39.

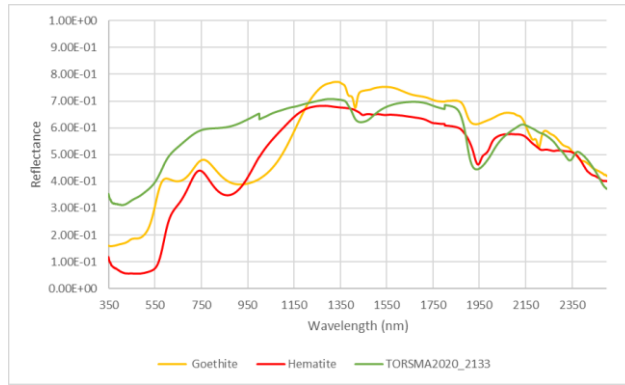


Figure 39 Group 7/a comparison with hematite and goethite

Shifts towards lower wavelengths can be related to factors such as, the number iron oxides contained as well as the clays that could be contained and that effect is more prominent in yellow ochres as opposed to red ones, another factor is related to the relative percentage of the iron oxide mineral contained and the poorness of the chromophore.⁶¹ Reflectance spectra of hematite always exhibit a small band at about 450 nm related to the electronic transition typical of Fe^{3+} ions arranged in octahedral symmetry. The shape of the spectra with an inflection point at 550 suggests a major contribution of goethite than hematite.⁶² Giving the opportunity to differentiate the red pieces with a major content of goethite from the ones containing hematite.

On the other hand, the spectra that show minima at 876 nm, 1446nm, 1934 nm, 1928 nm, 2312 nm, and shoulders at 1839 nm, and 2226 nm, and maxima at 2138 nm are consistent with a lower reflectance version of a pure hematite spectrum, except the signal at 2310 nm and 2226 nm. Indicative of a mixture either with other minerals such as dolomite or calcite. Figure 40.

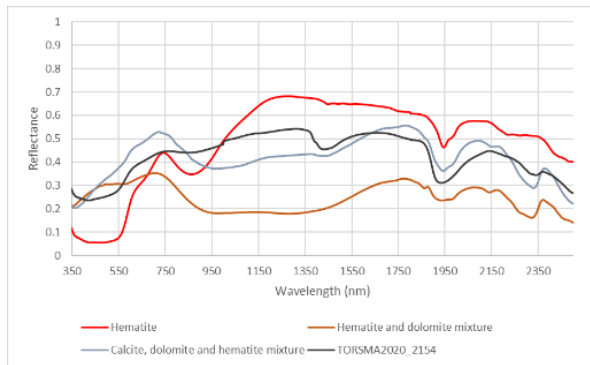


Figure 40 Sample comparison with theoretical mixtures of hematite with other minerals containing calcium carbonate

The green hue groups, previously divided into 2 categories, and thoroughly described were compared to the Glauconite reflectance spectrum (Figure 41) that also has a prominent peak at 575 nm, and a shoulder at 865 nm. Although, the rest of the relevant points present in wavelengths over 1000 nm are not accounted for by this identification. Green earth pigments have a characteristic maximum in their reflectance spectrum at about 560 nm and a shoulder near 480 nm common to celadonite and glauconite.⁶³

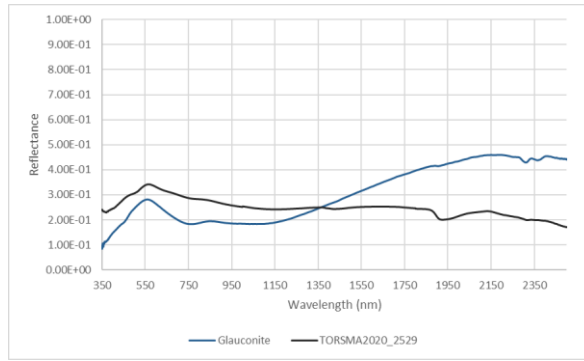


Figure 41 Comparison of green group to glauconite spectrum

The blue hue category had as preliminary results the presence of either Egyptian blue or Lazurite mineral. The relevant points in the spectra obtained with a longer wavelength range of the category include maxima at 454 nm, 2150 nm, and 2387 nm, minima at 646 nm, shoulders at 749 nm and 1904 nm, that are more like the ones present in lazurite than on the Egyptian blue. Figure 42. Lazurite pigments usually is well detectable by its strong large absorbance around 600 nm.⁶² For this reason an accurate identification of the pigment present in the fragment could be done at this point of the investigation.

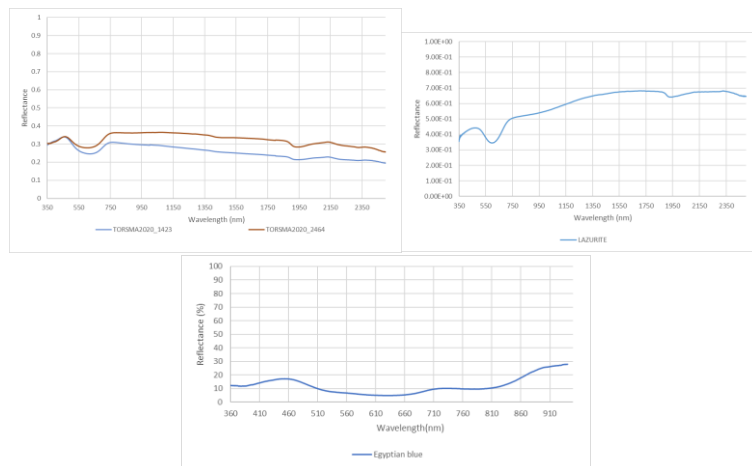


Figure 42 Group 2/a (left), lazurite (centre), Egyptian blue (right).

Contrary to the hyperspectral imaging analysis, this analysis did give more information regarding the reflectance spectrum of the white hue group (23/a). Relevant signals were observed at 382 nm, 1429 nm, 1932 nm, 2204 nm, and 2350 nm. A comparison was made with minerals rich in calcium carbonate, it is possible that minerals present are either calcite or dolomite, though a complete identification can be done. Figure 43.

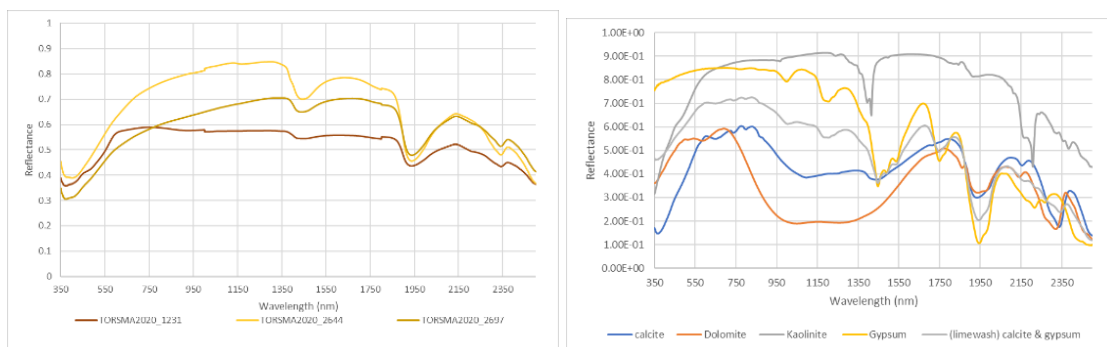


Figure 43 Group 23/a (left), minerals rich in calcium carbonate(right).

FORS spectra can give information about binder and pigment-binder interaction.³⁰Overtones bands of methylene (-CH₂-), methyl (-CH₃) and alkenyl (-CH=CH-) stretching modes can be observed in the range of 1720–1760 nm, while the respective second-overtone bands are observed between 1200 and 1215 nm. Combination bands for the -CH=CH- and -CH₂-/-CH₃ stretching modes were observed in the ranges of 2100–2190 nm and 2300–2490 nm, respectively. Overtones of OH vibrations are consistently observed in the FORS spectra at 1441 nm for fats and oils at 1441 nm and the corresponding peak from egg binder fell within a 10 nm range of this.⁶⁴ Some samples from all the groups show peaks around 1350, 1900, 2100 and 2350 nm that coincide with the peaks of the spectrum of whole egg and linseed oil, indicating a high probability of either of them being used as a binder or a varnish. Table 13

Material	Wavelength	Assignments
Whole egg	1725	First overtones of -CH ₃ , -CH ₂ -, -CH = CH- groups Combination bands of -OH Combination bands of -NH Combination bands of -CH ₃ and -CH ₂ -
	1759	
	1933	
	2058	
	2306	
	2348	
Linseed oil	1723	First overtones of -CH ₃ , -CH ₂ -, -CH = CH- groups Combination bands of -OH Combination bands of -CH = CH- Combination bands of -CH ₃ and -CH ₂ -
	1755	
	1922	
	2131	
	2302	
	2347	

Table 13 Reflectance spectra assignments to materials compared to⁶⁴

6.3 RAMAN SPECTROSCOPY

During the Raman spectroscopy analysis some difficulties arose, and an accurate identification of pigments could not be made in some samples, for reasons related to the characteristics of the instrument, particularly the acquisition range of the instrument as many of the bands that would enable pigment identification are found between 200 and 400 cm⁻¹ which were not included in the recorded spectra. Some characteristic bands are visible in the acquired spectra though.

Red, yellow, orange, and purple colours were analysed in bulk as their FORS spectra show similar characteristics and groups 4/a, and 6/a were identified as hematite. Goethite was also found in the rest of the groups that contained yellow, orange, pink, and brown colours (bands at 665, 1686, 1808, 2232, 1849, 2133, 2317, 2659, 2795, 2796, and 2886).

Both pigments have been used extensively since pre-historical times, and a variety of different shades of yellow and red colour can be obtained heating goethite,^{18,65} different shades of red colour can be obtained by thermal decomposition of goethite to hematite at relatively low temperatures allows to obtain darker shades as the temperature raises, hues ranging from brownish-orange, brownish red, bright red, marron/purple and grey can be observed.^{18,65-67}

Goethite Raman bands occurring at 223 and 675 cm^{-1} were assigned to Fe-O mode and Fe-O stretching, respectively.⁶⁶ Although archaeological samples exhibit quite weak Raman spectra, mainly dominated by bands that correspond to calcite, an intense band corresponding to goethite at around 390 cm^{-1} could be sometimes identified.⁶¹ The replacing of its bands for the ones of hematite are the most significant feature, and are larger than the usually observed form hematite, indicating a smaller degree of crystallinity.^{63,65,68} Hematite obtained in this way shows its characteristic bands in the region 200-700 cm^{-1} ,^{63,66} specially 657 cm^{-1} band appears with high intensity.^{21,65} Another important feature is the presence of an intense peak between 1316 and 1323 cm^{-1} while acquiring spectra at 632.8 nm²¹ as in this case.

The spectra obtained and identified as iron oxides, especially the ones identified as goethite, show weak spectra, this is due to the important presence of CaCO_3 and the presence of other clays, as they affect spectra by fluorescence.²¹

The green colour groups FORS taken previously indicate the presence of one of the four green earths groups pigments, the clayey micas and particularly the glauconite, is derived from a sedimentary geological origin.^{69,70}

The chemical composition of glauconite is similar to the one of celadonite, but with a major content of Al due to a partial substitution of Al^{3+} for Si^{4+} in the tetrahedrally coordinated layer.⁶⁹ The Raman spectrum shows characteristic bands in the range of 100-800 cm^{-1} , the most important bands are 264, 447, 591, 700 and 955 cm^{-1} , at higher laser excitations, the spectrum is dominated by the 385 and 549 cm^{-1} .^{69,71}

Peaks at 548 cm^{-1} and 713 cm^{-1} could be seen in the samples' spectra, confirming the presence of the mineral in the pictorial layer.

The green earth pigment, glauconite pigment was identified in fragments 1671, 1681, 1866, 2516, and 2814.

Blue pigments in the samples analysed by FORS suggested the possibility of having Egyptian blue and lazurite as pigments, the first being a synthetic material sometimes used in mixture with a green earth or a yellow ochre under coat to improve adhesion,⁷⁰ and the second a natural one obtained from lapis lazuli.

The ancient and artificial pigment shows only three Raman bands, situated at 1087, 430 and 114 cm^{-1} , this usually appears with calcite and carbon, used to modify the colour tone. The mineral lazurite crystallizes in the isometric group, giving it a quite simple Raman Spectrum that at higher laser wavelengths exhibits bands at 546 and 2539 cm^{-1} and at lower intensities the strongest band is at 547 cm^{-1} , and a minor bands at 1093 and 1635 cm^{-1} , other weaker bands are situated at 258 and 804 cm^{-1} .^{70,72-74}

The group 2/a pieces have two different shades of blue, the lighter shade Raman spectra show the main band at 545 cm^{-1} that corresponds to lazurite. This band is also present in the samples corresponding to greyer shadows such as the ones pertaining to group 13/a.

The Raman of the darker colours does not exhibit any of the characteristic band. Instead, two different spectra types were identified, one exhibits two broad bands between 1300 and 1600 cm^{-1} indicative of a black pigment (carbon black, ivory black, lamp black), it's impossible to distinguish between them by Raman means.⁷⁵

The grey Raman spectra (fragment 1867) showed the two characteristic broad bands between 1300 and 1600 cm^{-1} of black pigments, along with the band at 1085 cm^{-1} of calcium carbonate to give the grey colour.

The Raman spectra data can give indication regarding not only the pigments present in the samples, but of the binders and the interaction between the two of them. And information regarding the binder used was obtained.

The white sample served to appreciate better the presence of it as not only the peaks of CaCO_3 were visible (1087 and 710 cm^{-1}) but also peaks in zones between 1100 and 1350 cm^{-1} and 1547 and 1727 cm^{-1} indicate the presence of an organic binder.

Samples containing egg only have strong C–H and C–C stretching frequencies and ring breathing modes, with only the C–H stretching frequencies being observed in the pigment–binder samples. The phenylalanine ring breathing and C–C stretching (1000 cm^{-1}) modes are represented in pure samples but are lost in the presence of certain pigments. On the other hand, the C=O stretching frequencies observed in oil-binder samples are not easily discernible against the background in the pigment binder samples.⁶⁴ Though proteins do show the presence of amides related to proteins, amide I peak appears between 1640-1670 cm^{-1} , amide III between 1280 and 1100 cm^{-1} . Albumin can be distinguished by the position of the CH_2 and CC aromatic bands near 1450 and 1000 cm^{-1} . Between 800 and 900 cm^{-1} the characteristic bands of tyrosine amino acid residues appear. In proteinaceous material there may be increased band intensity around 650 cm^{-1} for partially degraded sulphur-containing proteins due to the formation of cysteine.⁷⁶

The use of drying oils is mentioned to be in use of a mixture, the linseed oil is by far the most used drying oil. In the Raman spectra of Linseed oil contains linolenic acid and the relative intensities of the two peaks at 1670-1640 cm^{-1} and 1100-1280 cm^{-1} peaks are higher than in the case of the other drying oils.⁷⁶

Material	Raman deviation (cm^{-1})	Assignments
Whole egg ⁶⁴	1072	Phenylalanine C–C stretching Amide III / =C–H symmetric rocking C–H vending Amide I / C = C stretching Aliphatic C–H stretching
	1255	
	1297	
	1436	
	1649	
	1746	
	1813	
	2710	
	2851	
	2887	
2915		
Linseed oil ⁶⁴	955	C–C, C–N stretching Amide III / =C–H symmetric rocking
	1078	
	1257	
	1297	

	1303 1438 1651 1735 2700 2792 2853 2905	CH ₂ deformation CH ₂ deformation Amide I / C = C stretching C = O stretching Aliphatic C–H stretching Aromatic / unsaturated C–H stretching
Poppy oil ⁶⁴	1074 1162 1297 1436 1673 1715 2710 2732 2853 2895 2915	Phenylalanine C–C stretching Aliphatic anti-symmetric stretching and aromatic rocking Amide III / =C–H symmetric rocking C–H vending Amide I / C = C stretching C = O stretching Aliphatic C–H stretching Aromatic / unsaturated C–H stretching
Walnut oil ⁶⁴	1076 1136 1295 1436 1657 1717 2712 2853 2901 2979	C–C, C–N stretching Aliphatic anti-symmetric stretching and aromatic rocking Amide III / =C–H symmetric rocking C–H vending Amide I / C = C stretching C = O stretching Aliphatic C–H stretching Aromatic / unsaturated C–H stretching
Goethite ^{65,66}	299 400 550	Fe-OH sym. Bend Fe-O-Fe/-OH symmetric stretching Fe-OH asymmetric stretching
Hematite ^{65,66}	225 247 293 412 498 613 660 820 1086 1320	Fe-O symmetric stretching Fe-O symmetric bend Fe-O symmetric bend Fe-O symmetric bend Fe-O symmetric stretching Fe-O symmetric bend
Glauconite ⁶⁹	146, 256, 385, 547, 703.	

(K, Na) (Fe ³⁺ , Al, Mg) ₂ (Si, Al) ₄ O ₁₀ (OH) ₂ ,	145, 266, 384, 439, 543, 694.	
Celadonite ⁶⁹ K [(Al, Fe ³⁺), (Fe ²⁺ , Mg)] (AlSi ₃ , Si ₄) O ₁₀ (OH) ₂	140, 169, 196, 279, 347, 392, 435, 538, 698. 141, 168, 202, 274, 392, 440, 536, 700. 136, 175, 274, 383, 393, 551, 676, 703. 133, 171, 276, 382, 393, 545, 699.	
Azurite 2CuCO ₃ · ⁷² Cu (OH) ₂	252 m, 334w, 404vs, 769 m, 843 m, 943 m, 1098 m, 1425 m, 1581 m	

Table 14 Raman numbers and assignments of reported materials

6.4 FOURIER TRANSFORM INFRARED (FT-IR)

Given the information obtained in the previous analysis made by using different techniques, the presence of CaCO₃ was appointed and confirmed by FTIR means, as the bands in the spectra confirmed the information obtained previously as the ν_3 , asymmetric stretching of CO₃²⁻ observed in every sample corresponds to the very strong band observed between 1410 and 1450 cm⁻¹, the bands observed at 1800 cm⁻¹ corresponds to the $\nu_1+\nu_4$, $\nu_1+\nu_3$ at 2500 cm⁻¹ and $2\nu_3$ at about 2900 cm⁻¹, all correspond to the carbonate anion. The band at 873 cm⁻¹ corresponds to the O-C-O bending band.^{13,31} This is present in every fragment studied.

The Raman results also pointed out to the use of whole eggs as part of the binding media, and their presence may be an indication of the painting technique used as the spectral features in IR are affected not only by the substrate and the pigment, but also be the painting technique.

The spectra of egg *fresco* plaster, whose characteristics favour the masking of the vibrational modes of organic materials, differ from the egg *secco* and *stancco*, where the binder special features become more important and the mortar contribution is less important, this enabled the identification of the bands that correspond to the proteinic content of the egg, by the confirmation of CH stretching at 2900-2800 cm⁻¹. Proteinaceous content was confirmed due to the bands of NH stretching present between 3300-3280 cm⁻¹, The band due that belongs to a carbonyl in a proteinaceous binder appears shifted, in this case at 1621 cm⁻¹ along with the bands at 1574 and 1545 cm⁻¹ corresponding to the polyamide absorption. All in stair-step type intensities.¹³ This pattern is clearly visible in fragments 1384, 1423, 1672, 1683, 1808, 1866, 2053, 2317 and 2659.

Moreover, the presence of a lipidic medium was assessed and confirmed, as during the process of oil drying after its exposition to the air, the bands assigned to double *cis* bonds (3010, 1654, and 722 cm⁻¹) disappear or turn into shoulders, as well as CH bonds bands related to methyl and methylene groups (2960, 2954, 2925 and 1450 cm⁻¹). Though the oxidative polymerization that oils undergo entail the appearance of hydroxyl groups whose bands appear at 3600-3000 cm⁻¹, the broadening of its carbonyl band, as well as the additional increase of the intensity of the stretching of the CO band,⁷⁷ the former feature was crucial to confirm the presence of an oil along with the egg, though the latter cannot be distinguished as it is being overshadowed by the stretching band corresponding to the carbonate present in the sample. It is possible to identify the type of oil as the bands (873, 1793, 1795 and 1153 cm⁻¹) corresponding to the linolenic group

(R-OO-R) from linseed oil.⁷⁸⁻⁸¹ All the signals are present in the following fragment's spectra: 1423, 1672, 1686, 1808, 1866, 2232, 2317, 2464, 2516, 2659, 2814 and 2832.

All this information regarding the binding media leads to think that the *secco* technique was used employing *tempera grassa* made with whole egg and linseed oil.

Regarding the colour identification via IR analysis, gave information to completely identify and discard hypothesis made during the review of the results of Raman spectra results.

The green colour identification as green earths were confirmed and could be distinguished between glauconite and celadonite, both components of the green earths pigment but they occasionally are used separately as in this case, where the spectra show that glauconite is the mineral contained in the samples.

The celadonite spectrum shows sharp bands, three bands between 3400 and 3700 cm^{-1} , that correspond to hydroxyl groups, dependent of octahedral cations, and four bands between 1110 and 950 cm^{-1} that correspond to stretching vibration within the tetrahedral sheet, the Si-O vibration perpendicular to SiO_4 and in plane. OH, bending modes involving octahedral cations are responsible of the bands between 840 and 665 cm^{-1} . Glauconite IR spectrum is weaker, the 3400-3700 cm^{-1} region shows broader bands, and the region 1110-950 cm^{-1} has only one broad band. And in the 950-650, a reduction of the spectrum can be observed.^{69,73} This is the case of the green and light green groups samples studied via IR.

Raman, FORS and hyperspectral imaging studies made before, left doubts about the probable presence of either Egyptian blue, lazurite or a combination of both pigments, so the infrared analysis gave light on the identity of the pigment used on the crypt samples recovered. The blue pigment could finally be distinguished as lazurite as it presents a prominent band (460 cm^{-1}) that can be used as marker of the silicate group that relates to the O-Si-O deformation bond⁸². The bands at 1070 and 960 cm^{-1} correspond to the Si-O-Si group and Si-O-Al. Finally, the 2340 cm^{-1} band is characteristic of lazurite pigments as corresponds to sulphur ion stretching band.⁷³ This is especially true for the light blue part of samples belonging to group 2, and for the grey and blue samples that belong to group 13 (1384).

Material	Wave number (cm^{-1})	Assignments
Calcium Carbonate ³¹	1410-1450 873	Asymmetric stretching CO_3^{2-} O-C-O bending band
Egg tempera ^{13,77,78}	1754 s 1650 1550 1450	C=O stretching lipidic binder C=O amide I (protein) Amide II Bending asymmetric vibrations of CH_3
Lazurite ^{73,77}	2340 1627w, 1426m, 1077sh, 995vs, 925sh, 877m, 746sh, 710w, 637w, 610w, 516m, 458s	Si-O-Si and Si-O-Al
Hematite ^{77,83}	1630w, 1432m, 1085w, 1030m, 911w, 877w, 646s, 530vs, 450vs	
Yellow ochre ^{77,83}	3694w 3619w,	OH Si-O-Si

	3435w, 3141s, 2959vw, 2925w, 2848w, 1639m, 1163sh, 1101w, 1029vs, 1010sh, 904s, 800s, 692sh, 671w, 593w, 528w, 469vs, 420w	Si-O-Al Al-O-H
Green earth ^{69,77}	3541w, 1630w, 1426m, 1083vs, 955vs, 879sh, 797m, 781sh, 691w, 493sh, 460s, 438sh	
Glauconite ^{69,77}	3610(br) 3545 (br) 1630 1110 (br) 970 (br) 861, 826 566(br)	Hydroxyl stretching Hydroxyl bending Si-O stretching R-O-H bending Si-O-R and R-O-H bending
Celadonite ^{69,77}	3601, 3555, 3534 1640 1115, 1075, 975, 956 840,799, 746,681,665 494, 460, 440	Hydroxyl stretching Hydroxyl bending Si-O stretching R-O-H bending Si-O-R and R-O-H bending

Table 15 FTIR Wavenumbers and assignments from reported materials

6.5 PYROLYSIS COUPLED TO GAS CHROMATOGRAPHY AND MASS SPECTROMETRY (PY-GCMS).

Identifying binders in historical paintings entails solving problems due to the complexity of their composition and the degradation of the materials, even more so in mixed binders such as *tempera grassa*. Generally, the characterization of proteinaceous binders is based on the determination of amino acids and that of lipid binders on the determination of fatty acids. Acid hydrolysis is adopted to release amino acids from proteins and fatty acids for triglycerides, with a subsequent derivatization reaction, which produces suitable derivatives for a single run gas chromatography analysis. Though this methods are unable to identify several amino acids, some dicarboxylic acids and cholesterol.⁸⁴ Moreover, diversity of markers not only on the derivatisation agent used but on the pyrolyzing conditions.⁴⁵

As it has been said, egg can be detected through the presence of lipidic and proteic markers. Under normal pyrolysis conditions a pattern of fatty acids similar to that obtained from drying oils is detected.^{84,85} Moreover, the presence of hexadecanitrile can often be noted as a possible marker of the simultaneous presence of lipidic and proteic fractions and indole and methyl indole as degradation fragments of tryptophane. These markers are of low intensity with respect to fatty acids and for this reason it is hard to distinguish egg from a drying oil.⁸⁴⁻⁸⁶ As is the case of the samples studied and whose results are included in Table 10, proteinaceous and lipid markers were found in samples in which a previous extraction was made.

Simultaneous pyrolysis and methylation on proteinaceous binders produce low intensity pyrolytic markers for this reason difficult to detect.⁸⁷ However an important marker has been detected in samples 2832 and 1866, Heptadecanenitrile, a marker associated with whole egg and particularly with egg yolk.^{45,88} Indole a degradation fragment of tryptophane,^{51,85} was also found in the same samples.

Cyclic dimers are observed for simple amino acids with no bulky side chains. 2,5-diketopiperazines (DKPs) are known to be important thermal condensation products of amino

amino acid mixtures and is formed from the dipeptide Pro-Pro, though it could not be found in the present samples, as it is common to coelute.⁸⁷

The pyrolysis of dipeptides or long peptides lead to the formation of the cyclic dipeptides piperazine-2,5-diones, these are formed by rearrangement of dipeptides by dehydration and cyclization.⁸⁷

The presence of palmitic and stearic acids alone, it is not enough to distinguish the presence of oil from egg, normal pyrolytic conditions lead to the formation mainly palmitic and stearic acid, but also a sequence of shorter chain acids, characterised with distribution similar from the lipidic fraction of the egg.^{85,90} The methylation thus enables the detection of azelaic and suberic acids,⁸⁵ this dicarboxylic acids have been reported to be less abundant in egg yolk than linseed oil in samples containing pigments possibly to the higher reactivity of bifunctional compounds during the aging process when there are in contact with other substances present in the layer.⁹⁰

In the “tempera grassa”, the content of fatty acids is very similar to that of egg binder except for an increase in dicarboxylic acids. To completely differentiate them, an statistical approach involving PCA is needed.⁸⁴

7 CONCLUSIONS

The range of techniques used has enabled to identify the use of inorganic pigments in each of the painted layers via the study of the recovered fragments.

By analysing the colours encountered in the double- and three-layered fragments, a change in colour scheme across each layer was detected.

A distinction in pigments could be made, a set of ochre and red fragments (groups 4/a, and 6/a) were identified as hematite, whereas goethite was identified in the fragments with colour hues ranging from yellow, orange, red, pink and brown. To obtain said colours, the mineral must have been heated.

The green colour pigment was identified as green earth, particularly glauconite, finally the blue pigment was identified as lazurite.

Indicating a rather austere palette, in terms of number of pigments, but with a budget as the lazurite mineral had not an extended use before the XIX century when the synthetic variety was developed.

As the FTIR and Raman analysis suggested the presence of binders, further analyses were made using Py-GC/MS in that enabled the identification of proteic and lipidic markers, though to completely identify the painting technique used as *tempera grassa* further studies with a statistical approach are suggested to be made.

- (1) Battaglini, N. *Torcello Antica e Moderna: Studii*; Online access with subscription: JISC Historical Texts; Marco Visentini, 1871.
- (2) Conton, L. *Torcello : il suo estuario e i suoi monumenti*; Bortoli: Venezia, 1927.
- (3) Calaon, D. Ecologia Della Venetia Prima Di Venezia: Uomini, Acqua e Archeologia. *Hortus Artium Medievalium* **2014**, *20* (2), 804–816. <https://doi.org/10.1484/J.HAM.5.102695>.
- (4) Calaon, D. *Quando Torcello era Abitata*; Regione del Veneto, 2013. <https://doi.org/10.13140/RG.2.1.4929.9680>.
- (5) Cattaneo, R. *L'architettura in Italia dal secolo VI al mille circa: ricerche storico-critiche*; Tip. emiliana, 1888.
- (6) *Per l'arte da Venezia all'Europa. 1: Dall'antichità al Caravaggio*; Arte documento Liber extra; Edizioni della Laguna: Monfalcone (Gorizia), 2001.
- (7) Agazzi, M. Torcello Medioevale, Scultura e Architettura. *Hortus Artium Medievalium* **2014**, *20* (2), 817–829. <https://doi.org/10.1484/J.HAM.5.102696>.
- (8) Fabbri, L. La Cripta Di Santa Maria Assunta a Torcello: Il Richiamo a Bizanzio All'Interno Della Politica Di Legittimazione Orseoliana Padova. Citazioni, modelli e tipologie nella produzione dell'opera d'arte. Atti delle Giornate di studio.29-30 maggio 2008 2011.
- (9) TORSMA 2020 Relazione tecnica sugli scavi. Assistenza archeologica alle opere di consolidamento e restauro della Basilica Rettoria di Santa Maria Assunta. Soprintendenza Archeologia, Belle Arti e Paesaggio per il Comune di Venezia e Laguna November 2020.
- (10) Project Report, Organic Materials in Wall Paintings. **2015**, 140.
- (11) Cuní, J. What Do We Know of Roman Wall Painting Technique? Potential Confounding Factors in Ancient Paint Media Analysis. *Herit Sci* **2016**, *4* (1), 44. <https://doi.org/10.1186/s40494-016-0111-4>.
- (12) Kakoulli, I. Late Classical and Hellenistic Painting Techniques and Materials: A Review of the Technical Literature. *Studies in Conservation* **2002**, *47* (Supplement-1), 56–67. <https://doi.org/10.1179/sic.2002.47.Supplement-1.56>.
- (13) Rosi, F.; Daveri, A.; Miliani, C.; Verri, G.; Benedetti, P.; Piqué, F.; Brunetti, B. G.; Sgamellotti, A. Non-Invasive Identification of Organic Materials in Wall Paintings by Fiber Optic Reflectance Infrared Spectroscopy: A Statistical Multivariate Approach. *Anal Bioanal Chem* **2009**, *395* (7), 2097–2106. <https://doi.org/10.1007/s00216-009-3108-y>.
- (14) Casoli, A. Research on the Organic Binders in Archaeological Wall Paintings. *Applied Sciences* **2021**, *11* (19), 9179. <https://doi.org/10.3390/app11199179>.
- (15) Murat, Z. Wall Paintings through the Ages: The Medieval Period (Italy, Twelfth to Fifteenth Century). *Archaeol Anthropol Sci* **2021**, *13* (11), 191. <https://doi.org/10.1007/s12520-021-01410-4>.
- (16) Casadio, F.; Giangualano, I.; Piqué, F. Organic Materials in Wall Paintings: The Historical and Analytical Literature. *Studies in Conservation* **2004**, *49* (sup1), 63–80. <https://doi.org/10.1179/sic.2004.49.Supplement-1.63>.
- (17) Siddall, R. Mineral Pigments in Archaeology: Their Analysis and the Range of Available Materials. *Minerals* **2018**, *8* (5), 201. <https://doi.org/10.3390/min8050201>.
- (18) Pomiés, M.-P.; Menu, M.; Vignaud, C. RED PALAEOOLITHIC PIGMENTS: NATURAL HEMATITE OR HEATED GOETHITE? *Archaeometry* **1999**, *41* (2), 275–285. <https://doi.org/10.1111/j.1475-4754.1999.tb00983.x>.
- (19) Bersani, D.; Lottici, P. P. Raman Spectroscopy of Minerals and Mineral Pigments in Archaeometry: Raman Spectroscopy of Minerals in Archaeometry. *J. Raman Spectrosc.* **2016**, *47* (5), 499–530. <https://doi.org/10.1002/jrs.4914>.
- (20) Costantini, I.; Castro, K.; Madariaga, J. M. Portable and Laboratory Analytical Instruments for the Study of Materials, Techniques and Environmental Impacts in

- Mediaeval Mural Paintings. *Anal. Methods* **2018**, *10* (40), 4854–4870. <https://doi.org/10.1039/C8AY00871J>.
- (21) Marucci, G.; Beeby, A.; Parker, A. W.; Nicholson, C. E. Raman Spectroscopic Library of Medieval Pigments Collected with Five Different Wavelengths for Investigation of Illuminated Manuscripts. *Anal. Methods* **2018**, *10* (10), 1219–1236. <https://doi.org/10.1039/C8AY00016F>.
- (22) Marić-Stojanović, M.; Bajuk-Bogdanović, D.; Uskoković-Marković, S.; Holclajtner-Antunović, I. Spectroscopic Analysis of XIV Century Wall Paintings from Patriarchate of Peć Monastery, Serbia. *Spectrochimica Acta Part A: Molecular and Biomolecular Spectroscopy* **2018**, *191*, 469–477. <https://doi.org/10.1016/j.saa.2017.10.043>.
- (23) Madariaga, J. M. Analytical Chemistry in the Field of Cultural Heritage. *Anal. Methods* **2015**, *7* (12), 4848–4876. <https://doi.org/10.1039/C5AY00072F>.
- (24) Cucci, C.; Casini, A. Hyperspectral Imaging for Artworks Investigation. In *Data Handling in Science and Technology*; Elsevier, 2020; Vol. 32, pp 583–604. <https://doi.org/10.1016/B978-0-444-63977-6.00023-7>.
- (25) Liang, H.; Keita, K.; Vajzovic, T. PRISMS: A Portable Multispectral Imaging System for Remote in Situ Examination of Wall Paintings; Fotakis, C., Pezzati, L., Salimbeni, R., Eds.; Munich, Germany, 2007; p 661815. <https://doi.org/10.1117/12.726034>.
- (26) Fischer, C.; Kakoulli, I. Multispectral and Hyperspectral Imaging Technologies in Conservation: Current Research and Potential Applications. *Studies in Conservation* **2006**, *51* (sup1), 3–16. <https://doi.org/10.1179/sic.2006.51.Supplement-1.3>.
- (27) Cucci, C.; Picollo, M.; Chiarantini, L.; Uda, G.; Fiori, L.; De Nigris, B.; Osanna, M. Remote-Sensing Hyperspectral Imaging for Applications in Archaeological Areas: Non-Invasive Investigations on Wall Paintings and on Mural Inscriptions in the Pompeii Site. *Microchemical Journal* **2020**, *158*, 105082. <https://doi.org/10.1016/j.microc.2020.105082>.
- (28) Picollo, M.; Cucci, C.; Casini, A.; Stefani, L. Hyper-Spectral Imaging Technique in the Cultural Heritage Field: New Possible Scenarios. *Sensors* **2020**, *20* (10), 2843. <https://doi.org/10.3390/s20102843>.
- (29) Cavaleri, T.; Giovagnoli, A.; Nervo, M. Pigments and Mixtures Identification by Visible Reflectance Spectroscopy. *Procedia Chemistry* **2013**, *8*, 45–54. <https://doi.org/10.1016/j.proche.2013.03.007>.
- (30) Dupuis, G.; Elias, M.; Simonot, L. Pigment Identification by Fiber-Optics Diffuse Reflectance Spectroscopy. *Appl Spectrosc* **2002**, *56* (10), 1329–1336. <https://doi.org/10.1366/000370202760354803>.
- (31) Derrick, M. R.; Stulik, D.; Landry, J. M. *Infrared Spectroscopy in Conservation Science*; Scientific tools for conservation; Getty Conservation Institute: Los Angeles, 1999.
- (32) Bitossi, G.; Giorgi, R.; Mauro, M.; Salvadori, B.; Dei, L. Spectroscopic Techniques in Cultural Heritage Conservation: A Survey. *Applied Spectroscopy Reviews* **2005**, *40* (3), 187–228. <https://doi.org/10.1081/ASR-200054370>.
- (33) La Russa, M. F.; Ruffolo, S. A.; Barone, G.; Crisci, G. M.; Mazzoleni, P.; Pezzino, A. The Use of FTIR and Micro-FTIR Spectroscopy: An Example of Application to Cultural Heritage. *International Journal of Spectroscopy* **2009**, *2009*, 1–5. <https://doi.org/10.1155/2009/893528>.
- (34) Franquelo, M. L.; Duran, A.; Herrera, L. K.; Jimenez de Haro, M. C.; Perez-Rodriguez, J. L. Comparison between Micro-Raman and Micro-FTIR Spectroscopy Techniques for the Characterization of Pigments from Southern Spain Cultural Heritage. *Journal of Molecular Structure* **2009**, *924–926*, 404–412. <https://doi.org/10.1016/j.molstruc.2008.11.041>.
- (35) Prati, S.; Joseph, E.; Sciutto, G.; Mazzeo, R. New Advances in the Application of FTIR Microscopy and Spectroscopy for the Characterization of Artistic Materials. *Acc. Chem. Res.* **2010**, *43* (6), 792–801. <https://doi.org/10.1021/ar900274f>.

- (36) Bell, J.; Nel, P.; Stuart, B. Non-Invasive Identification of Polymers in Cultural Heritage Collections: Evaluation, Optimisation and Application of Portable FTIR (ATR and External Reflectance) Spectroscopy to Three-Dimensional Polymer-Based Objects. *Herit Sci* **2019**, *7* (1), 95. <https://doi.org/10.1186/s40494-019-0336-0>.
- (37) Casadio, F.; Toniolo, L. The Analysis of Polychrome Works of Art: 40 Years of Infrared Spectroscopic Investigations. *Journal of Cultural Heritage* **2001**, *2* (1), 71–78. [https://doi.org/10.1016/S1296-2074\(01\)01107-4](https://doi.org/10.1016/S1296-2074(01)01107-4).
- (38) Kendix, E. L.; Prati, S.; Mazzeo, R.; Joseph, E.; Sciutto, G.; Fagnano, C. Far Infrared Spectroscopy in the Field of Cultural Heritage. **2010**, *7*.
- (39) Poliszuk, A.; Ybarra, G. ANALYSIS OF CULTURAL HERITAGE MATERIALS BY INFRARED SPECTROSCOPY. **19**.
- (40) Raman Spectroscopy in Cultural Heritage: Background Paper. *Anal. Methods* **2015**, *7* (12), 4844–4847. <https://doi.org/10.1039/C5AY90036K>.
- (41) Caggiani, M. C.; Colomban, P. Raman Microspectroscopy for Cultural Heritage Studies. *Physical Sciences Reviews* **2018**, *3* (11). <https://doi.org/10.1515/psr-2018-0007>.
- (42) Casadio, F.; Daher, C.; Bellot-Gurlet, L. Raman Spectroscopy of Cultural Heritage Materials: Overview of Applications and New Frontiers in Instrumentation, Sampling Modalities, and Data Processing. *Top Curr Chem (Z)* **2016**, *374* (5), 62. <https://doi.org/10.1007/s41061-016-0061-z>.
- (43) Analytical Pyrolysis in Cultural Heritage. *Anal. Methods* **2018**, *10* (46), 5463–5467. <https://doi.org/10.1039/C8AY90151A>.
- (44) Colombini, M. P.; Modugno, F. Characterisation of Proteinaceous Binders in Artistic Paintings by Chromatographic Techniques. *J. Sep. Science* **2004**, *27* (3), 147–160. <https://doi.org/10.1002/jssc.200301625>.
- (45) Bonaduce, I.; Andreotti, A. Py-GC/MS of Organic Paint Binders. In *Organic Mass Spectrometry in Art and Archaeology*; Colombini, M. P., Modugno, F., Eds.; John Wiley & Sons, Ltd: Chichester, UK, 2009; pp 303–326. <https://doi.org/10.1002/9780470741917.ch11>.
- (46) Sam, K. D.; Wampler, T. P. *Analytical Pyrolysis Handbook*; CRC Press, 2021.
- (47) Tamburini, D.; Iucejko, J. J.; Ribechini, E.; Colombini, M. P. New Markers of Natural and Anthropogenic Chemical Alteration of Archaeological Lignin Revealed by in Situ Pyrolysis/Silylation-Gas Chromatography-mass Spectrometry. *Journal of Analytical and Applied Pyrolysis* **2016**, *118*, 249–258. <https://doi.org/10.1016/j.jaap.2016.02.008>.
- (48) Degano, I.; Modugno, F.; Bonaduce, I.; Ribechini, E.; Colombini, M. P. Recent Advances in Analytical Pyrolysis to Investigate Organic Materials in Heritage Science. *Angew. Chem. Int. Ed.* **2018**, *57* (25), 7313–7323. <https://doi.org/10.1002/anie.201713404>.
- (49) La Nasa, J.; Biale, G.; Ferriani, B.; Colombini, M. P.; Modugno, F. A Pyrolysis Approach for Characterizing and Assessing Degradation of Polyurethane Foam in Cultural Heritage Objects. *Journal of Analytical and Applied Pyrolysis* **2018**, *134*, 562–572. <https://doi.org/10.1016/j.jaap.2018.08.004>.
- (50) Tamburini, D. Analytical Pyrolysis Applied to the Characterisation and Identification of Asian Lacquers in Cultural Heritage Samples – A Review. *Journal of Analytical and Applied Pyrolysis* **2021**, *157*, 105202. <https://doi.org/10.1016/j.jaap.2021.105202>.
- (51) Chiavari, G.; Gandini, N.; Russo, P.; Fabbri, D. Characterisation of Standard Tempera Painting Layers Containing Proteinaceous Binders by Pyrolysis (/Methylation)-Gas Chromatography-Mass Spectrometry. *Chromatographia* **1998**, *47* (7–8), 420–426. <https://doi.org/10.1007/BF02466473>.
- (52) Chiavari, G.; Fabbri, D.; Galletti, G. C.; Mazzeo, R. Use of Analytical Pyrolysis to Characterize Egyptian Painting Layers. *Chromatographia* **1995**, *40* (9–10), 594–600. <https://doi.org/10.1007/BF02290274>.
- (53) Čukovska, L. R.; Minčeva – Šukarova, B.; Lluveras-Tenorio, A.; Andreotti, A.; Colombini, M. P.; Nastova, I. Micro-Raman and GC/MS Analysis to Characterize the Wall Painting

- Technique of Dicho Zograph in Churches from Republic of Macedonia. *J. Raman Spectrosc.* **2012**, *43* (11), 1685–1693. <https://doi.org/10.1002/jrs.4183>.
- (54) Germinario, G.; van der Werf, I. D.; Sabbatini, L. Chemical Characterisation of Spray Paints by a Multi-Analytical (Py/GC–MS, FTIR, μ -Raman) Approach. *Microchemical Journal* **2016**, *124*, 929–939. <https://doi.org/10.1016/j.microc.2015.04.016>.
- (55) Dorez, G.; Otazaghine, B.; Taguet, A.; Ferry, L.; Lopez-Cuesta, J. M. Use of Py-GC/MS and PCFC to Characterize the Surface Modification of Flax Fibres. *Journal of Analytical and Applied Pyrolysis* **2014**, *105*, 122–130. <https://doi.org/10.1016/j.jaap.2013.10.011>.
- (56) Grabowska, B.; Kaczmarska, K.; Bobrowski, A.; Żymankowska-Kumon, S.; Kurleto-Kozioł, Ż. TG-DTG-DSC, FTIR, DRIFT and Py-GC-MS Studies of Thermal Decomposition for Poly(Sodium Acrylate)/Dextrin (PAANA/D) – New Binder BioCo3. *jcme* **2017**, *1* (1), 27. <https://doi.org/10.7494/jcme.2017.1.1.27>.
- (57) The Color of Soil | NRCS Soils https://www.nrcs.usda.gov/wps/portal/nrcs/detail/soils/edu/?cid=nrcs142p2_054286 (accessed 2021 -07 -08).
- (58) Bruni, S.; Caglio, S.; Guglielmi, V.; Poldi, G. The Joined Use of n.i. Spectroscopic Analyses – FTIR, Raman, Visible Reflectance Spectrometry and EDXRF – to Study Drawings and Illuminated Manuscripts. *Appl. Phys. A* **2008**, *92* (1), 103–108. <https://doi.org/10.1007/s00339-008-4454-x>.
- (59) Guglielmi, V.; Comite, V.; Andreoli, M.; Demartin, F.; Lombardi, C. A.; Fermo, P. Pigments on Roman Wall Painting and Stucco Fragments from the Monte d’Oro Area (Rome): A Multi-Technique Approach. *Applied Sciences* **2020**, *10* (20), 7121. <https://doi.org/10.3390/app10207121>.
- (60) Pearson, N. C.; Livo, K. E.; Driscoll, R. L.; Lowers, H. A.; Hoefen, T. M.; Swayze, G. A.; Klein, A. J.; Kokaly, R. F.; Wise, R. A.; Benzel, W. M.; Clark, R. N. USGS Spectral Library Version 7 Data, 2017. <https://doi.org/10.5066/F7RR1WDJ>.
- (61) Guglielmi, V.; Andreoli, M.; Comite, V.; Baroni, A.; Fermo, P. The Combined Use of SEM-EDX, Raman, ATR-FTIR and Visible Reflectance Techniques for the Characterisation of Roman Wall Painting Pigments from Monte d’Oro Area (Rome): An Insight into Red, Yellow and Pink Shades. *Environ Sci Pollut Res* **2021**. <https://doi.org/10.1007/s11356-021-15085-w>.
- (62) Bersani, D.; Berzioli, M.; Caglio, S.; Casoli, A.; Lottici, P. P.; Medeghini, L.; Poldi, G.; Zannini, P. An Integrated Multi-Analytical Approach to the Study of the Dome Wall Paintings by Correggio in Parma Cathedral. *Microchemical Journal* **2014**, *114*, 80–88. <https://doi.org/10.1016/j.microc.2013.11.014>.
- (63) Cheilakou, E.; Troullinos, M.; Kouli, M. Identification of Pigments on Byzantine Wall Paintings from Crete (14th Century AD) Using Non-Invasive Fiber Optics Diffuse Reflectance Spectroscopy (FORS). *Journal of Archaeological Science* **2014**, *41*, 541–555. <https://doi.org/10.1016/j.jas.2013.09.020>.
- (64) Pallipurath, A.; Skelton, J.; Ricciardi, P.; Bucklow, S.; Elliott, S. Multivariate Analysis of Combined Raman and Fibre-Optic Reflectance Spectra for the Identification of Binder Materials in Simulated Medieval Paints: Multivariate Analysis of Combined Raman and Fibre-Optic Reflectance. *J. Raman Spectrosc.* **2013**, *44* (6), 866–874. <https://doi.org/10.1002/jrs.4291>.
- (65) de Faria, D. L. A.; Lopes, F. N. Heated Goethite and Natural Hematite: Can Raman Spectroscopy Be Used to Differentiate Them? *Vibrational Spectroscopy* **2007**, *45* (2), 117–121. <https://doi.org/10.1016/j.vibspec.2007.07.003>.
- (66) Legodi, M.; Dewaal, D. The Preparation of Magnetite, Goethite, Hematite and Maghemite of Pigment Quality from Mill Scale Iron Waste. *Dyes and Pigments* **2007**, *74* (1), 161–168. <https://doi.org/10.1016/j.dyepig.2006.01.038>.
- (67) Gialanella, S.; Belli, R.; Dalmeri, G.; Lonardelli, I.; Mattarelli, M.; Montagna, M.; Toniutti, L. ARTIFICIAL OR NATURAL ORIGIN OF HEMATITE-BASED RED PIGMENTS IN

- ARCHAEOLOGICAL CONTEXTS: THE CASE OF RIPARO DALMERI (TRENTO, ITALY): Origin of Hematite-Based Red Pigments. *Archaeometry* **2011**, 53 (5), 950–962. <https://doi.org/10.1111/j.1475-4754.2011.00594.x>.
- (68) Bell, I. M.; Clark, R. J. H.; Gibbs, P. J. Raman Spectroscopic Library of Natural and Synthetic Pigments (Pre- ≈ 1850 AD). *Spectrochimica Acta Part A: Molecular and Biomolecular Spectroscopy* **1997**, 53 (12), 2159–2179. [https://doi.org/10.1016/S1386-1425\(97\)00140-6](https://doi.org/10.1016/S1386-1425(97)00140-6).
- (69) Ospitali, F.; Bersani, D.; Di Lonardo, G.; Lottici, P. P. ‘Green Earths’: Vibrational and Elemental Characterization of Glauconites, Celadonites and Historical Pigments. *J. Raman Spectrosc.* **2008**, 39 (8), 1066–1073. <https://doi.org/10.1002/jrs.1983>.
- (70) Jorge-Villar, S. E.; Edwards, H. G. M. Green and Blue Pigments in Roman Wall Paintings: A Challenge for Raman Spectroscopy. *J Raman Spectrosc* **2021**, jrs.6118. <https://doi.org/10.1002/jrs.6118>.
- (71) Aliatis, I.; Bersani, D.; Campani, E.; Casoli, A.; Lottici, P. P.; Mantovan, S.; Marino, I.-G.; Ospitali, F. Green Pigments of the Pompeian Artists’ Palette. *Spectrochimica Acta Part A: Molecular and Biomolecular Spectroscopy* **2009**, 73 (3), 532–538. <https://doi.org/10.1016/j.saa.2008.11.009>.
- (72) Bicchieri, M.; Nardone, M.; Russo, P. A.; Sodo, A.; Corsi, M.; Cristoforetti, G.; Palleschi, V.; Salvetti, A.; Tognoni, E. Characterization of Azurite and Lazurite Based Pigments by Laser Induced Breakdown Spectroscopy and Micro-Raman Spectroscopy. *Spectrochimica Acta Part B: Atomic Spectroscopy* **2001**, 56 (6), 915–922. [https://doi.org/10.1016/S0584-8547\(01\)00228-2](https://doi.org/10.1016/S0584-8547(01)00228-2).
- (73) Zeng, Q. G.; Zhang, G. X.; Leung, C. W.; Zuo, J. Studies of Wall Painting Fragments from Kaiping Diaolou by SEM/EDX, Micro Raman and FT-IR Spectroscopy. *Microchemical Journal* **2010**, 96 (2), 330–336. <https://doi.org/10.1016/j.microc.2010.05.013>.
- (74) Bersani, D.; Antonioli, G.; Lottici, P. P.; Fornari, L.; Castrichini, M. Restoration of a Parmigianino’s Fresco: A Micro-Raman Investigation of the Pictorial Surface; Salimbeni, R., Ed.; Munich, Germany, 2001; p 221. <https://doi.org/10.1117/12.445667>.
- (75) Coccato, A.; Jehlicka, J.; Moens, L.; Vandenabeele, P. Raman Spectroscopy for the Investigation of Carbon-Based Black Pigments: Investigation of Carbon-Based Black Pigments. *J. Raman Spectrosc.* **2015**, 46 (10), 1003–1015. <https://doi.org/10.1002/jrs.4715>.
- (76) Vandenabeele, P.; Wehling, B.; Moens, L.; Edwards, H.; De Reu, M.; Van Hooydonk, G. Analysis with Micro-Raman Spectroscopy of Natural Organic Binding Media and Varnishes Used in Art. *Analytica Chimica Acta* **2000**, 407 (1–2), 261–274. [https://doi.org/10.1016/S0003-2670\(99\)00827-2](https://doi.org/10.1016/S0003-2670(99)00827-2).
- (77) Sarmiento, A.; Pérez-Alonso, M.; Olivares, M.; Castro, K.; Martínez-Arkarazo, I.; Fernández, L. A.; Madariaga, J. M. Classification and Identification of Organic Binding Media in Artworks by Means of Fourier Transform Infrared Spectroscopy and Principal Component Analysis. *Anal Bioanal Chem* **2011**, 399 (10), 3601–3611. <https://doi.org/10.1007/s00216-011-4677-0>.
- (78) Vornicu, N.; Bibire, C.; Murariu, E.; Ivanov, D. Analysis of Mural Paintings Using *in Situ* Non-Invasive XRF, FTIR Spectroscopy and Optical Microscopy: Analysis of Mural Paintings Using *in Situ* Non-Invasive XRF Portable. *X-Ray Spectrom.* **2013**, 42 (5), 380–387. <https://doi.org/10.1002/xrs.2459>.
- (79) González-Cabrera, M.; Domínguez-Vidal, A.; Ayora-Cañada, M. J. Monitoring UV-Accelerated Alteration Processes of Paintings by Means of Hyperspectral Micro-FTIR Imaging and Chemometrics. *Spectrochimica Acta Part A: Molecular and Biomolecular Spectroscopy* **2021**, 253, 119568. <https://doi.org/10.1016/j.saa.2021.119568>.
- (80) Haghghi, Z.; Karimy, A.-H.; Karami, F.; Bagheri Garmarudi, A.; Khanmohammadi, M. Infrared Spectroscopic and Chemometric Approach for Identifying Binding Medium in

- Sukias Mansion's Wall Paintings. *Natural Product Research* **2019**, *33* (7), 1052–1060. <https://doi.org/10.1080/14786419.2015.1108974>.
- (81) van der Weerd, J.; van Loon, A.; Boon, J. J. FTIR Studies of the Effects of Pigments on the Aging of Oil. *Studies in Conservation* **2005**, *50* (1), 3–22. <https://doi.org/10.1179/sic.2005.50.1.3>.
- (82) Navas, N.; Romero-Pastor, J.; Manzano, E.; Cardell, C. Benefits of Applying Combined Diffuse Reflectance FTIR Spectroscopy and Principal Component Analysis for the Study of Blue Tempera Historical Painting. *Analytica Chimica Acta* **2008**, *630* (2), 141–149. <https://doi.org/10.1016/j.aca.2008.10.008>.
- (83) Genestar, C.; Pons, C. Earth Pigments in Painting: Characterisation and Differentiation by Means of FTIR Spectroscopy and SEM-EDS Microanalysis. *Anal Bioanal Chem* **2005**, *382* (2), 269–274. <https://doi.org/10.1007/s00216-005-3085-8>.
- (84) Colombini, M. P.; Modugno, F.; Giacomelli, M.; Francesconi, S. Characterisation of Proteinaceous Binders and Drying Oils in Wall Painting Samples by Gas Chromatography–Mass Spectrometry. *Journal of Chromatography A* **1999**, *846* (1–2), 113–124. [https://doi.org/10.1016/S0021-9673\(99\)00344-1](https://doi.org/10.1016/S0021-9673(99)00344-1).
- (85) Chiavari, G.; Prati, S. Analytical Pyrolysis as Diagnostic Tool in the Investigation of Works of Art. **2003**, No. 9, 12.
- (86) Sotiropoulou, S.; Sciutto, G.; Tenorio, A. L.; Mazurek, J.; Bonaduce, I.; Prati, S.; Mazzeo, R.; Schilling, M.; Colombini, M. P. Advanced Analytical Investigation on Degradation Markers in Wall Paintings. *Microchemical Journal* **2018**, *139*, 278–294. <https://doi.org/10.1016/j.microc.2018.03.007>.
- (87) Chiavari, G.; Lanterna, G.; Luca, C.; Matteini, M.; Prati, S.; Sandu, I. C. A. Analysis of Proteinaceous Binders by In-Situ Pyrolysis and Silylation. *Chromatographia* **2003**, *57* (9–10), 645–648. <https://doi.org/10.1007/BF02491743>.
- (88) Orsini, S.; Parlanti, F.; Bonaduce, I. Analytical Pyrolysis of Proteins in Samples from Artistic and Archaeological Objects. *Journal of Analytical and Applied Pyrolysis* **2017**, *124*, 643–657. <https://doi.org/10.1016/j.jaap.2016.12.017>.
- (89) Chiavari, G.; Fabbri, D.; Prati, S. Gas Chromatographic–Mass Spectrometric Analysis of Products Arising from Pyrolysis of Amino Acids in the Presence of Hexamethyldisilazane. *Journal of Chromatography A* **2001**, *922* (1–2), 235–241. [https://doi.org/10.1016/S0021-9673\(01\)00936-0](https://doi.org/10.1016/S0021-9673(01)00936-0).
- (90) Chiavari, G.; Galletti, G. C.; Lanterna, G.; Mazzeo, R. The Potential of Pyrolysis—Gas Chromatography/Mass Spectrometry in the Recognition of Ancient Painting Media. *Journal of Analytical and Applied Pyrolysis* **1993**, *24* (3), 227–242. [https://doi.org/10.1016/0165-2370\(93\)85003-H](https://doi.org/10.1016/0165-2370(93)85003-H).

9 ANNEX 1

ID	US	Group_class	Main_pictorial_layer	Main_color	Munsell_code	Average_surface_cm ²	Plaster_thickness	Plaster_color	Plaster_munsell	Paint_layers	Dino	Specim	FORS	Raman	IR
TORSMA2020_0436	1816	5	1820	ochre	10YR 6/8	8.64	0.6	grey	5Y8/1	1	Y	Y	N	N	N
TORSMA2020_1266	1814	2	1820	blue	5PB 2.5/1	17.4	0.7	grey	5Y8/1	1	Y	Y	N	N	N
TORSMA2020_1274	1814	14	1820	light greyish green	5GY 3/2	11.61	1.3	grey	5Y8/1	1	Y	Y	N	N	N
TORSMA2020_1290	1814	14	1821	light greyish green	5GY 3/2	12.96	0.8	grey	5Y8/1	1	Y	Y	Y	N	N
TORSMA2020_1296	1814	2	1820	blue	5PB 2.5/1	15	0.6	grey	5Y8/1	1	Y	Y	N	N	N
TORSMA2020_1321	1814	25	1821	bluish grey	10B 6/1	6.21	0.7	white	10YR9.5/2	2	Y	Y	N	N	N
TORSMA2020_1348	1814	15	1821	red green yellow grey	10YR 2/1	7.14	0.7	white	10YR9.5/2	1	Y	Y	N	N	N
TORSMA2020_1365	1814	1	1820	green	5G 2.5/2	4.5	1.2	grey	5Y8/1	1	Y	Y	N	N	N
TORSMA2020_1384	1814	13	1821	blue grey	10B 4/1	21.08	0.6	white	10YR9.5/2	1	Y	Y	Y	Y	Y
TORSMA2020_1407	1814	2	1821	blue	5PB 2.5/1	12.71	0.7	white	10YR9.5/2	1	Y	Y	N	N	N
TORSMA2020_1423	1814	2	1820	blue	5PB 2.5/1	49.41	0.6	grey	5Y8/1	1	Y	Y	Y	Y	Y
TORSMA2020_1443	1814	1	1820	green	5G 2.5/2	5.46	0.4	grey	5Y8/1	2	Y	Y	N	N	N
TORSMA2020_1444	1814	3	1821	blue-black	N 3/	7.2	0.5	white	10YR9.5/2	2	Y	Y	N	N	N
TORSMA2020_1450	1814	1	1820	green	5G 2.5/2	2.75	0.1	grey	5Y8/1	2	Y	Y	N	N	N
TORSMA2020_1451	1814	3	1821	blue-black	N 3/	14.26	0.8	white	10YR9.5/2	2	Y	Y	N	N	N
TORSMA2020_1458	1814	1	1820	green	5G 2.5/2	4.06	0.3	grey	5Y8/1	2	Y	Y	N	N	N
TORSMA2020_1459	1814	3	1821	blue-black	N 3/	4.25	0.6	white	10YR9.5/2	2	Y	Y	N	N	N
TORSMA2020_1476	1814	26	1821	dark reddish grey	5YR 4/2	18.24	0.7	white	10YR9.5/2	1	Y	Y	Y	N	N
TORSMA2020_1486	1814	26	1821	dark reddish grey	5YR 4/2	12.92	0.9	white	10YR9.5/2	1	Y	Y	Y	N	N
TORSMA2020_1493	1814	26	1821	dark reddish grey	5YR 4/2	12.04	0.8	white	10YR9.5/2	1	Y	Y	N	N	N
TORSMA2020_1494	1814	14	1821	light greyish green	5GY 3/2	9.52	0.5	white	10YR9.5/2	1	Y	Y	N	N	N
TORSMA2020_1500	1814	13	1821	blue grey	10B 4/1	35.1	1.6	white	10YR9.5/2	1	Y	Y	Y	N	Y
TORSMA2020_1505	1814	19	1820	greyish green	5G 4/2	6.96	0.9	grey	5Y8/1	1	Y	Y	N	N	N
TORSMA2020_1512	1814	26	1821	dark reddish grey	5YR 4/2	25.6	1	white	10YR9.5/2	1	Y	Y	N	N	N
TORSMA2020_1514	1814	26	1821	dark reddish grey	5YR 4/2	16.4	1.1	white	10YR9.5/2	1	Y	Y	Y	N	N
TORSMA2020_1526	1814	15	1821	red green yellow grey	10YR 2/1	8.84	0.8	white	10YR9.5/2	1	Y	Y	N	N	N
TORSMA2020_1532	1814	26	1821	dark reddish grey	5YR 4/2	52.93	1.1	white	10YR9.5/2	1	Y	Y	Y	N	N
TORSMA2020_1539	1814	16	1821	ochre	7.5YR 5/6	9.24	0.8	white	10YR9.5/2	1	Y	Y	N	N	N
TORSMA2020_1543	1814	4	1821	ochre	7.5YR 5/6	10.71	0.8	white	10YR9.5/2	1	Y	Y	N	N	N
TORSMA2020_1560	1814	3	1821	blue-black	N 3/	11.84	0.7	white	10YR9.5/2	1	Y	Y	Y	N	N
TORSMA2020_1575	1814	13	1821	blue grey	10B 4/1	6.6	1	white	10YR9.5/2	1	Y	Y	N	N	N
TORSMA2020_1585	1814	2	1821	blue	5PB 2.5/1	10.15	1.5	white	10YR9.5/2	1	Y	Y	N	N	N
TORSMA2020_1607	1814	3	1820	blue-black	N 3/	5.2	0.4	grey	5Y8/1	1	Y	Y	N	N	N

TORSMA2020_1611	18 14	3	182 0	blue-black	N 3/	7.38	0. 8	gre y	5Y8/1	1	Y	Y	N	N	N
TORSMA2020_1629	18 14	1 4	182 1	light greyish green	5GY 3/2	26.7 9	1	whi te	10YR9. 5/2	1	Y	Y	Y	N	N
TORSMA2020_1641	18 14	1 4	182 1	blue	5PB 3/1	24	1. 1	whi te	10YR9. 5/2	1	Y	Y	Y	N	N
TORSMA2020_1643	18 14	2 7	182 0	red	2.5YR 5/8	12.7 6	0. 7	gre y	5Y8/1	1	Y	Y	Y	N	N
TORSMA2020_1644	18 14	1 2	182 0	bluish black	10B 2.5/1	13.1 6	1. 2	gre y	5Y8/1	1	Y	N	Y	N	N
TORSMA2020_1647	18 14	1 2	182 0	bluish black	10B 2.5/1	22.0 5	1. 6	gre y	5Y8/1	1	Y	N	N	N	N
TORSMA2020_1648	18 14	1 2	182 0	bluish black	10B 2.5/1	458. 2	1. 2	gre y	5Y8/1	1	Y	Y	N	N	N
TORSMA2020_1653	18 14	9	182 0	light reddish brown	2.5YR 6/4	9.86	0. 7	gre y	5Y8/1	1	Y	Y	N	N	N
TORSMA2020_1660	18 14	8	182 0	greenish grey	5G 6/1	9.8	0. 7	gre y	5Y8/1	1	Y	Y	Y	N	N
TORSMA2020_1671	18 14	8	182 0	greenish grey	5G 6/1	19.6	0. 5	gre y	5Y8/1	2	Y	Y	N	N	N
TORSMA2020_1674	18 14	8	182 0	greenish grey	5G 6/1	5.7	0. 4	gre y	5Y8/1	1	Y	Y	N	N	N
TORSMA2020_1676	18 14	8	182 0	greenish grey	5G 6/1	8.64	0. 5	whi te	10YR9. 5/2	1	Y	Y	N	N	N
TORSMA2020_1677	18 14	2 1	182 1	light grey	N 7/	4.08	1. 3	gre y	5Y8/1	1	Y	Y	N	N	N
TORSMA2020_1681	18 14	1 9	182 0	greyish green	5G 4/2	11.2	0. 9	gre y	5Y8/1	1	Y	Y	Y	Y	N
TORSMA2020_1686	18 14	5	182 0	ochre	10YR 6/8	20.0 9	0. 5	gre y	5Y8/1	2	Y	Y	N	Y	Y
TORSMA2020_1691	18 14	5	182 0	ochre	10YR 6/8	12.7 1	1	gre y	5Y8/1	1	Y	Y	Y	N	N
TORSMA2020_1698	18 14	2 0	182 1	yellow	10YR 7/8	7.2	0. 8	whi te	10YR9. 5/2	1	Y	Y	N	N	N
TORSMA2020_1702	18 14	2 0	182 0	yellow	10YR 7/8	8.96	0. 4	gre y	5Y8/1	1	Y	Y	N	N	N
TORSMA2020_1711	18 14	2 0	182 1	yellow	10YR 7/8	7.83	0. 5	gre y	5Y8/1	1	Y	Y	N	N	N
TORSMA2020_1713	18 14	1 5	182 1	red green yellow grey	10YR 2/1	10.4	1. 2	gre y	5Y8/1	1	Y	Y	N	N	N
TORSMA2020_1726	18 14	7	182 1	red	2.5YR 3/6	25.2	0. 9	whi te	10YR9. 5/2	1	Y	Y	Y	N	N
TORSMA2020_1730	18 14	6	182 0	red	10R 4/6	13.7 2	0. 6	gre y	5Y8/1	1	Y	Y	N	N	N
TORSMA2020_1754	18 14	1 5	182 0	red green yellow grey	10YR 2/1	13.5 3	1. 1	whi te	10YR9. 5/2	1	Y	Y	Y	N	N
TORSMA2020_1776	18 14	7	182 1	red	2.5YR 3/6	6.6	0. 8	whi te	10YR9. 5/2	1	Y	Y	N	N	N
TORSMA2020_1785	18 14	2 8	182 1	black	2.5Y 2.5/1	5.28	0. 4	whi te	10YR9. 5/2	1	Y	Y	N	N	N
TORSMA2020_1787	18 14	2 8	182 1	black	2.5Y 2.5/1	6.84	0. 9	whi te	10YR9. 5/2	1	Y	Y	N	N	N
TORSMA2020_1791	18 14	1 3	182 1	blue grey	10B 4/1	8	0. 7	whi te	10YR9. 5/2	1	Y	Y	N	N	N
TORSMA2020_1794	18 14	2 8	182 1	black	2.5Y 2.5/1	7.98	0. 6	whi te	10YR9. 5/2	1	Y	Y	N	N	N
TORSMA2020_1795	18 14	2 8	182 1	black	2.5Y 2.5/1	9.84	1. 2	whi te	10YR9. 5/2	1	Y	Y	N	N	N
TORSMA2020_1796	18 14	2 8	182 1	black	2.5Y 2.5/1	5.5	0. 5	whi te	10YR9. 5/2	1	Y	Y	N	N	N
TORSMA2020_1797	18 14	2 8	182 0	black	2.5Y 2.5/1	9.86	0. 4	gre y	5Y8/1	1	Y	Y	N	N	N
TORSMA2020_1799	18 14	2 8	182 0	black	2.5Y 2.5/1	4.14	0. 5	gre y	5Y8/1	1	Y	Y	N	N	N
TORSMA2020_1803	18 14	3	182 1	blue-black	N 3/	1.1	0. 1	gre y	5Y8/1	1	Y	Y	N	N	N
TORSMA2020_1806	18 14	2 8	182 1	black	2.5Y 2.5/1	8.64	0. 6	whi te	10YR9. 5/2	1	Y	Y	Y	N	N
TORSMA2020_1807	18 14	2 8	182 1	black	2.5Y 2.5/1	5.88	0. 5	whi te	10YR9. 5/2	1	Y	Y	N	N	N
TORSMA2020_1808	18 14	9	182 0	light reddish brown	2.5YR 6/4	24.9 6	0. 8	gre y	5Y8/1	1	Y	Y	Y	Y	Y
TORSMA2020_1811	18 14	2 4	182 0	pale red	7.5R6/4	14.5 7	0. 5	gre y	5Y8/1	1	Y	Y	N	N	N
TORSMA2020_1818	18 14	9	182 0	light reddish brown	2.5YR 6/4	9.18	0. 7	gre y	5Y8/1	1	Y	Y	N	N	N
TORSMA2020_1819	18 14	9	182 0	light reddish brown	2.5YR 6/4	5.75	0. 8	gre y	5Y8/1	1	Y	Y	N	N	N

TORSMA2020_1824	18 14	9	182 1	light reddish brown	2.5YR 6/4	17.2 8	0. 5	whi te	10YR9. 5/2	1	Y	Y	N	N	N
TORSMA2020_1825	18 14	1 7	182 0	dusky red	10R 3/2	7.2	0. 6	gre y	5Y8/1	1	Y	Y	Y	N	N
TORSMA2020_1833	18 14	3	182 0	blue-black	N 3/	22.6 3	0. 6	gre y	5Y8/1	2	Y	Y	N	N	N
TORSMA2020_1841	18 14	1 0	182 1	reddish-black	5R 2.5/1	11.2	0. 5	whi te	10YR9. 5/2	1	Y	Y	N	N	N
TORSMA2020_1843	18 14	1 0	182 1	reddish-black	5R 2.5/1	8.61	0. 8	whi te	10YR9. 5/2	1	Y	Y	N	N	N
TORSMA2020_1844	18 14	1 0	182 1	reddish-black	5R 2.5/1	10.5	0. 7	whi te	10YR9. 5/2	1	Y	Y	N	N	N
TORSMA2020_1849	18 14	1 0	182 1	reddish-black	5R 2.5/1	15.5 4	0. 8	whi te	10YR9. 5/2	1	Y	Y	Y	Y	N
TORSMA2020_1859	18 14	1 1	182 1	dark reddish grey	2.5YR 4/1	15.4 8	1. 3	whi te	10YR9. 5/2	1	Y	Y	N	N	N
TORSMA2020_1866	18 14	1 4	182 1	light greyish green	5GY 3/2	17	0. 9	whi te	10YR9. 5/2	1	Y	Y	Y	Y	Y
TORSMA2020_1875	18 14	2 7	182 1	black	10G 2.5/1	11.0 7	0. 9	whi te	10YR9. 5/2	1	Y	Y	N	N	N
TORSMA2020_1877	18 14	1 4	182 1	light greyish green	5GY 3/2	8.1	0. 6	whi te	10YR9. 5/2	1	Y	Y	N	N	N
TORSMA2020_1879	18 14	1 4	182 1	light greyish green	5GY 3/2	11.4 7	0. 7	whi te	10YR9. 5/2	1	Y	Y	N	N	N
TORSMA2020_1898	18 14	2 9	182 1	light greyish olive	10Y 6/2	11.5 5	1	whi te	10YR9. 5/2	1	Y	N	N	N	N
TORSMA2020_1915	18 14	2 3	182 1	white	10YR 9.5/1	5.13	0. 7	whi te	10YR9. 5/2	1	Y	Y	N	N	N
TORSMA2020_1916	18 14	2 3	182 0	white	10YR 9.5/1	6.9	0. 9	gre y	5Y8/1	1	Y	Y	N	N	N
TORSMA2020_1918	18 14	2 0	182 0	yellow	10YR 7/8	10.8	0. 7	whi te	10YR9. 5/2	1	Y	Y	N	N	N
TORSMA2020_1919	18 14	2 3	182 1	white	10YR 9.5/1	28.8	0. 7	whi te	10YR9. 5/2	1	Y	Y	N	N	N
TORSMA2020_1924	18 14	2 3	182 0	white	10YR 9.5/1	12.9	0. 5	gre y	5Y8/1	1	Y	Y	N	N	N
TORSMA2020_1926	18 14	1 9	182 0	greyish green	5G 4/2	7.2	0. 7	whi te	10YR9. 5/2	1	Y	Y	N	N	N
TORSMA2020_1928	18 14	9	182 0	light reddish brown	2.5YR 6/4	41.3 1	1	gre y	5Y8/1	1	Y	Y	N	N	N
TORSMA2020_1934	18 14	1 1	182 0	dark reddish grey	2.5YR 4/1	12.9 6	1	gre y	5Y8/1	1	Y	Y	N	N	N
TORSMA2020_1939	18 14	7	182 1	red	2.5YR 3/6	5.76	0. 6	whi te	10YR9. 5/2	1	Y	Y	N	N	N
TORSMA2020_1956	18 14	6	182 1	red	10R 4/6	15.3 6	0. 8	whi te	10YR9. 5/2	1	Y	Y	Y	N	N
TORSMA2020_1959	18 14	7	182 1	red	2.5YR 3/6	6.16	0. 8	whi te	10YR9. 5/2	1	Y	Y	N	N	N
TORSMA2020_1970	18 14	6	182 0	red	10R 4/6	8.97	0. 3	gre y	5Y8/1	2	Y	Y	N	N	N
TORSMA2020_1973	18 14	6	182 0	red	10R 4/6	10.4 4	0. 7	gre y	5Y8/1	1	Y	Y	Y	N	N
TORSMA2020_1979	18 14	2 0	182 0	yellow	10YR 7/8	5.8	0. 4	gre y	5Y8/1	1	Y	Y	N	N	N
TORSMA2020_1980	18 14	3 0	182 0	reddish yellow	7.5YR 6/6	14.7	0. 4	gre y	5Y8/1	2	Y	Y	N	N	N
TORSMA2020_1982	18 14	1	182 0	green	5G 2.5/2	21.2	0. 6	gre y	5Y8/1	2	Y	Y	Y	N	N
TORSMA2020_1986	18 14	3 0	182 0	reddish yellow	7.5YR 6/6	13.7 6	0. 4	gre y	5Y8/1	2	Y	Y	Y	N	N
TORSMA2020_1993	18 14	3 0	182 0	reddish yellow	7.5YR 6/6	12.7 4	0. 6	gre y	5Y8/1	2	Y	Y	N	N	N
TORSMA2020_1995	18 14	5	182 0	ochre	10YR 6/8	5.88	0. 3	gre y	5Y8/1	2	Y	Y	N	N	N
TORSMA2020_2001	18 14	1 6	182 1	strong brown	7.5YR 4/6	18.0 6	0. 5	whi te	10YR9. 5/2	2	Y	Y	N	N	N
TORSMA2020_2006	18 14	1	182 0	green	5G 2.5/2	6.6	0. 5	gre y	5Y8/1	1	Y	Y	N	N	N
TORSMA2020_2011	18 14	5	182 0	ochre	10YR 6/8	7.92	0. 8	gre y	5Y8/1	1	Y	Y	N	N	N
TORSMA2020_2024	18 14	5	182 0	ochre	10YR 6/8	5.76	0. 9	gre y	5Y8/1	1	Y	Y	N	N	N
TORSMA2020_2028	18 14	6	182 1	red	10R 4/6	35.7 7	0. 7	whi te	10YR9. 5/2	1	Y	Y	N	N	N
TORSMA2020_2034	18 14	3 1	182 1	very dark greenish grey	10GY 3/1	16.5	0. 6	whi te	10YR9. 5/2	1	Y	Y	Y	N	N
TORSMA2020_2053	18 14	1 3	182 1	blue grey	10B 4/1	15.9 8	0. 9	whi te	10YR9. 5/2	1	Y	Y	Y	Y	Y

TORSMA2020_2059	18 14	2	182 1	blue	5PB 2.5/1	17.1	0. 7	whi te	10YR9. 5/2	1	Y	Y	N	N	N
TORSMA2020_2062	18 14	2	182 0	blue	5PB 2.5/1	13.4 4	0. 5	gre y	5Y8/1	2	Y	Y	N	N	N
TORSMA2020_2063	18 14	6	182 1	red	10R 4/6	8.64	0. 4	whi te	10YR9. 5/2	2	Y	Y	N	N	N
TORSMA2020_2068	18 14	1	182 0	green	5G 2.5/2	10.4	0. 6	gre y	5Y8/1	1	Y	Y	N	N	N
TORSMA2020_2076	18 14	3	182 1	blue-black	N 3/	5.04	0. 7	whi te	10YR9. 5/2	1	Y	Y	N	N	N
TORSMA2020_2091	18 14	1	182 0	green	5G 2.5/2	28.1 4	0. 6	gre y	5Y8/1	2	Y	Y	N	N	N
TORSMA2020_2100	18 14	7	182 0	red	2.5YR 3/6	18	0. 8	gre y	5Y8/1	1	Y	Y	Y	N	N
TORSMA2020_2103	18 14	6	182 0	red	10R 4/6	14.8 2	0. 3	gre y	5Y8/1	2	Y	Y	N	N	N
TORSMA2020_2131	18 14	6	182 1	red	10R 4/6	22.0 4	0. 7	whi te	10YR9. 5/2	1	Y	Y	Y	Y	Y
TORSMA2020_2133	18 14	7	182 0	red	2.5YR 3/6	14.7	0. 7	gre y	5Y8/1	1	Y	Y	Y	Y	N
TORSMA2020_2134	18 14	7	182 0	red	2.5YR 3/6	5.04	0. 7	gre y	5Y8/1	1	Y	Y	N	N	N
TORSMA2020_2136	18 14	7	182 0	red	2.5YR 3/6	8.16	0. 7	gre y	5Y8/1	1	Y	Y	N	N	N
TORSMA2020_2139	18 14	6	182 0	red	10R 4/6	26.5 2	0. 2	gre y	5Y8/1	2	Y	Y	N	N	N
TORSMA2020_2154	18 14	7	182 1	red	2.5YR 3/6	28.5 6	0. 9	whi te	10YR9. 5/2	1	Y	Y	Y	N	N
TORSMA2020_2155	18 14	7	182 1	red	2.5YR 3/6	5.04	1. 1	whi te	10YR9. 5/2	1	Y	Y	N	N	N
TORSMA2020_2159	18 14	2	182 7	red	2.5YR 5/8	3.99	0. 9	gre y	5Y8/1	1	Y	Y	N	N	N
TORSMA2020_2163	18 14	7	182 0	red	2.5YR 3/6	6.72	0. 5	gre y	5Y8/1	1	Y	Y	N	N	N
TORSMA2020_2180	18 14	2	182 0	yellow	10YR 7/8	12.7 4	0. 7	whi te	10YR9. 5/2	1	Y	Y	N	N	N
TORSMA2020_2181	18 14	2	182 0	yellow	10YR 7/8	6.12	0. 6	whi te	10YR9. 5/2	1	Y	Y	N	N	N
TORSMA2020_2182	18 14	2	182 0	yellow	10YR 7/8	12.2 1	0. 9	whi te	10YR9. 5/2	1	Y	Y	Y	N	N
TORSMA2020_2185	18 14	2	182 0	yellow	10YR 7/8	7	0. 6	whi te	10YR9. 5/2	1	Y	Y	N	N	N
TORSMA2020_2186	18 14	5	182 0	ochre	10YR 6/8	3.9	0. 7	gre y	5Y8/1	1	Y	Y	N	N	N
TORSMA2020_2193	18 14	2	182 0	yellow	10YR 7/8	12.8 8	0. 6	whi te	10YR9. 5/2	1	Y	Y	N	N	N
TORSMA2020_2202	18 14	2	182 0	yellow	10YR 7/8	12.9 6	0. 6	whi te	10YR9. 5/2	1	Y	Y	N	N	N
TORSMA2020_2210	18 14	2	182 0	ochre	7.5YR 5/6	6.4	0. 7	whi te	10YR9. 5/2	1	Y	Y	N	N	N
TORSMA2020_2214	18 14	2	182 0	yellow	10YR 7/8	27.7 3	0. 9	whi te	10YR9. 5/2	1	Y	Y	Y	N	N
TORSMA2020_2224	18 14	2	182 6	dark reddish grey	5YR 4/2	23.4 5	0. 5	whi te	10YR9. 5/2	1	Y	Y	Y	N	N
TORSMA2020_2225	18 14	2	182 9	light greyish olive	10Y 6/2	5.8	0. 6	whi te	10YR9. 5/2	1	Y	Y	N	N	N
TORSMA2020_2230	18 14	9	182 0	light reddish brown	2.5YR 6/4	29.9	0. 9	gre y	5Y8/1	1	Y	Y	N	N	N
TORSMA2020_2232	18 14	9	182 0	light reddish brown	2.5YR 6/4	36.9 6	0. 5	gre y	5Y8/1	2	Y	Y	Y	Y	Y
TORSMA2020_2241	18 14	3	182 1	very dark greenish grey	10GY 3/1	17.2	0. 7	whi te	10YR9. 5/2	1	Y	Y	N	N	N
TORSMA2020_2242	18 14	2	182 9	light greyish olive	10Y 6/2	2.85	0. 9	whi te	10YR9. 5/2	1	Y	Y	N	N	N
TORSMA2020_2246	18 14	2	182 9	light greyish olive	10Y 6/2	5.52	0. 5	whi te	10YR9. 5/2	1	Y	Y	N	N	N
TORSMA2020_2248	18 14	2	182 9	light greyish olive	10Y 6/2	8.51	0. 5	whi te	10YR9. 5/2	1	Y	Y	N	N	N
TORSMA2020_2252	18 14	3	182 1	very dark greenish grey	10GY 3/1	2.42	0. 8	whi te	10YR9. 5/2	1	Y	Y	N	N	N
TORSMA2020_2263	18 14	1	182 1	dark reddish grey	2.5YR 4/1	11.7 8	1	whi te	10YR9. 5/2	1	Y	Y	N	N	N
TORSMA2020_2264	18 14	1	182 1	dark reddish grey	2.5YR 4/1	5.12	0. 6	whi te	10YR9. 5/2	1	Y	Y	N	N	N
TORSMA2020_2265	18 14	2	182 3	white	10YR 9.5/1	12.7 5	0. 7	whi te	10YR9. 5/2	1	Y	Y	N	N	N
TORSMA2020_2271	18 14	2	182 3	white	10YR 9.5/1	9.02	0. 5	whi te	10YR9. 5/2	1	Y	Y	N	N	N

TORSMA2020_2277	18 14	1 1	182 1	dark reddish grey	2.5YR 4/1	4.16	0. 6	whi te	10YR9. 5/2	1	Y	Y	N	N	N
TORSMA2020_2290	18 14	1 1	182 1	dark reddish grey	2.5YR 4/1	10.8 5	0. 7	whi te	10YR9. 5/2	1	Y	Y	N	N	N
TORSMA2020_2291	18 14	2 6	182 1	dark reddish grey	5YR 4/2	13.8 6	0. 7	whi te	10YR9. 5/2	1	Y	Y	N	N	N
TORSMA2020_2294	18 14	2 4	182 1	pale red	7.5R6/4	9.62	1	whi te	10YR9. 5/2	1	Y	Y	N	N	N
TORSMA2020_2295	18 14	3 1	182 1	very dark greenish grey	10GY 3/1	5	0. 6	whi te	10YR9. 5/2	1	Y	Y	N	N	N
TORSMA2020_2308	18 14	2 1	182 1	light grey	N 7/	13	0. 7	whi te	10YR9. 5/2	1	Y	Y	N	N	N
TORSMA2020_2310	18 14	2 1	182 0	light grey	N 7/	4	0. 7	gre y	5Y8/1	1	Y	Y	N	N	N
TORSMA2020_2314	18 14	4 1	182 1	ochre	7.5YR 5/6	22.5 4	0. 6	whi te	10YR9. 5/2	1	Y	Y	Y	N	N
TORSMA2020_2317	18 14	1 0	182 1	reddish-black	5R 2.5/1	27	1. 2	whi te	10YR9. 5/2	1	Y	Y	Y	Y	Y
TORSMA2020_2328	18 14	1 2	182 0	ochre	10YR 6/8	31.8	0. 6	gre y	5Y8/1	2	Y	Y	N	N	N
TORSMA2020_2332	18 14	1 3	182 0	blue grey	10B 4/1	34.1 6	1. 1	gre y	5Y8/1	1	Y	Y	Y	N	N
TORSMA2020_2344	18 14	1 3	182 1	blue grey	10B 4/1	13.5 2	1. 2	whi te	10YR9. 5/2	1	Y	Y	N	N	N
TORSMA2020_2356	18 14	2 3	182 1	white	10YR 9.5/1	6.8	0. 6	whi te	10YR9. 5/2	1	Y	Y	N	N	N
TORSMA2020_2358	18 14	2 3	182 0	white	10YR 9.5/1	10.4 4	1	gre y	5Y8/1	1	Y	Y	N	N	N
TORSMA2020_2362	18 14	2 1	182 0	light grey	N 7/	42.5	1. 1	gre y	5Y8/1	1	Y	Y	N	N	N
TORSMA2020_2363	18 14	9 0	182 0	light reddish brown	2.5YR 6/4	33	0. 5	gre y	5Y8/1	2	Y	Y	N	N	N
TORSMA2020_2384	18 14	3 1	182 1	blue-black	N 3/	7.98	0. 7	whi te	10YR9. 5/2	1	Y	Y	N	N	N
TORSMA2020_2388	18 14	1 0	182 0	green	5G 2.5/2	8.88	0. 4	gre y	5Y8/1	2	Y	Y	N	N	N
TORSMA2020_2398	18 14	3 1	182 1	blue-black	N 3/	8	0. 7	whi te	10YR9. 5/2	1	Y	Y	N	N	N
TORSMA2020_2424	18 14	3 0	182 0	blue-black	N 3/	3.6	0. 4	gre y	5Y8/1	1	Y	Y	N	N	N
TORSMA2020_2443	18 14	1 0	182 1	reddish-black	5R 2.5/1	12.4 7	0. 7	whi te	10YR9. 5/2	1	Y	Y	N	N	N
TORSMA2020_2464	18 14	2 0	182 0	blue	5PB 2.5/1	40.9 2	0. 7	gre y	5Y8/1	2	Y	Y	Y	Y	Y
TORSMA2020_2465	18 14	1 3	182 1	blue grey	10B 4/1	36.5 8	0. 7	whi te	10YR9. 5/2	2	Y	Y	N	N	N
TORSMA2020_2468	18 14	3 1	182 0	very dark greenish grey	10GY 3/1	10.5 3	0. 7	gre y	5Y8/1	1	Y	Y	N	N	N
TORSMA2020_2471	18 14	2 9	182 1	light greyish olive	10Y 6/2	11.1 8	0. 7	whi te	10YR9. 5/2	1	Y	Y	N	N	N
TORSMA2020_2474	18 14	1 1	182 1	dark reddish grey	2.5YR 4/1	10.7 3	0. 8	whi te	10YR9. 5/2	1	Y	Y	N	N	N
TORSMA2020_2495	18 14	2 6	182 1	dark reddish grey	5YR 4/2	12.8 8	0. 8	whi te	10YR9. 5/2	1	Y	Y	N	N	N
TORSMA2020_2498	18 14	1 1	182 1	dark reddish grey	2.5YR 4/1	8.36	0. 8	whi te	10YR9. 5/2	1	Y	Y	N	N	N
TORSMA2020_2500	18 14	2 0	182 0	blue	5PB 2.5/1	7.2	0. 6	gre y	5Y8/1	1	Y	Y	N	N	N
TORSMA2020_2508	18 14	1 1	182 1	dark reddish grey	2.5YR 4/1	11.5 2	0. 8	whi te	10YR9. 5/2	1	Y	Y	N	N	N
TORSMA2020_2512	18 14	3 0	182 0	blue-black	N 3/	26.9 8	1. 8	gre y	5Y8/1	1	Y	Y	N	N	N
TORSMA2020_2515	18 14	1 3	182 1	blue grey	10B 4/1	35.8 8	1. 6	whi te	10YR9. 5/2	2	Y	Y	N	N	N
TORSMA2020_2516	18 14	1 0	182 0	green	5G 2.5/2	49.2 9	0. 6	gre y	5Y8/1	2	Y	Y	Y	Y	Y
TORSMA2020_2519	18 14	1 3	182 1	blue grey	10B 4/1	87.8 7	0. 8	whi te	10YR9. 5/2	2	Y	Y	Y	N	N
TORSMA2020_2522	18 14	3 2	182 1	dark greyish green	5GY 4/2	11.5 5	0. 7	whi te	10YR9. 5/2	1	Y	N	N	N	N
TORSMA2020_2523	18 14	3 2	182 1	dark greyish green	5GY 4/2	10.2	1. 1	whi te	10YR9. 5/2	1	Y	N	N	N	N
TORSMA2020_2526	18 14	3 2	182 1	dark greyish green	5GY 4/2	9.36	0. 7	whi te	10YR9. 5/2	1	Y	N	N	N	N
TORSMA2020_2528	18 14	3 2	182 0	dark greyish green	5GY 4/2	9.86	0. 4	gre y	5Y8/1	1	Y	N	Y	N	N
TORSMA2020_2529	18 14	3 2	182 0	dark greyish green	5GY 4/2	20.6 4	0. 5	whi te	10YR9. 5/2	1	Y	N	Y	N	N

TORSMA2020_2533	18 14	1	182 1	green	5G 2.5/2	4.8	0. 6	whi te	10YR9. 5/2	1	Y	Y	N	N	N
TORSMA2020_2535	18 14	2 9	182 1	light greyish olive	10Y 6/2	10.3 5	0. 8	whi te	10YR9. 5/2	1	Y	Y	N	N	N
TORSMA2020_2539	18 14	3 2	182 1	dark greyish green	5GY 4/2	4.62	0. 1	whi te	10YR9. 5/2	2	Y	N	N	N	N
TORSMA2020_2542	18 14	2 9	182 1	light greyish olive	10Y 6/2	6.66	0. 6	whi te	10YR9. 5/2	1	Y	Y	N	N	N
TORSMA2020_2546	18 14	2 9	182 1	light greyish olive	10Y 6/2	4.2	0. 4	whi te	10YR9. 5/2	1	Y	Y	N	N	N
TORSMA2020_2572	18 14	2 9	182 1	light greyish olive	10Y 6/2	15.7 5	1. 5	whi te	10YR9. 5/2	1	Y	Y	Y	N	N
TORSMA2020_2614	18 14	1 3	182 0	blue grey	10B 4/1	15.7 5	0. 5	whi te	10YR9. 5/2	1	Y	Y	Y	N	N
TORSMA2020_2627	18 14	6	182 1	red	10R 4/6	5.1	0. 8	whi te	10YR9. 5/2	1	Y	Y	N	N	N
TORSMA2020_2644	18 14	2 3	182 0	white	10YR 9.5/1	18.4	0. 6	gre y	5Y8/1	1	Y	Y	Y	N	N
TORSMA2020_2645	18 14	2 3	182 1	white	10YR 9.5/1	3.74	0. 7	whi te	10YR9. 5/2	1	Y	Y	N	N	N
TORSMA2020_2654	18 14	2 3	182 0	white	10YR 9.5/1	7.68	0. 3	whi te	10YR9. 5/2	2	Y	Y	N	N	N
TORSMA2020_2655	18 14	2 3	182 1	white	10YR 9.5/1	3.4	0. 2	gre y	5Y8/1	2	Y	Y	N	N	N
TORSMA2020_2659	18 14	4	182 0	ochre	7.5YR 5/6	26.6 5	0. 5	gre y	5Y8/1	2	Y	Y	Y	Y	Y
TORSMA2020_2663	18 14	4	182 1	ochre	7.5YR 5/6	11.8 4	0. 5	gre y	5Y8/1	2	Y	Y	N	N	N
TORSMA2020_2668	18 14	5	182 0	ochre	10YR 6/8	6.46	0. 5	gre y	5Y8/1	1	Y	Y	N	N	N
TORSMA2020_2669	18 14	1 6	182 1	strong brown	7.5YR 4/6	20.4	1. 2	whi te	10YR9. 5/2	1	Y	Y	Y	N	N
TORSMA2020_2673	18 14	1 6	182 1	strong brown	7.5YR 4/6	17.4 8	1	whi te	10YR9. 5/2	1	Y	Y	Y	N	N
TORSMA2020_2675	18 14	5	182 0	ochre	10YR 6/8	5.76	0. 8	gre y	5Y8/1	1	Y	Y	N	N	N
TORSMA2020_2676	18 14	4	182 1	ochre	7.5YR 5/6	23.9 4	1. 3	whi te	10YR9. 5/2	1	Y	Y	Y	Y	Y
TORSMA2020_2681	18 14	2 0	182 0	yellow	10YR 7/8	2.47	0. 8	gre y	5Y8/1	1	Y	Y	N	N	N
TORSMA2020_2684	18 14	5	182 0	ochre	10YR 6/8	2.72	0. 4	gre y	5Y8/1	1	Y	Y	N	N	N
TORSMA2020_2695	18 14	5	182 0	ochre	10YR 6/8	20.5 2	1	gre y	5Y8/1	1	Y	Y	N	N	N
TORSMA2020_2697	18 14	2 3	182 0	white	10YR 9.5/1	77.3 8	0. 6	whi te	10YR9. 5/2	1	Y	Y	Y	N	N
TORSMA2020_2700	18 14	7	182 1	red	2.5YR 3/6	8.5	0. 6	whi te	10YR9. 5/2	1	Y	Y	N	N	N
TORSMA2020_2701	18 14	7	182 0	red	2.5YR 3/6	8.4	0. 2	gre y	5Y8/1	2	Y	Y	Y	N	N
TORSMA2020_2704	18 14	3	182 1	blue-black	N 3/	14.5	0. 2	whi te	10YR9. 5/2	3	Y	Y	N	N	N
TORSMA2020_2706	18 14	4	182 1	ochre	7.5YR 5/6	12.7 4	1. 2	whi te	10YR9. 5/2	1	Y	Y	N	N	N
TORSMA2020_2713	18 14	3	182 1	blue-black	N 3/	9.88	0. 7	whi te	10YR9. 5/2	1	Y	Y	N	N	N
TORSMA2020_2716	18 14	3 1	182 1	very dark greenish grey	10GY 3/1	8.75	0. 7	whi te	10YR9. 5/2	1	Y	Y	N	N	N
TORSMA2020_2717	18 14	3	182 1	blue-black	N 3/	9.52	0. 7	whi te	10YR9. 5/2	1	Y	Y	N	N	N
TORSMA2020_2720	18 14	3	182 0	blue-black	N 3/	13.8	0. 6	gre y	5Y8/1	1	Y	Y	N	N	N
TORSMA2020_2728	18 14	2 6	182 1	dark reddish grey	5YR 4/2	38.6 9	0. 9	whi te	10YR9. 5/2	2	Y	Y	Y	N	N
TORSMA2020_2733	18 14	2 3	182 1	white	10YR 9.5/1	6.3	0. 5	whi te	10YR9. 5/2	1	Y	Y	N	N	N
TORSMA2020_2735	18 14	1 1	182 1	dark reddish grey	2.5YR 4/1	9.28	0. 6	whi te	10YR9. 5/2	1	Y	Y	N	N	N
TORSMA2020_2736	18 14	3	182 1	blue-black	N 3/	17.9 2	0. 8	whi te	10YR9. 5/2	1	Y	Y	N	N	N
TORSMA2020_2742	18 14	1 5	182 1	red green yellow grey	10YR 2/1	4.08	0. 5	whi te	10YR9. 5/2	1	Y	Y	N	N	N
TORSMA2020_2746	18 14	2	182 0	blue	5PB 2.5/1	48.6	1. 1	gre y	5Y8/1	1	Y	Y	Y	N	N
TORSMA2020_2747	18 14	2	182 0	blue	5PB 2.5/1	45.9 9	0. 6	gre y	5Y8/1	1	Y	Y	N	N	N
TORSMA2020_2748	18 14	3	182 1	blue-black	N 3/	74.8 2	0. 7	whi te	10YR9. 5/2	1	Y	Y	N	N	N

TORSMA2020_2749	18 14	2	182 0	blue	5PB 2.5/1	14.0 4	0. 6	gre y	5Y8/1	1	Y	Y	N	N	N
TORSMA2020_2764	18 14	1 3	182 1	blue grey	10B 4/1	23.6 5	1. 4	whi te	10YR9. 5/2	1	Y	Y	N	N	N
TORSMA2020_2765	18 14	2 1	182 0	light grey	N 7/	15.0 5	0. 7	whi te	10YR9. 5/2	1	Y	Y	N	N	N
TORSMA2020_2768	18 14	1 1	182 1	dark reddish grey	2.5YR 4/1	7.7	0. 8	whi te	10YR9. 5/2	1	Y	Y	N	N	N
TORSMA2020_2770	18 14	2 1	182 0	light grey	N 7/	51.0 4	0. 5	gre y	5Y8/1	1	Y	Y	Y	N	N
TORSMA2020_2777	18 14	3	182 0	blue-black	N 3/	7	1	gre y	5Y8/1	1	Y	Y	N	N	N
TORSMA2020_2781	18 14	1	182 0	green	5G 2.5/2	3.15	0. 5	gre y	5Y8/1	1	Y	Y	N	N	N
TORSMA2020_2785	18 14	1 6	182 1	strong brown	7.5YR 4/6	9.68	0. 8	whi te	10YR9. 5/2	1	Y	Y	N	N	N
TORSMA2020_2789	18 14	2 1	182 1	light grey	N 7/	20.6 4	0. 7	whi te	10YR9. 5/2	1	Y	Y	N	N	N
TORSMA2020_2795	18 14	1 1	182 1	dark reddish grey	2.5YR 4/1	22.3 6	0. 5	whi te	10YR9. 5/2	1	Y	Y	Y	Y	Y
TORSMA2020_2796	18 14	1 1	182 1	dark reddish grey	2.5YR 4/1	29.1 5	0. 7	whi te	10YR9. 5/2	1	Y	Y	Y	Y	N
TORSMA2020_2798	18 14	1 4	182 1	light greyish green	5GY 3/2	15.9 9	0. 6	whi te	10YR9. 5/2	1	Y	Y	Y	N	N
TORSMA2020_2802	18 14	2 4	182 1	dark brown	7.5YR3/4	6.16	0. 7	whi te	10YR9. 5/2	1	Y	Y	N	N	N
TORSMA2020_2804	18 14	2	182 0	blue	5PB 2.5/1	34.0 4	0. 4	gre y	5Y8/1	1	Y	Y	Y	N	N
TORSMA2020_2805	18 14	3	182 1	blue-black	N 3/	41.0 4	1. 1	whi te	10YR9. 5/2	1	Y	Y	N	N	N
TORSMA2020_2814	18 14	8	182 1	greenish grey	5G 6/1	25.8 5	0. 6	whi te	10YR9. 5/2	1	Y	Y	Y	Y	Y
TORSMA2020_2822	18 14	2 3	182 0	white	10YR 9.5/1	6.21	0. 2	gre y	5Y8/1	1	Y	Y	N	N	N
TORSMA2020_2831	18 14	2 7	182 1	red	2.5YR 5/8	5.5	0. 2	whi te	10YR9. 5/2	1	Y	Y	N	N	N
TORSMA2020_2832	18 14	2 4	182 0	pale red	7.5R6/4	22.3 6	1	gre y	5Y8/1	1	Y	Y	Y	Y	Y
TORSMA2020_2834	18 14	2 3	182 0	white	10YR 9.5/1	18.5 5	0. 3	gre y	5Y8/1	1	Y	Y	N	N	N
TORSMA2020_2843	18 14	1	182 1	green	5G 2.5/2	26.6 5	0. 4	whi te	10YR9. 5/2	2	Y	Y	Y	N	N
TORSMA2020_2845	18 14	2	182 0	blue	5PB 2.5/1	17.1 1	0. 2	gre y	5Y8/1	2	Y	Y	N	N	N
TORSMA2020_2848	18 14	5	182 0	ochre	10YR 6/8	15.1 2	0. 3	gre y	5Y8/1	2	Y	Y	N	N	N
TORSMA2020_2852	18 14	5	182 0	ochre	10YR 6/8	13.1 1	0. 4	gre y	5Y8/1	2	Y	Y	N	N	N
TORSMA2020_2855	18 14	1	182 0	green	5G 2.5/2	21.1 6	0. 5	gre y	5Y8/1	2	Y	N	N	N	N
TORSMA2020_2872	18 14	5	182 0	ochre	10YR 6/8	14	0. 5	gre y	5Y8/1	2	Y	Y	Y	N	N
TORSMA2020_2881	18 14	1	182 1	green	5G 2.5/2	8.05	0. 5	whi te	10YR9. 5/2	1	Y	Y	N	N	N
TORSMA2020_2885	18 14	1	182 0	green	5G 2.5/2	7.2	1. 1	gre y	5Y8/1	1	Y	Y	N	N	N
TORSMA2020_2886	18 14	5	182 0	ochre	10YR 6/8	4.62	0. 7	whi te	10YR9. 5/2	1	Y	Y	N	Y	N
TORSMA2020_3117	18 14	7	182 2	red	2.5YR 3/6	7.2	0. 5	whi te	10YR9. 5/2	1	Y	Y	N	N	N
TORSMA2020_3119	18 14	2	182 0	yellow	10YR 7/8	8.25	0. 6	whi te	10YR9. 5/2	1	Y	Y	N	N	N
TORSMA2020_3120	18 14	6	182 1	red	10R 4/6	5.94	0. 7	whi te	10YR9. 5/2	1	Y	Y	N	N	N
TORSMA2020_3123	18 14	9	182 0	light reddish brown	2.5YR 6/4	5.75	0. 6	gre y	5Y8/1	1	Y	Y	N	N	N
TORSMA2020_3129	18 14	7	182 0	red	2.5YR 3/6	4.5	0. 9	gre y	5Y8/1	1	Y	Y	N	N	N
TORSMA2020_3133	18 14	8	182 0	greenish grey	5G 6/1	5.4	0. 5	whi te	10YR9. 5/2	1	Y	Y	N	N	N
TORSMA2020_3158	18 14	1 9	182 1	greyish green	5G 4/2	2.28	0. 7	whi te	10YR9. 5/2	1	Y	Y	N	N	N
TORSMA2020_3159	18 14	1 9	182 1	greyish green	5G 4/2	1.68	0. 4	whi te	10YR9. 5/2	1	Y	Y	N	N	N
TORSMA2020_3160	18 14	1 9	182 1	greyish green	5G 4/2	2.28	0. 3	whi te	10YR9. 5/2	1	Y	Y	N	N	N